PNAS
www.pnas.org

Supplementary Information for

Click-to-lead design of a picomolar ABA receptor antagonist with potent activity *in vivo*

Aditya S. Vaidya[1,2], Francis C. Peterson[3], James Eckhardt[1,2], Zenan Xing[1,2], Sang-Youl Park[1,2], Wim Dejonghe[1,2], Jun Takeuchi[4,5], Oded Pri-Tal[6], Julianna Faria[1,2], Dezi Elzinga[1,2], Brian F. Volkman[3], Yasushi Todoroki[4,5], Assaf Mosquna[6], Masanori Okamoto[7], Sean R. Cutler[1,2].

Affiliations
1. Institute for Integrative Genome Biology, University of California, Riverside, CA, USA, 92521
2. Botany and Plant Sciences, University of California, Riverside, CA, USA, 92521
3. Biochemistry, Medical College of Wisconsin, Milwaukee, WI, USA, 53226
4. Faculty of Agriculture, Shizuoka University, Shizuoka 422-8529, Japan

5. Research Institute of Green Science and Technology, Shizuoka University, Shizuoka 422-8529.
6. The Robert H. Smith Institute of Plant Sciences and Genetics in Agriculture, Hebrew University of Jerusalem, Rehovot 7610001, Israel.
7. Center for Bioscience Research and Education, Utsunomiya University, 350 Mine, Utsunomiya, Tochigi 321-8505, Japan.

Corresponding author: Sean R.Cutler
Email: cutler@ucr.edu

This PDF file includes:

Supplementary text
Figures S1 to S13
Tables S1
Legends for Datasets S1-S2
SI References

Other supplementary materials for this manuscript include the following:
Datasets S1-S2

Supplementary Materials and Methods

Model click reactions using OPZ and 4-ethynyltoluene. Prior to synthesizing a library of OP-4-triazoles we conducted model click reactions to establish the feasibility and efficiency of using unpurified reaction mixtures directly in ABA receptor activation assays. These reactions were performed using OPZ and 4-ethynyltoluene as follows: we mixed OPZ (4 µL, 25 mM), alkyne (10 µL, 10 mM), sodium ascorbate (2 µL, 20 mM), BTTAA (2 µL, 20 mM) and copper(II) sulfate (2 µL, 10 mM) in a 200 µL PCR tube and incubated the reaction at 37°C for 48 hr. The reaction was monitored using TLC. In parallel, we ran a scaled-up synthesis of the triazole using similar ratios of the reagents and conditions, followed by precipitation of the product by the addition of 2N HCl and subsequent filtration to yield triazole **T1** (Supplementary Fig. 2A) from 4-ethynyltoluene as white powder in quantitative yields. The purified triazole and unpurified click reaction were both tested in receptor-mediated phosphatase inhibition assays. We also tested the effects of the individual click reagents on PP2C activity by running PP2C assays in the presence of sodium ascorbate (50 µM), BTTAA ligand (100 µM), copper (II) sulfate (50 µM), or a combination of all the click-reaction reagents. The Arabidopsis receptors and PP2C ΔN-HAB1 used for this assay were expressed and purified using previously described expression clones and methods (1, 2). Phosphatase assays for were conducted in an assay buffer (100 mM Tris-HCl –pH7.9, 100 mM NaCl, 30 µg/ml BSA, 0.1% 2-mercaptoethanol) supplemented with 100 nM PYR1 (active receptor-titrated against HAB1), 25 nM ΔN-HAB1, 50 µM test compound (triazole product or OPZ precursor), in the presence or absence of 5 µM ABA. Reactions were mixed, equilibrated for 20 minutes, substrate added (4-methylumbelliferyl phosphate, 1 mM final), and fluorescence data were collected (λ exc = 360 nm, λ emm = 460 nm) using a Tecan Infinite F200 Pro fluorimeter. PP2C activity was calculated relative to solvent-only control wells (i.e. receptors and PP2C in assay buffer, but no test compound); compounds were tested in duplicate.

Synthesis and screening of a 4002 member OP-4-triazole library. 4002 commercially available alkynes were purchased from Enamine, Asinex, Chembridge, and Urosy and solvated in DMSO as 10 mM stocks in 96-well Matrix plates (80 compounds per plate); these stock solutions were used directly in click reactions. Reactions were performed as follows (per well): OPZ (4 µL, 25 mM, solution in DMSO) was mixed with library alkyne (10 µL, 10 mM, solution in DMSO), freshly prepared-sodium ascorbate (2 µL, 20 mM, solution in water), BTTAA (2 µL, 20 mM, solution in DMSO), and copper(II) sulfate (2 µL, 10 mM, solution in water) in a 96-well polypropylene PCR plate, which was covered with sealing tape and incubated at 37°C for 48 hours. Plates were stored at -20 °C prior to their use in receptor activation assays. The crude reactions were diluted 100-fold for receptor-mediated phosphatase inhibition assays (~50 µM OP-4-triazole, assuming quantitative conversion) in 96-well plates and conducted in presence of (PYR1 and HAB1 at 25 nM) in a volume of 100 µL. Both ABA (5 µM) and mock PP2C controls (no ABA) were included in each plate. Duplicate measurements of %-PP2C activity were averaged and wells that enabled recovery of PP2C activity to ≥ 90% relative to mock PP2C control were classified as hits. A total of 204 hits were obtained, which were combined into a small sub-library and retested for antagonist activity at a 10-fold lower concentration using receptors from the three receptor subfamilies: PYR1 (25 nM), PYL4 (100 nM), or PYL8 (50 nM), using assays conditions that were otherwise identical to those described above **(S. Data file 1**). To gauge the efficiency of library synthesis, LC-MS analyses of the 204 hit reactions were conducted to estimate OPZ consumption, which indicated an average reaction efficiency of 86% (± 11%); however this subset is biased towards reactions that were successful.

Arabidopsis receptor-mediated phosphatase inhibition assays. Recombinant Arabidopsis PYR/PYL proteins and ΔN-HAB1 used for phosphatase assays were expressed and purified using previously described expression clones and methods. (1–3). The PYR/PYL proteins were titrated against ΔN-HAB1 to determine active concentration (see detailed description in section-determination of active receptor). Phosphatase assays were conducted in an assay buffer (100 mM Tris-HCl –pH7.9, 100 mM NaCl, 30 µg/ml BSA, 0.1% 2-mercaptoethanol) supplemented with 25 nM PYR/PYL proteins (active receptors-titrated against HAB1), 25 nM ΔN-HAB1, different concentrations of test chemicals ranging from 100 µM to 4 nM, in the presence of 5 µM ABA. Reactions were mixed, equilibrated for 20 minutes, substrate (4-methylumbelliferyl phosphate, 1 mM final) added, and fluorescence data were collected (λ exc = 360 nm, λ emm = 460 nm) using a Tecan Infinite F200 Pro fluorimeter. PP2C activity was calculated relative to solvent-only control wells (i.e. receptors and PP2C in assay buffer, but no test compound); compounds were tested in triplicate. Dose response data fitted to a single site log-logistic model using the drc (dose response curves) package to obtain EC_{50} values in nM (effective concentrations at which 50% recovery in phosphatase activity is observed).

Synthesis and characterization of a focused combinatorial propargyl amide library Solid phase coupling reagents were used to rapidly synthesize a 106 member library of diverse aryl/heteroaryl propargyl amides by coupling diverse carboxylic acids (obtained from Combiblocks) with propargyl amine in presence of polymer supported EDCI. Reactions were carried out in a 10 mL glass vial fitted with a small stir bar. Polymer supported EDCI (2 equiv, with labeling of 1.4 mmol/g, Sigma Aldrich) was weighed into siliconized vials (coated with Sigmacote) and 2 mL of anhydrous chloroform was added to swell the resin as it was being stirred. Carboxylic acid (1 equiv) was added to the polymer suspension and the resultant mixture stirred at RT for 30 mins, after which propargyl amine (1 equiv) was added and the reaction stirred for 48 hrs at RT. The reaction mixture was subsequently filtered through a polypropylene syringe filter to separate the resin from the reaction, and the resin washed with 3 mL anhydrous chloroform. The filtrate was concentrated under vacuum to yield the crude propargyl amides, which were used directly (without further purification) as a 10 mM stock in DMSO to react with OPZ as described using click conditions described earlier. The *in situ* formed triazoles were then tested at ~50 µM OP-4-triazole, assuming quantitative conversion in phosphatase assays as described earlier in presence of 5 µM ABA and PYR1, PYL4 or PYL8 at 25 nM with ΔN-HAB1 at 25 nM. Hits that gave 90% recovery in phosphatase activity were resynthesized and tested for antagonistic activity *in vitro* using Arabidopsis receptor mediated phosphatase inhibition assays as described in previous section and *in vivo* in Arabidopsis thaliana seedling establishment assays as described in the following sections **(S. Data file 2**). These efforts produced a quinoline derivative (**4d**) which was modified to incorporate fluorine to improve hydrophobicity, yielding ligand **4o** or **Antabactin (ANT).**

***Arabidopsis thaliana* seedling establishment assays.** Greening experiments were performed in 96-well polystyrene petri plates using surface sterilized Arabidopsis (Col) seeds plated (20-25 seeds per well) on to 0.7% agar medium containing 1/2-X MS salts, 0.5% sucrose, 1 µM ABA, and one of the 204 click reactions products (~10 µM). Each experiment also included ABA (1 µM ABA, no antagonist) and mock (no ABA) controls. After 4 days of stratification (4 °C), the plates were transferred to a growth chamber under 16 hour day/8 hour night illumination and photographed 4 days later. Green pixel counts were quantified using ImageJ (v1.53c) through Hue, Saturation and Brightness thresholding parameters (H: 38,79; S: 134, 255; B: 42, 255) selected to include only green cotyledons. The resulting pixel count was used to calculate greening area per seed and

the greening area per seed in each well was normalized to mock greening per seed to obtain % greening. Purified triazoles were evaluated for their ability to block the effects of exogenous ABA in inhibiting seed germination/greening alongside PanMe, AA1, and OPZ at concentrations ranging from 200 nM to 50000 nM in triplicate in presence of 1 μM ABA. Green pixel area (normalized to mock control) was fitted to log(inhibitor) vs. response-(variable slope) model using non-linear regression to infer the EC_{50}s (concentration at which 50% of green area is observed relative to mock controls), using GraphPad Prism 6.0.

X-ray crystallography & structure determination. $PYL10^{25-183}$ was expressed in *E. coli* and purified as described previously (4). Purified protein was stored at -80 °C in a buffer containing 20 mM HEPES (pH 7.6), 50 mM sodium chloride, 10 mM DTT and 30% glycerol. Purified $PYL10^{25-183}$ was exchange into a buffer containing 20 mM HEPES (pH 7.6), 50 mM sodium chloride, 10 mM dithiothreitiol, and 5 mM magnesium chloride, mixed with a 5-fold molar excess of **4a** and concentrated to 25 mg/mL. Crystallization of the $PYL10^{25-183}$:**4a** complex was conducted by sitting drop vapor diffusion at 19 °C. Drops were formed by mixing equal volumes of the Purified $PYL10^{25-183}$:4a complex with well solution containing 200 mM tribasic ammonium citrate (pH 7.0) and 20% (w/v) PEG 3,350. The resulting crystals were flash frozen after passing through a cryoprotection solution consisting of well solution plus 20% glycerol. The $PYL10^{25-183}$:ANT complex was prepared by mixing a 5-fold molar excess of ANT with $PYL10^{25-183}$ in a buffer containing 20 mM HEPES (pH 7.6), 50 mM sodium chloride, 10 mM dithiothreitiol, and 5 mM magnesium chloride and concentrating to 25 mg/mL. Crystallization was conducted by hanging drop vapor diffusion at 19 °C by mixing equal volumes of the $PYL10^{25-183}$:ANT complex with well solution containing 200 mM tribasic ammonium citrate (pH 7.0) and 22% (w/v) PEG 3,350. Crystals were flash frozen after passing through a cryoprotection solution consisting of 200 mM tribasic ammonium citrate (pH 7.0), 25% (w/v) PEG 3,350 and 20% glycerol. X-ray diffraction data for each complex were gathered from a single crystal. Diffraction data was collected at 100 K using a Rigaku MicroMax–007 X-ray generator equipped with VariMax-HF optics and a R-Axis 4++ detector. Diffraction data were indexed, integrated, and scaled using HKL2000 software package (5) . The $PYL10^{25-183}$:**4a** and $PYL10^{25-183}$:ANT complexes were solved by molecular replacement using a $PYL10^{25-183}$:hexabactin complex (PDB ID 6NWB) devoid of ligand and water molecules as the search model to evaluate the initial phases. Phenix.AutoMR solved the initial phases and automatically built the majority of residues for both complexes (6). The resulting models were completed through iterative rounds of manual model building in Coot (7) and refinement with Phenix.refine (6) using translational libration screw-motion (TLS) and individual atomic displacement parameters. Phenix topology files for novel **4a** and ANT ligands were generated using the PRODRG server (http://davapc1.bioch.dundee.ac.uk/cgi-bin/prodrg/). Geometry of the final structures were validated using Molprobity (8). Data collection and refinement statistics for the final models are listed in Supplementary Table 1 and the coordinates for $PYL10^{25-183}$:**4a** and $PYL10^{25-183}$:ANT complexes deposited in the Protein Data Bank, PDB IDs 7MLC and 7MLD, respectively. $PYL10^{25-183}$:**4a** collection date: 2019-5-23, $PYL10^{25-183}$:ANT collection date: 2019-7-1. Ligand-protein contacts were determined and visualized using PLIP (9, 10) and Ligplot+ (11). The structure images shown in Figure 3 were rendered in Cinema 4D (Maxon) using OctaneRender (OTOY) after importing scenes generated using ANT/PYL10 coordinates and PLIP analyses from Pymol (Schroedinger).

Fluorescence polarization assays. FP assays were conducted in a buffer of 100 mM Tris-HCl, pH 7.9, 100 mM NaCl, 0.1%v/v 2-mercaptoethanol, 0.1mg/mL BSA, and 0.006%

v/v Tween 20 at 25 °C in black, non-binding 96 well microplates (100 µL; 1%v/v DMSO). Fluorescence polarization was quantified using a Tecan Infinite Pro 200 with λ_{exc} = 535 nm, λ_{emm} = 590 nm (G factor-1). Fraction bound was determined according to the equation $\Theta = (FP_{max} - FP) / (FP_{max} - FP_{min})$, where FP_{max} is the maximum FP signal (signal obtained at highest receptor concentration tested), FP_{min} is the minimum FP signal (signal from no receptor control) and FP is the signal obtained at a certain protein concentration.
To establish conditions for conducting equilibrium binding measurements, titration experiments were performed with 2.5, 5, and 10 nM TAMRA-ANT with receptor concentrations ranging from 0.4 to 100 nM; FP was measured at regular intervals over 120 minutes. Based on these experiments, dissociation constants were inferred in FP experiments using 5 nM TAMRA-ANT equilibrated with receptors for either 30 mins (PYR1) or 60 mins (PYL5 and PYL8) prior to measurements. To estimate dissociation constants, titration data were fit to the following quadratic equation in GraphPad Prism:

$$\text{Fraction bound} = \frac{([L]_{total} + [P]_{total} + K_d) - ([L]_{total} + [P]_{total} + K_d)^2 - (4 \times [L]_{total} \times [P]_{total})^{1/2}}{2 \times [L]_{total}}$$

Where, $[L]_{total}$ = total concentration of probe and $[P]_{total}$ is total concentration of protein. $[P]_{total}$ was determined by titration experiments of each receptor preparation assay using TAMRA-ANT as described by Jarmoskite *et al. (12)*.

Determination of active receptor concentrations by titration. The concentration of active Arabidopsis receptors used in each biochemical assay was determined by one of two titration methods. In the first method, the active receptor concentration was inferred from IC_{50} values for inhibition of ΔN-HAB1. To ascertain this, HAB1 (25 nM) was titrated with different concentrations of total ABA receptor protein (6.25 nM - 400 nM) in presence of 10 µM ABA in PP2C assays, as described above. Reactions were mixed, substrate added, and phosphatase activity data were collected. PP2C activity was calculated relative to no receptor control wells. The dose response data fit using non-linear regression (4 parameter logistic model) to determine the receptor concentration that gives 50% inhibition (IC_{50}). The fraction of active receptors was determined by dividing theoretical IC_{50} (12.5 nM) by the experimental IC_{50}. In the second method, receptors were titrated against TAMRA-ANT, to identify the concentration at which FP saturates (which occurs when active receptor concentration matches TAMRA-ANT concentration). ABA receptors (7.8 nM to 500 nM) were incubated for 90 minutes at 25 °C for 90 mins in the buffer described above and FP data collected and used to infer fraction, as described above by breakpoint analysis (12), see supplemental Figure 9C. Using this method, we determined the percent active receptors used in our FP experiments to be 85% for PYR1, 71% for PYL5, and 67% PYL8.

FP-based TAMRA-ANT competition Assays In case of competition experiments (n = 3), 10 nM of PYR/PYL protein were chosen as it produced a dynamic range of ≥100 mP with Z factor 0.6-0.7. Different concentrations of antagonists/competitors (0.97 nM - 10000 nM for ANT) and (9.7 nM to 100000 nM for AA1) were incubated with probe (5 nM) and PYR/PYL protein (10 nM) at 25 °C for 120 mins (total reaction volume-100 µL with 2%v/v DMSO).

Isothermal titration calorimetry (ITC). The ITC experiments were performed with an iTC_{200} calorimeter (Microcal, GE Healthcare Bio-Sciences AB) as described previously (13). Briefly, His_6-tagged PYL5 was assayed at a concentration of 50 mM with AA1 and ABA stock solutions in the injection syringe at a concentration of 500 µM. All titrations

were carried out via a series of 25 injections of 1.25 µL each. The data were corrected by subtracting the mixing enthalpies for the AA1 or ABA solutions into protein-free solutions and fitted by Origin for ITC (GE Healthcare Bio-Sciences AB) with a 1/1 binding model.

Wheat receptor-mediated PP2C inhibition assays. Wheat ABA receptor (TaPYL) and PP2C4 proteins were obtained as previously described (14). The concentration of enzymatically active TaPP2C4 protein was determined by titration against AtPYL10 protein in the presence of saturating 10 µM ABA. Subsequently active wheat ABA receptor concentrations were estimated using various concentrations of active TaPP2C4 protein in the presence of ABA. For PP2C activity assays, purified proteins were preincubated in 80 µl of buffer containing 12.5 mM MnCl2, 0.125% 2-mercaptoethanol, 3 µg BSA and test compounds at 30 °C for 10 min. Reactions containing 25 nM TaPP2C4 and 50 nM TaPYL proteins were started by adding 20 µl of substrate buffer (165 mM Tris-acetate, pH 7.9, 330 mM potassium acetate, 1 mg/mL BSA and 5 mM 4-methylumbelliferyl phosphate) (13). Fluorescence intensities were immediately measured using 360 nm excitation filter and 465 nm emission filter on a SPARK 10M (TECAN). EC_{50} values were calculated for recovery of PP2C activities in the presence of 5,000 nM ABA with different concentrations of test compound using a model using the drc (dose response curves) package (9).

Brachypodium receptors mediated phosphatase inhibition assays. Recombinant proteins were purified as described previously (15) and were used for PP2C inhibition assay. Each reaction contained 1.2 µm recombinant PP2C and 3.6µM recombinant receptor in 33 mM Tris acetate (pH 7.9), 66 mM potassium acetate, 0.1% bovine serum albumin, 10 mM $MnCl_2$, 0.1% β-ME, 50 mM pNPP, 0.25 µM +ABA and increasing concentrations of AA1 (0, 1, 5, 10, 25, and 50µM). The reaction was monitored for pNPP hydrolysis at A_{405}. Recombinant GST-BdPP2C44 activity (as a percentage) was measured in the presence of recombinant 6XHIS-BdPYL1, 6XHIS-BdPYL2 and GST-BdPYL3. The activity of BdPP2C44 was measured for 10 minutes and phosphatase activity was calculated during 2 minutes in the linear phase of the reaction with three replicates. All reactions were analysed three minutes after the reaction started. Values represent percentage activity compared with phosphatase activity in the presence of a receptor only (without ABA or AA1).

Yeast two-hybrid assays with Brachypodium receptors. *Arabidopsis* receptors were examined for PP2C interactions by using X-gal staining to monitor β-*galactosidase* reporter gene expression levels. Individual clones were spotted onto SD–LT glass round plates containing 1µM ABA, 1µM ABA with 50uM AA1 and 0.1% Mock control (DMSO). Following incubation at 28°C for 2 days, colonies were chloroform lysed and stained to estimate β-galactosidase accumulation, as described previously (4).

***In vitro* pull-down assays.** GST-HAB1 used in this assay was expressed and purified as previously described (4). Reaction mixtures including 25 µg of His6-Pyr1 and 250 µg of GST-HAB1 (1.05 and 3.05 µM each) in 1ml of TBS buffer with 1 mM MnCl2 and chemicals were incubated at RT for 1.5 hr and extended incubation with 30mg of His-tagged protein purification resin (PrepEase, USB) for 30min. The resin was collected by brief centrifugation and washed 5 times with TBS containing 1 mM MnCl2. Proteins were released by boiling with SDS sample buffer and analyzed by SDS PAGE. ABA and ANT reactions included 10µM each, and ABA/ANT ratio was 10:50 in µM respectively.

Arabidopsis ABA-reporter gene analyses. For ABA-responsive reporter gene analyses, transgenic Arabidopsis expressing β-glucuronidase (GUS) under the control of the

AtMAPKKK18 promoter were used as previously described (3). Seedlings were grown on agar plates containing 1/2 MS and 0.5% sucrose for 6 days at 22°C and an 18/6-h light/dark cycle. Transgenic seedlings were transferred to an incubation solution containing 1/2 MS and 0.5% sucrose and acclimated in the incubation solution overnight before chemical treatment. For ABA agonist and antagonist analyses, a single chemical or a mixture was added to the incubation solution with seedlings and then incubated for 6 h under the 22°C light condition. For osmotic stress analysis, seedlings were transferred to 400 mM mannitol solution containing 1/2 MS, 0.5% sucrose and chemicals, and incubated for 6 h under the 22°C light condition. GUS detection was performed in reaction buffer containing 50 mM sodium phosphate (pH 7.0), 0.05% Tween-20, 5 mM potassium ferrocyanide, 5 mM potassium ferricyanide and 1 mM 5-bromo-4-chloro-3-indolyl-β-D-glucuronide (X-gluc) at 37°C. The reaction was stopped by adding ethanol (EtOH), and the chlorophyll pigment of the seedlings was bleached with 70% EtOH at 65°C. GUS staining was observed using stereo and optical microscopes.

Arabidopsis qRT-PCR experiments. Eight-day-old seedlings of *Arabidopsis thaliana* wild-type (Col-0) were pretreated with ½ Murashige-Skoog (MS) liquid medium (0.25% sucrose, pH 5.7) supplemented with either DMSO control or 25 μM ANT for 4 hours, and then exposed to either DMSO or 25 μM ANT in the presence or absence of 20% PEG for another 6 hours. Each treatment was conducted in biological triplicate. The total RNA was extracted using the RNeasy Plant Mini Kit (QIAGEN, Cat No. 74904), and cDNA was synthesized by QuantiTect Reverse Transcription Kit (QIAGEN, Cat No. 205311). Quantitative RT-PCR was performed with CFX Connect Real-Time PCR Detection System using Maxima SYBR Green/Fluorescein qPCR Master Mix (Thermo Scientific, Cat No. K0242). The relative expression level of the ABA-responsive genes was normalized against the reference gene *AtPEX4* by ΔC_T Method. Statistical tests were performed using the raw ΔC_T values, the two-way ANOVA test was performed to test the significance of the differences between all the treatments, different lowercase letters indicate significant differences as assessed by the pairwise Tukey test.

The primers used in the experiments are listed as follows.
AtPEX4: 5'CAGTCCTCTTAACTGCGACTC3', 5'GGCGAGGCGTGTATACATTT3'
AtMAPKKK18: 5'CACACTTGTCGGTGAGTTCG3', 5'GGAGAGATGGACAGCGAGTC3'
AtRD29B: 5'TGGTGGGGAAAGTTAAAGGA3', 5'GGAATCCGAAAACCCCATAGTCC3'

Wheat qRT-PCR experiments. Wheat (cv. Chinese Spring) seeds were imbibed in water for 2 days at 4°C, and subsequently placed under the light condition at 22°C for 2days. Germinated seeds were hydroponically cultivated in 1/10× Hoagland's solution at 22/18 °C (day/night) under a 14-h light/10-h dark photoperiod in a growth chamber. Root parts of seven-day-old seedlings were soaked in 1/10× Hoagland's solution containing each 5 μM compound for 12h. The shoot and root parts were cut off, and frozen in liquid nitrogen and then ground to a powder with Mixer Mill MM 400 (Verder Scientific). Total RNA was extracted using a Plant Total RNA purification kit (GMbiolab, Taichung, Taiwan) and was reverse-transcribed using RevTra Ace qPCR RT Master Mix with gDNA Remover (Toyobo). qRT-PCR was performed on a LightCycler 96 System (Roche) using KOD SYBR qPCR Mix (Toyobo). The relative amounts of target transcripts were determined using the relative standard curve method and were normalized by the relative amount of internal control transcripts. *TaActin* (forward primer 5'-CCTCTCTGCGCCAATCGT-3', reverse primer 5'-TCAGCCGAGCGGGAAATTGT-3') was used as internal standards, whereas *TaLEA* (forward primer 5'-GACAACACCATCACCACCAAGGACA-3', reverse primer 5'-TAATACAGAACCGGACACGAGGAGT-3'), *TaPP2C6* (forward primer 5'-

ACGAGTGCCTGATCCTAGCCAG-3', reverse primer 5'-GGAGATGTTGTCCGAGCTGTTCTT-3') were used as ABA responsive genes. Significance was determined using Tukey's test.

Thermoinhibition assays. To establish if ANT blocks thermoinhibition, we conducted assays as follows. Surface sterilized Arabidopsis seeds (n>25 seeds; seeds were harvested six months prior to the experiment) were plated in 24 well polystyrene petri plates on 0.7% agar medium containing 1/2-x MS salts, 0.5% sucrose, and 30 µM ANT, fluridione, or mock untreated control (0.3% v/v DMSO). After 96hrs of stratification at 4°C, the plates were either heat treated at 37°C (in darkness for 48 hrs), or transferred directly to an imaging cabinet used to acquire images at regular intervals. After heat treatment, the plates were transferred to the imaging cabinet and photographed every 5h. Germination was scored as positive based on radicle emergence and the ET_{50} (time at which 50% of seeds have germinated) values were inferred by fitting the germination data over time to a 4 parameter log-logistic model in the drc (dose response curves) package (9). Continuous monitoring of germination was conducted under dim illumination (under LED illumination at 12 µmol/m^2/s) at room temperature (25 °C).

Seed germination rate (ET_{50}) measurements. Experiments examining the effects of ANT on germination were conducted as follows. Surface sterilized seeds were plated onto polystyrene petri plates on 0.7% agar medium containing ½X- MS salts and carrier solvent (DMSO; 0.2% v/v) or ANT (Arabidopsis 50 µM, tomato 25 µM, barley 100 µM). All experiments were completed in triplicate with 15 tomato and barley seeds per replicate. Plates were immediately transferred to a growth chamber with 22°C under 16 hour day/8hr night illumination. Germination was manually quantified and the ET_{50} (time at which 50% of seeds have germinated) was calculated using a log-logistic model using the drc (dose response curves) package in R.

Thermography experiments. Chemicals were directly applied to soil in case of Arabidopsis or as aerosols in case of tomato in a solution composed of 0.2 v/v% DMSO and 0.02% v/v Silwet-77 (Lehle seeds) for Arabidopsis or 0.05% Silwet-77 for experiments with tomato and wheat. Pot positions within each experiment were randomized to control for microenvironmental differences in the growth cabinet. Leaf temperatures were obtained using a FLIR T62101 camera and averaged from 10-15 ~1 cm^2 leaf area spots per replicate pot using FLIR software. Col-0 seeds were either plated on ½ MS, 0.5% w/v sucrose, 0.7% agar plates containing no chemical (mock treated) or 100 µM ANT. Simultaneously abi1C seeds were also plated on ½ MS, 0.5% w/v sucrose, 0.7% agar plates. After 4 days of stratification at 4'C, plates were grown in a light chamber with controlled humidity for another 7 days, after which seedlings were transferred to soil in 4 inch pots (2 plants per pot; n = 12 pots per treatment). Seedlings germinated on ANT were continuously exposed to ANT by addition of 2.5 mL of solutions of ANT (100 µM in water + 0.2% v/v DMSO) every other day directly to the soil for three weeks, while mock treated seedlings were exposed identically to 2.5 mL mock solution treatment (water + 0.2% v/v DMSO). Plants were grown under 18 hour days at ~25 ºC. For a single treatment experiment, Col-0 seeds were plated on ½ MS, 0.5% w/v sucrose, 0.7% agar plates with or without added test chemical. After 4 days of stratification at 4'C, plates were grown in a light chamber with controlled humidity for another 7 days, after which seedlings were transferred to soil in 4 inch pots (2 plants per pot; n = 10 pots per treatment) and grown until the plants were 3 weeks old. Plants were sprayed with 20 mL of 100 µM ANT solution and images after 48 hr. Experiments conducted on tomato (UC82) used ~6 week old seedlings (1 plant per pot, n=8 for per treatment) and 20 mL solution of 100 µM ANT.

Experiments conducted on wheat (Patwin 515) used ~3 week old seedlings (10 - 15 plants per pot, n = 9 for per treatment) and 20 mL solution of 100uM ANT. Plants were grown under continuous exposure to light (under LED illumination at 120 μmol/m^2/s) at ~25 ºC and photographed after 2 hr.

Chemicals & syntheses. Target molecules were synthesized according to the schemes depicted in (**Supplemental Figure 1 and 3**). Reactions were carried out under an atmosphere of argon in oven-dried glassware, unless otherwise stated. Indicated reaction temperatures refer to those of the reaction bath, while room temperature (rt) is noted as 25 °C. All solvents were of anhydrous quality purchased from Aldrich Chemical Co. and used as received. Pure reaction products were typically dried under high vacuum. Commercially available starting materials and reagents were purchased from Aldrich, TCI, Fisher Scientific, Combiblocks and AK Scientific and used as received. Analytical thin layer chromatography (TLC) was performed on 60 Å, 250 µm silica TLC plates. ^{1}H NMR and ^{13}C NMR spectra were recorded on a Bruker 700 MHz NMR and chemical shifts reported in ppm using the solvent resonance as internal standard ([DMSO-d6 2.5 ppm] for ^{1}H, ^{13}C respectively). NMR data are reported as follows: chemical shift, multiplicity (s= singlet, d = doublet, dd = doublet of doublet, t = triplet, q = quartet, br = broad, m = multiplet), number of protons, and coupling constants. Product exact masses were obtained by analysis on an Agilent 6224 ESI TOF in positive ion mode after LC separation. All compounds used for biological testing were ≥ 95% pure. (+)-ABA was purchased from BioSynth, AA1 was purchased from Life Chemicals and its structure confirmed by ^{1}H NMR, which we collected after we observed numerous biochemical results that were inconsistent with previous reports of AA1-mediated antagonism of ABA receptor activity (16); our analytical data confirming the identity of AA1 are shown below along with analytical section for newly synthesized compounds. TAMRA-5-azide was purchased from LumiProbe, BTTAA was purchased from Click Chemistry Tools and PanMe was synthesized according to an established procedure (17).

Syntheses

Methyl (4-amino-3,5-dibromophenyl)acetate (**1a**). To a solution of Methyl (*p*-aminophenyl)acetate (5 g, 30.26 mmoles, 1 equiv) in anhydrous methanol was added ammonium bromide (5.93 g, 60.52 mmoles, 2 equiv) followed by oxone (9.21 g, 60.52 mmoles, 2 equiv) portion wise and the reaction stirred overnight. After completion of reaction (TLC), the reaction was concentrated in vacuo, adsorbed on silica and purified by silica gel flash chromatography using hexane/ethyl acetate gradient to yield 4.63 g of **1a** as a pale yellow solid in 48% yield.

Methyl (4-amino-3,5-dicyclopropylphenyl)acetate (**1b**). To a solution of **1a (**3.72 g, 11.52 mmoles, 1 equiv) in toluene/water (12 ml toluene: 600 µL water) was added K_3PO_4 (8.56 g, 40.31 mmoles, 3.5 equiv), $P(Cy)_3$ (323 mg, 1.15 mmoles, 0.1 equiv), $Pd(OAc)_2$ (129.3 mg, 0.578 mmoles, 0.05 equiv) and cyclopropyl boronic acid (2.47 g, 28.8 mmoles, 2.5 equiv) and heated in a pressure vessel at 110°C for 3 hours. After completion of reaction (TLC), the reaction was concentrated in vacuo, adsorbed on silica and purified by silica gel flash chromatography using hexane/ethyl acetate gradient to yield 2.63 g of **1b** as a off white crystalline solid in 93 % yield.

(4-Amino-3,5-dicyclopropylphenyl)acetic acid (**1c**). To a solution of **1b** (2.63 g, 10.73 mmoles, 1 equiv) in 20 mL of methanol/water (1:1 v/v) was added lithium hydroxide (2.57 g, 107.3 mmoles, 10 equiv) and stirred at room temperature for 24 hr. After completion of reaction (TLC), the reaction, 2N HCl was added to precipitate the product, **1c** as a white solid (near quantitative yield) which was filtered, dried and used in the next step without further purification.

(4-Azido-3,5-dicyclopropylphenyl)acetic acid (**1d**). To an ice cold solution of **1c** (0.9 g, 3.89 mmoles, 1 equiv) in acetonitrile/water (1:1) was added concentrated hydrochloric acid dropwise 5 mL, followed by a cold aqueous solution of sodium nitrite (0.4 g, 5.84 mmoles, 1.5 equiv). The reaction stirred at 0°C for 20 min. Thereafter a cold aqueous solution of sodium azide (0.76g, 11.67 mmoles, 3 equiv) was added dropwise so as to control the effervescence of nitrogen gas observed. The reaction was stirred at 0°C for a further 1 hr and left to attain room temperature overnight. After completion of reaction (TLC), 2N HCl was added to the reaction mixture, and the reaction extracted three times with ethyl acetate (30 mL). The organic extracts were combined and dried over anhydrous sodium sulfate and concentrated in vacuo. The residue was adsorbed on silica gel and purified by flash chromatography using a hexane/ethyl acetate gradient to yield 0.82 g of **1d** as an off white solid in 83% yield.

Methyl 1-[2-(4-azido-3,5-dicyclopropylphenyl)acetylamino]cyclohexanecarboxylate (**2a**). To an ice cold solution of **1d** (0.82 g, 3.18 mmoles, 1 equiv) in anhydrous dichloromethane was added 1-aminocyclohexanoate (0.6 g, 3.82 mmoles, 1.2 equiv), EDCI (0.91 g, 4.77 mmoles, 1.5 equiv) and DMAP (0.58g, 4.77 mmoles, 1.5 equiv) and the reaction stirred overnight at room temperature. After completion of reaction (TLC), the reaction was concentrated in vacuo, adsorbed on silica and purified by silica gel flash chromatography using hexane/ethyl acetate gradient to **2a** as a off white solid in near quantitative yield.

1-[2-(4-Azido-3,5-dicyclopropylphenyl)acetylamino]cyclohexanecarboxylic acid (2b; OPZ). To a solution of **2a** (0.4 g, 1.01 mmoles, 1 equiv) in methanol/water 20 mL (1:1 v/v) was added lithium hydroxide (0.48 g, 20.2 mmoles, 20 equiv) and stirred at RT for 24 hr. After completion of the reaction (TLC), 2N HCl was added to the reaction mixture to precipitate the product as a white solid in near quantitative yields. The product is extremely light sensitive and stored at -20°C until further use.

N-2 Propynyl-6-fluoro-2-quinolinecarboxamide (3o). To a solution of the precursor acid (250 mg, 1.31 mmoles, 1 equiv) in anhydrous DCM at 0°C was added propargyl amine (86.4 mg, 1.57 mmoles, 1.2 equiv). To this mixture were added EDCI (376 mg, 1.96 mmoles, 1.5 equiv) and DMAP (192 mg, 1.57 mmoles, 1.2 equiv) and the reaction allowed to come to room temperature and further stirred for 12 hrs. After completion of reaction, brine was added to the reaction and extracted three times with dichloromethane, the organic extracts were combined and dried over anhydrous sodium sulfate and concentrated *in vacuo*. The residue was purified using flash chromatography using a hexane/ethyl acetate gradient to yield the corresponding amides **3n** as a white powder. Similar protocol was applied for synthesis of propargyl amides **3a-3p** which were obtained in 70-90 % yields as solid powders.

Synthesis of ANT (4o). To a solution of the OPZ (75 mg, 0.19 mmoles, 1 equiv) in DMSO/Water (4:1 v/v) at RT was added propargyl amides **3o** (44.7 mg, 0.19 mmoles, 1 equiv). To this mixture was added BTTAA (33.7 mg, 0.078 mmoles, 4 equiv), sodium ascorbate (23.3 mg, 0.12 mmoles, 0.6 equiv) and copper sulfate (6.3 mg, 0.039 mmoles, 0.2 equiv) the reaction stirred at room temperature and stirred for further 48 hrs. After completion of reaction, 2N HCl was added to the reaction and the precipitated triazole antagonist filtered through a sintered funnel. The solid was thoroughly washed (3-5 times the reaction volume) with distilled water and dried in the oven to yield solid white powder **4o**. Similar protocol was applied for synthesis of other triazole antagonists **4a-4p** which were obtained in 80-90 % yields as solid powders.

Synthesis of alkyne 4q. Aryl bromide **4p** (400 mg, 0.6 mmoles, 1 equiv), CuI (22.8 mg, 0.12 mmoles, 0.2 equiv) and Palladium(II)bis(triphenylphosphine) dichloride (84.2 mg, 0.12 mmoles, 0.2 equiv) were added to oven-dried schlenk flask. The schlenk flask was evacuated and refilled with argon, this process repeated thrice. 5 mL of anhydrous DMF, trimethylsilylacetylene (294 mg, 3 mmoles, 5 equiv) and triethylamine (183 mg, 1.8 mmoles, 3 equiv) were added to the flask and the reaction mixture stirred in a heated oil bath at 60°C overnight. After completion of reaction, brine was added to the reaction and extracted three times with ethyl acetate, the organic extracts were combined and dried over anhydrous sodium sulfate and concentrated *in vacuo*. The residue so obtained was dissolved in anhydrous methanol (10 mL) and treated with catalytic quantities of potassium carbonate (~5-10 mg) at room temperature for 3 hrs to effect deprotection of trimethylsilyl group. After completion of the reaction, silica gel was directly added to the reaction and the reaction concentrated *in vacuo.* The product was purified using flash chromatography using a hexane/ethyl acetate gradient to yield 180 mg of a yellow solid- alkyne **4q** in 49 % yield over two steps.

Synthesis of TAMRA-ANT (4r). Commercially available TAMRA-5-azide (100 mg, 0.19 mmoles, 1 equiv) was dissolved in DMSO (3 mL) and added to a small glass vial covered with aluminum foil to protect from light. To this a solution of alkyne **4q** (120 mg, 0.19 mmoles, 1 equiv) in DMSO (1 mL) was added followed by BTTAA (67 mg, 0.16 mmoles, 0.8 equiv). To this was added a solution of sodium ascorbate (31 mg, 0.16 mmoles, 0.8 equiv) in 500 µL water followed by a solution of copper sulfate (12.5 mg, 0.08 mmoles, 0.4 equiv) in 500 µL water. The dark-pink reaction was protected from light and stirred at room temperature for 48 hrs. After completion of reaction distilled water (20 mL) was added to the reaction to precipitate the triazole which was filtered through a sintered funnel and washed 5 times with distilled water (10 mL) and subsequently dried to give the pure triazole as a dark pink powder in near quantitative yields. The product is light sensitive and stored at -20°C until further use.

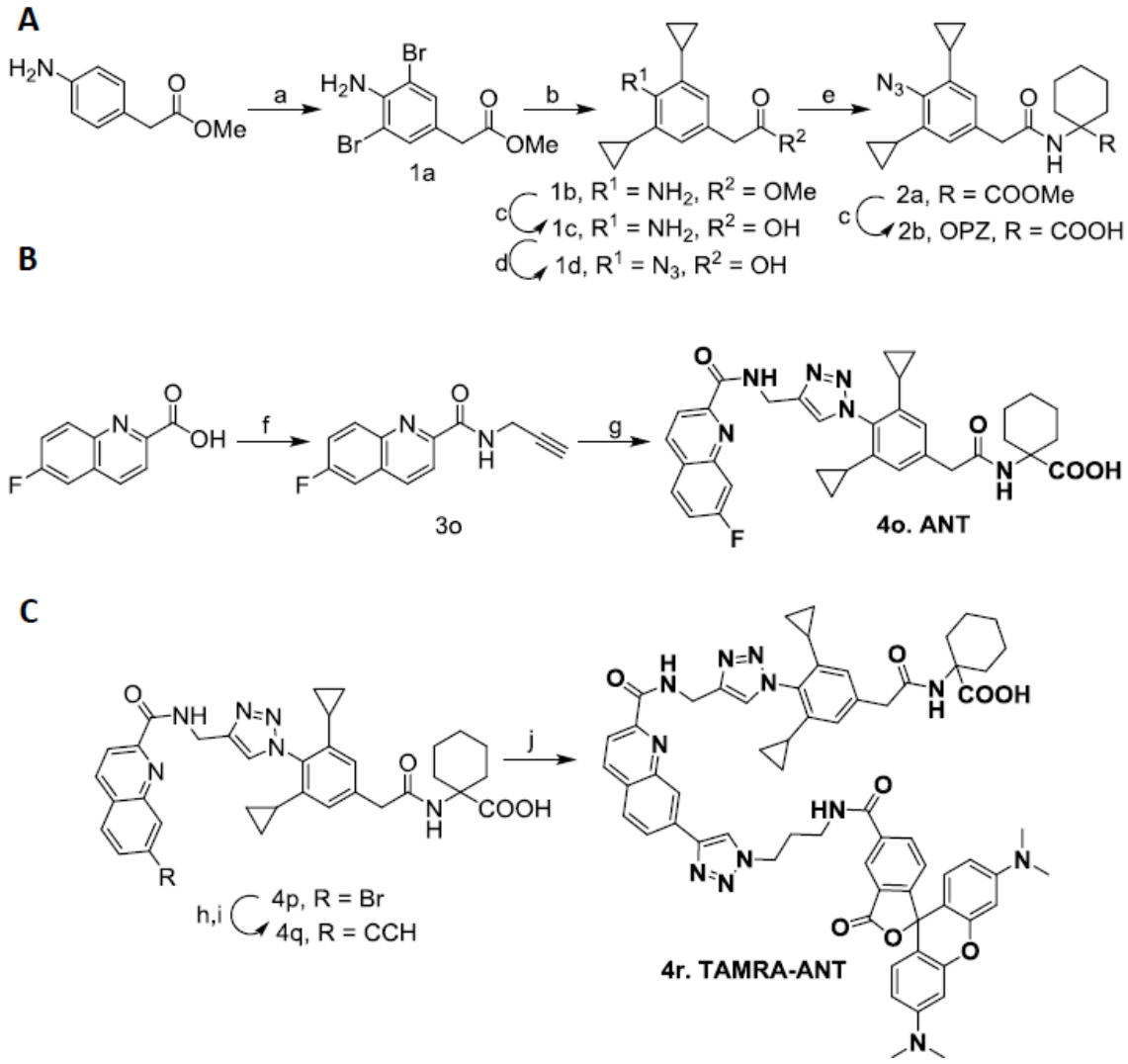

Fig. S1. Synthesis of OPZ (A), ANT (B) and TAMRA-ANT (C). Reagents and conditions: (a) Ammonium bromide, oxone, MeOH, 12 hr; (b) Cyclopropyl boronic acid, K_3PO_4, $P(Cy)_3$, $Pd(OAc)_2$, Toluene/water, 110°C, 3 hr; (c) LiOH, MeOH/H_20, RT, 24 hr; (d) $NaNO_2$, HCl, NaN_3, 0°C-RT, 12 hr; (e) Methyl 1-aminocyclohexanoate, EDCI, DMAP, DCM, 0°C-RT, 12 hr; (f) EDCI, DMAP, DCM, 0-RT, 12 hr; (g) OPZ, BTTAA, sodium ascorbate, copper (II) sulfate, DMSO/H_20, RT, 48 hr; (h) Aryl bromide-**4p**, Cu(I), Palladium (II)bis(triphenylphosphine)dichloride, trimethylsilylacetylene, 60°C, 12 hr; (i) catalytic potassium carbonate, MeOH, RT, 3 hrs. (j)TAMRA-5-azide, BTTAA, sodium ascorbate, copper (II) sulfate, DMSO/H_20, RT, 48 hr.

A

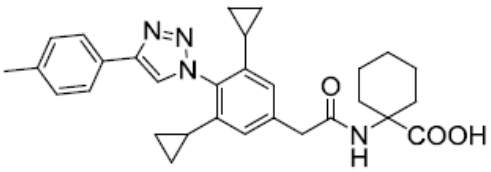

Ligand name: T1
Chemical Formula: $C_{30}H_{34}N_4O_3$
Expected Mass $(M+H)^+$ = 500.2742
Observed Mass $(M+H)^+$ = 500.2886

B

Ligand/Condition	Concentration	% HAB1 activity Mean ± S.D
DMSO	1%v/v	100.0 ± 2.5
ABA	5000 nM	9.5 ± 1.3
Pure triazole	50000 nM	101.3 ±1.8
Pure triazole + ABA	50000 nM + 5000 nM	66.3 ± 6.8
In situ triazole	50000 nM	98.1 ± 0.6
In situ triazole +ABA	50000 nM + 5000 nM	72.9 ± 1.8
OPZ	50000 nM	65.8 ±3.2
OPZ+ ABA	50000 nM + 5000 nM	51.1 ± 5.0
CuSO4	50000 nM	92.9 ± 1.7
BTTA	100000 nM	93.8 ± 0.6
Na ascorbate	100000 nM	96.5 ± 0.9
Click reagents-combination		97.3 ± 1.0

Fig. S2: **(A)** Structure and observed HRMS data for triazole T1 (detailed NMR characterization are provided in analytical section); **(B)** ABA/PYR1-mediated PP2C activity in different conditions tested: *in situ* generated versus purified OP-4-triazole, OPZ, and different click reagents on their own or combinations.

A

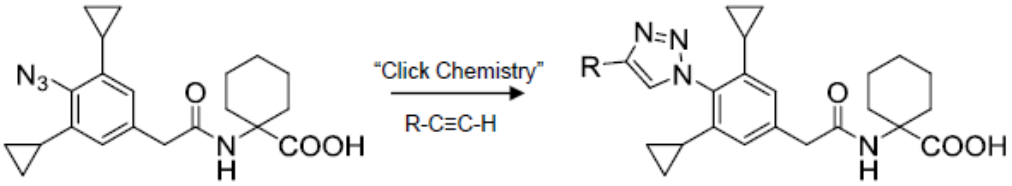

OPZ OP-triazoles

B

Class	Structure	No of hits
Propargyl amines	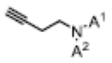	61
Propynoic acid derivatives		5
Propargyl ethers		6
Propargyl amides	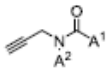	**121**
Propargyl Esters	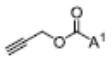	2
Propynes		2
Propargyl thioethers		2
Propragyl ureas	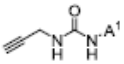	3
Propargyl sulfonamides	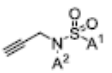	1
Propargyl carbamates	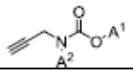	1
Total		204

Fig. S3. Structural diversity of R-groups identified as OP-4-triazole antagonists. **(A)** General scheme for the synthesis of 4-OP-triazoles by clicking OPZ against a collection of alkynes. **(B)** Classification of alkyne building blocks that produced PYR1 antagonist hits; propargyl amides, which produce OP-4-peptidotriazoles after clicking with OPZ, produced the most frequent hits. A1 and A2 represent aryl/alkyl substituents or hydrogen atoms. Building block structures, screening data, and details on specific hit molecules that were resynthesized are available in **S. Data file 1**.

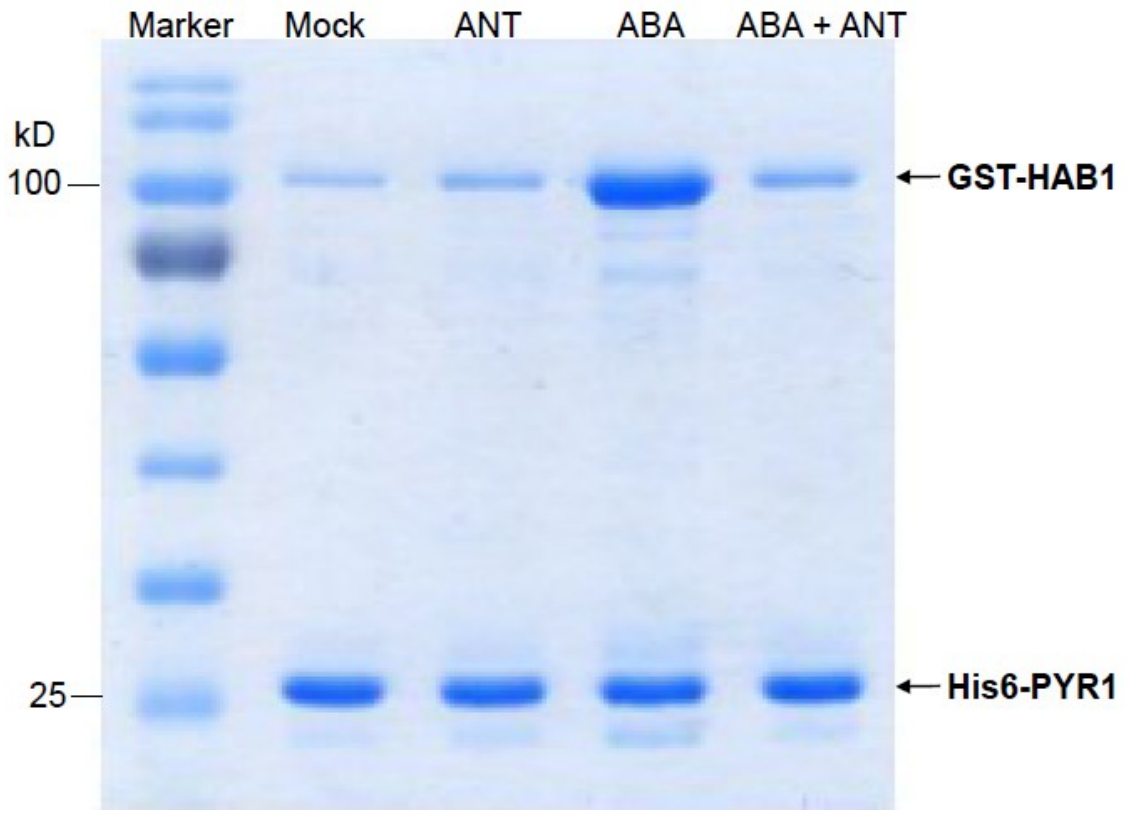

Fig. S4. ANT blocks the physical interaction between recombinant Arabidopsis PYR1 and HAB1 *in vitro*. Reaction mixtures including 25 µg of 6xHis-PYR1 and 250 µg of GST-HAB1 (1.05 and 3.05 µM each) in 1 ml of TBS buffer with 1 mM $MnCl_2$ and chemicals (ABA -10µM or ANT-10µM or their combination ABA(10µM) +ANT(50µM)) were incubated at room temperature for 1.5 hr, after which 30 mg of His-tagged protein purification resin (PrepEase, USB) was added for an additional 30 min. The resin was collected by brief centrifugation and washed 5 times with TBS containing 1 mM $MnCl_2$. Proteins were released by boiling with SDS sample buffer and analyzed on SDS-PAGE

.

A **Arabidopsis**

Subfamily	Receptor	EC_{50} (nM)		
		ANT	PanMe	AA1
III	PYR1	100 ± 18	20451 ± 855	-
	PYL1	172 ± 30	24263 ± 3498	-
	PYL2	13 ± 3	1438 ± 257	-
	PYL3	26 ± 5	6463 ± 800	-
II	PYL4	220 ± 34	7614 ± 2623	-
	PYL5	427 ± 99	3744 ± 947	-
	PYL6	846 ± 117	4716 ± 436	-
I	PYL8	149 ± 33	8857 ± 3621	-
	PYL9	465 ± 65	7734 ± 1238	-
	PYL10	77 ± 20	5212 ± 1469	-

B **Wheat**

Subfamily	Receptor	EC_{50} (nM)		
		ANT	PanMe	AA1
III	TaPYL1	24 ± 3	*	-
	TaPYL2	60 ± 8	6032 ± 549	-
	TaPYL3	22 ± 4	3362 ± 157	-
II	TaPYL4	22 ± 3	9468 ± 481	-
	TaPYL5	20 ± 4	1836 ± 305	-
	TaPYL6	37 ± 7	9030 ± 167	-
I	TAPYL7	16 ± 2	4393 ± 1491	-
	TaPYL8	70 ± 8	5626 ± 609	-

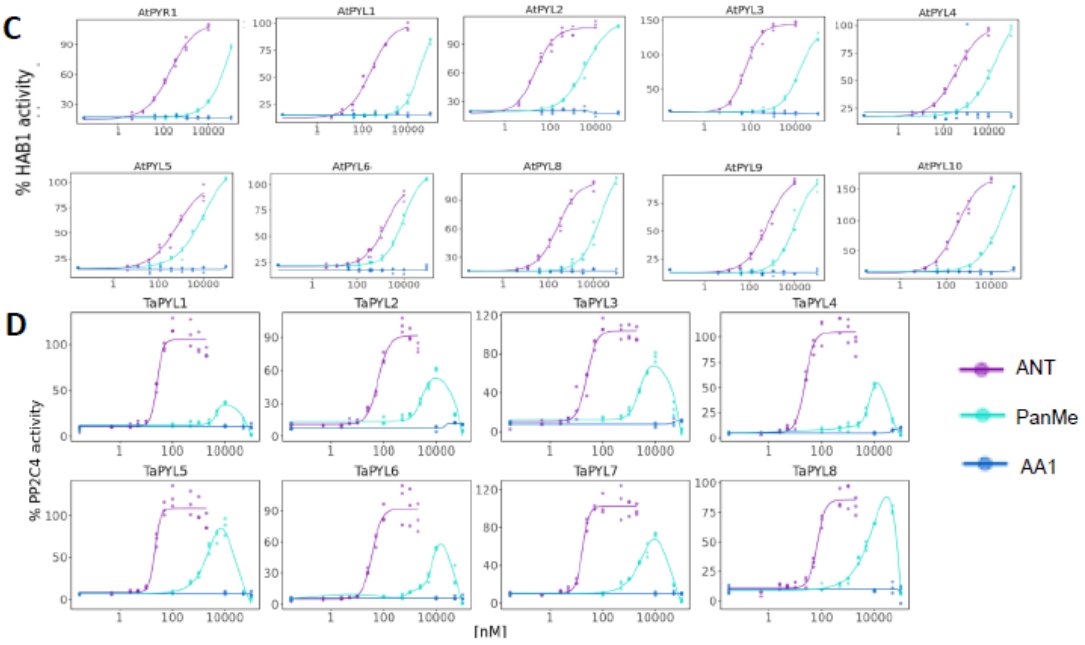

Fig. S5. ANT potently antagonizes effects of ABA mediated receptor activation in Arabidopsis and Wheat. (A) and **(B)** Quantification of antagonist-mediated recovery of Arabidopsis HAB1 or wheat PP2C4 activity for different ABA receptors at saturating ABA concentrations (5000 nM). Arabidopsis ABA receptors were tested at 25 nM, wheat receptors at 50 nM, PP2Cs tested 50 nM. The EC_{50} values indicate the concentration of antagonist (nM) at which 50% recovery of phosphatase activity is observed. Errors indicate the standard deviation of triplicate measurements. "**-**" indicates that no statistically significant change in HAB1 activity was observed up to 100 μM; "*****" indicates that the maximal PP2C recovery does not exceed 50%. (C and D) Dose response curves from which EC_{50} values were obtained. EC_{50} values were inferred by fitting the dose response data to the 4 parameter log-logistic equation using the drc R package. These data show the complete dose response data collected for Arabidopsis and wheat receptors; a subset of these data (for Arabidopsis PYR1, PYL5, and PYL8) are plotted and shown in Fig. 2 of the main text.

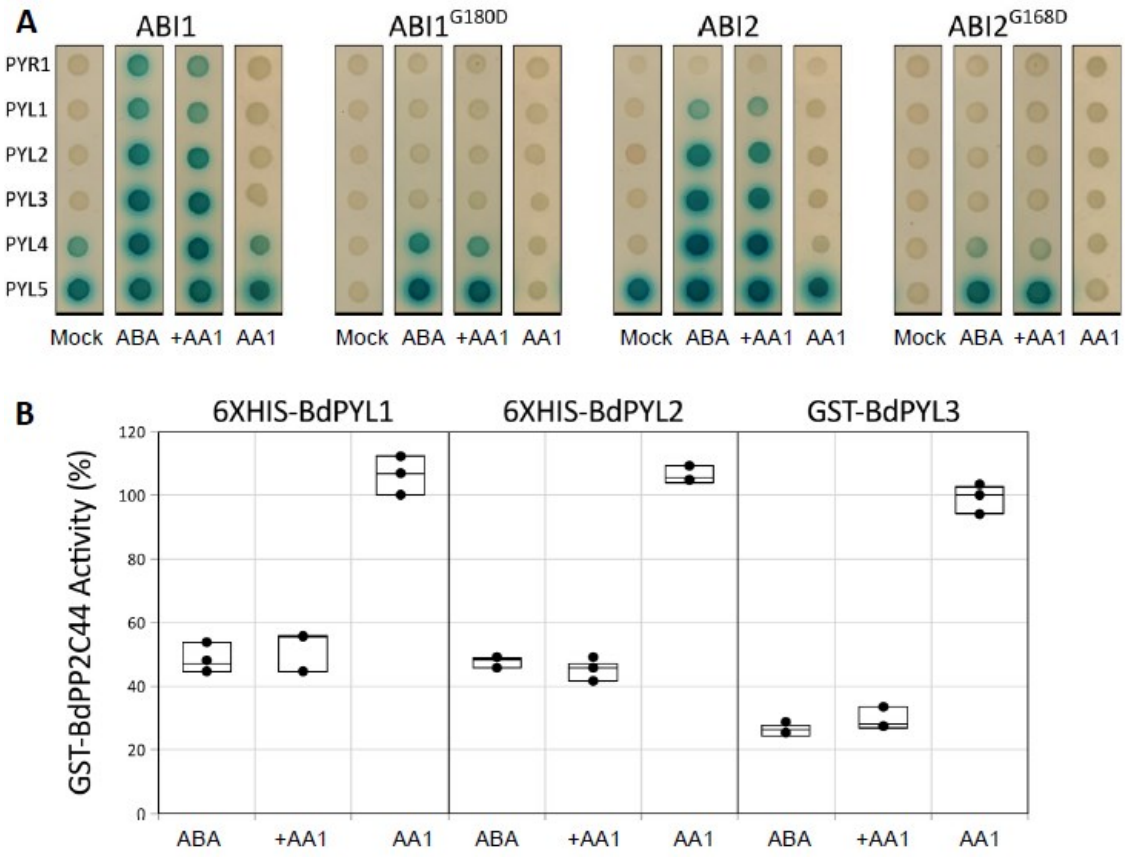

Fig. S6. AA1 does not antagonize Brachypodium ABA receptors. (A) AA1 has no effect on ABA-induced interaction between *Arabidopsis* receptors and PP2Cs as measured using a yeast two-hybrid assay. Binding domain fused receptors were tested for interaction with activating domain fused PP2C in yeast. Interactions were tested in the presence of AA1 (50 μM), ABA (0.25 μM), AA1 + ABA (50/0.25 μM; lane "+AA1"), or mock control. **(B)** AA1 has no effect on *Brachypodium* PP2C44 ABA-induced phosphatase activity inhibition. The phosphatase activity (% control) of recombinant GST-BdPP2C44 was measured in the presence of BdPYL recombinant receptors (6XHIS-BdPYL1, 6XHIS-BdPYL2, and GST-BdPYL3) and 5 μM AA1, 0.25 μM ABA or combination of the two and is presented relative to a no-agonist/antagonist mock control. GST-BdPP2C44 was measured using p-nitrophenyl phosphate(pNPP) substrate over 10 minutes with three technical replicates. Error bars represent ± 1 SE.

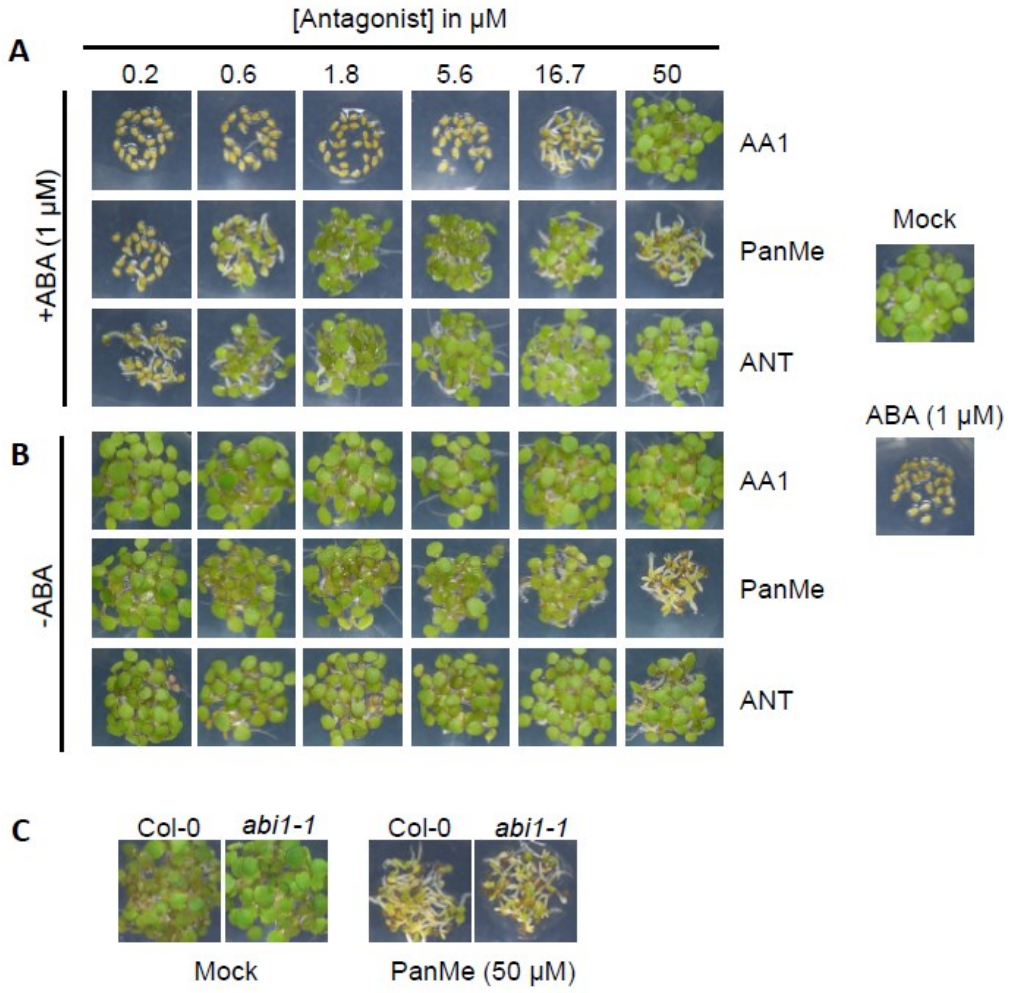

Fig. S7. ANT reverses the inhibitory effect of ABA on Arabidopsis seedling establishment. Dose-dependent effects of AA1, PanMe, and ANT on Columbia seedling establishment in the presence **(A)** or absence **(B)** of ABA (1 µM). **(C)** PanMe inhibits seedling establishment at high concentrations and its inhibitory effects are independent of ABA signaling. Seeds were sown on 1/2× MS agar plates containing chemicals, stratified at 4 °C for 4 days, and then transferred to a growth chamber at 22 °C under 16 hour days. Photographs were taken after 4 days. The high-concentration growth inhibitory effects of PanMe are evident in both *Col-0* and *abi1-1,* suggesting that PanMe has phytotoxicity unrelated to ABA signaling.

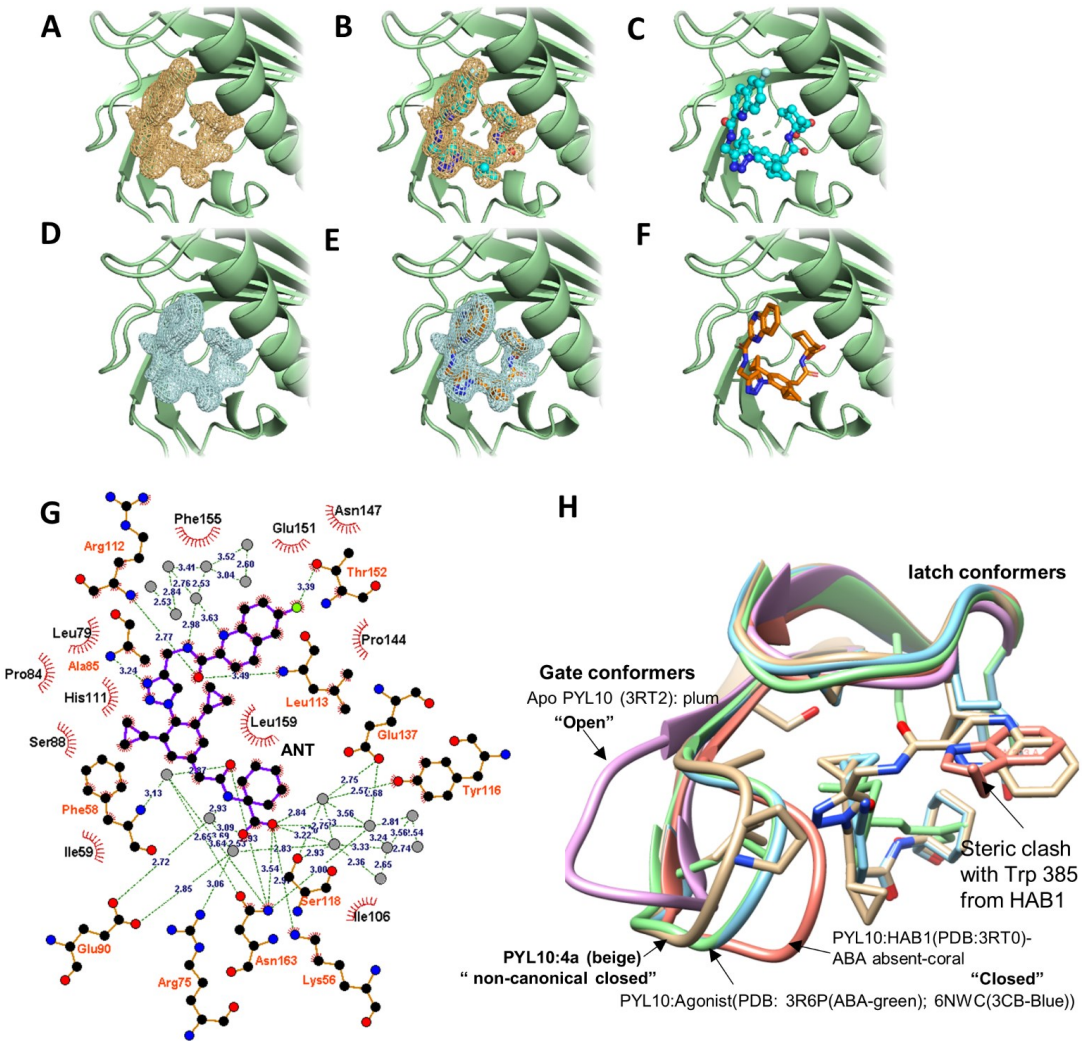

Fig. S8. Unbiased electron density in the PYL10 binding pocket. Omit maps contoured at 2 sigma show clear ligand density present in PYL10's ligand-binding pocket after several rounds of refining the **(A)** PYL10$^{24\text{-}183}$:ANT and **(D)** PYL10$^{24\text{-}183}$:**4a** structural models in the absence of ligand. The envelope of unbiased electron density allowed the unambiguous placement of **(B)** ANT and **(E) 4a** in the PYL10$^{24\text{-}183}$binding pocket. Correct ligand placement is supported by real-space correlation coefficients of 0.97 and 0.97 calculated between the unbiased density and the modeled ligand for ANT and 4a, respectively. Placement of **(C)** ANT and **(F) 4a** in the PYL10$^{24\text{-}183}$binding pocket. **(G)** Ligplot (48) of ANT interactions with PYL10 in the binary complex. Grey circles represent water molecules, values indicate H-bond distances **(H)** Conformations of the gate & latch loops in PYL10 in complex in presence/absence of different ligands i.e. ABA (green), 3CB (blue) (21) with HAB1 (coral)-closed conformation (49), ANT/**4a** (beige)-semi-open conformation and Apo PYL10 (plum)-open conformation. ANT's (quinoline ring)/**4a** (quinoxaline ring) is placed to block interaction with conserved Trp from PP2Cs by creating a steric clash. RMSD between open conformer/apo-PYL10 (PDB:3RT2) and ABA bound closed conformer (PDB:3R6P), between open conformer/apo-PYL10 (PDB:3RT2) and ANT bound non-canonical closed conformer and between ABA bound closed conformer (PDB:3R6P) and ANT bound non-canonical closed conformer are 1.4 Å, 1.2 Å and 0.6 Å respectively.

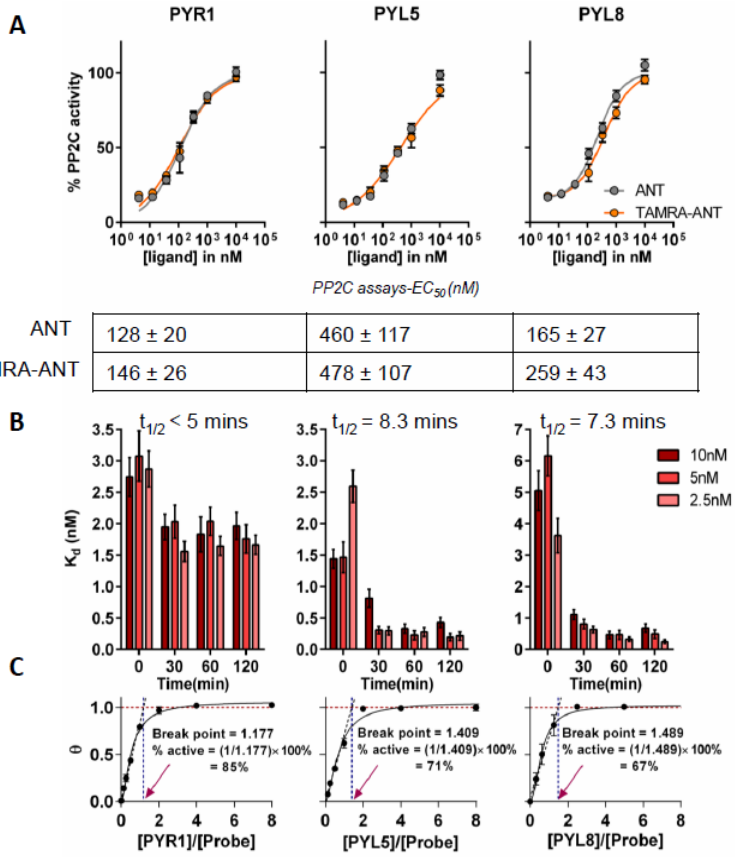

PP2C assays-EC_{50}(nM)

ANT	128 ± 20	460 ± 117	165 ± 27
TAMRA-ANT	146 ± 26	478 ± 107	259 ± 43

Fig. S9. TAMRA-ANT binds to ABA receptors with high affinity. (A) TAMRA-ANT and ANT are equipotent in antagonizing ABA receptors. Graphs show chemical dependent recovery of Arabidopsis HAB1 (25 nM) for the receptors shown (25 nM), at 5000 nM ABA. The EC_{50} values in the table below and were estimated by non-linear fits to the dose response data in the drc R package; SDs reported by drc are shown (n= 3). **(B)** Time-dependent binding of TAMRA-ANT to ABA receptors. TAMRA-ANT (10, 5 and 2.5 nM) was incubated with different concentrations of ABA receptors (shown) and incubated for different times in the FP assay buffer at 25 °C. FP data were fit to the quadratic Morrison equation of ligand binding and dissociation constant (***k_d*** shown in nM) plotted versus time for different probe concentrations. Inset values indicate half-lives of binding of probe to ABA receptors, as deduced by fitting ***k_d*** vs time for reactions with 5 nM TAMRA-ANT to a one-phase exponential decay in Graph Pad Prism; (n = 4, s.e.m shown). **(C)** Inference of the percent active receptors in receptor samples. Active receptor concentration was determined by extrapolation of the x-intercept to determine the receptor:probe ratio at which 100% occupancy occurs (as estimated by breakpoint method (*43*)). If a given receptor sample contained fully active receptors, 100% occupancy would occur at 1:1 ratio; deviations from this ratio are used to correct for the presence of inactive sub-populations of receptors in test samples. 50 nM of probe incubated with different amounts of ABA receptors in FP assay buffer at 25 °C for 90 mins. Fraction bound (θ) plotted against the ratio of receptor/probe (n = 12). Error bars represent SD. The reciprocal of the breakpoint shown indicates the fraction of active protein.

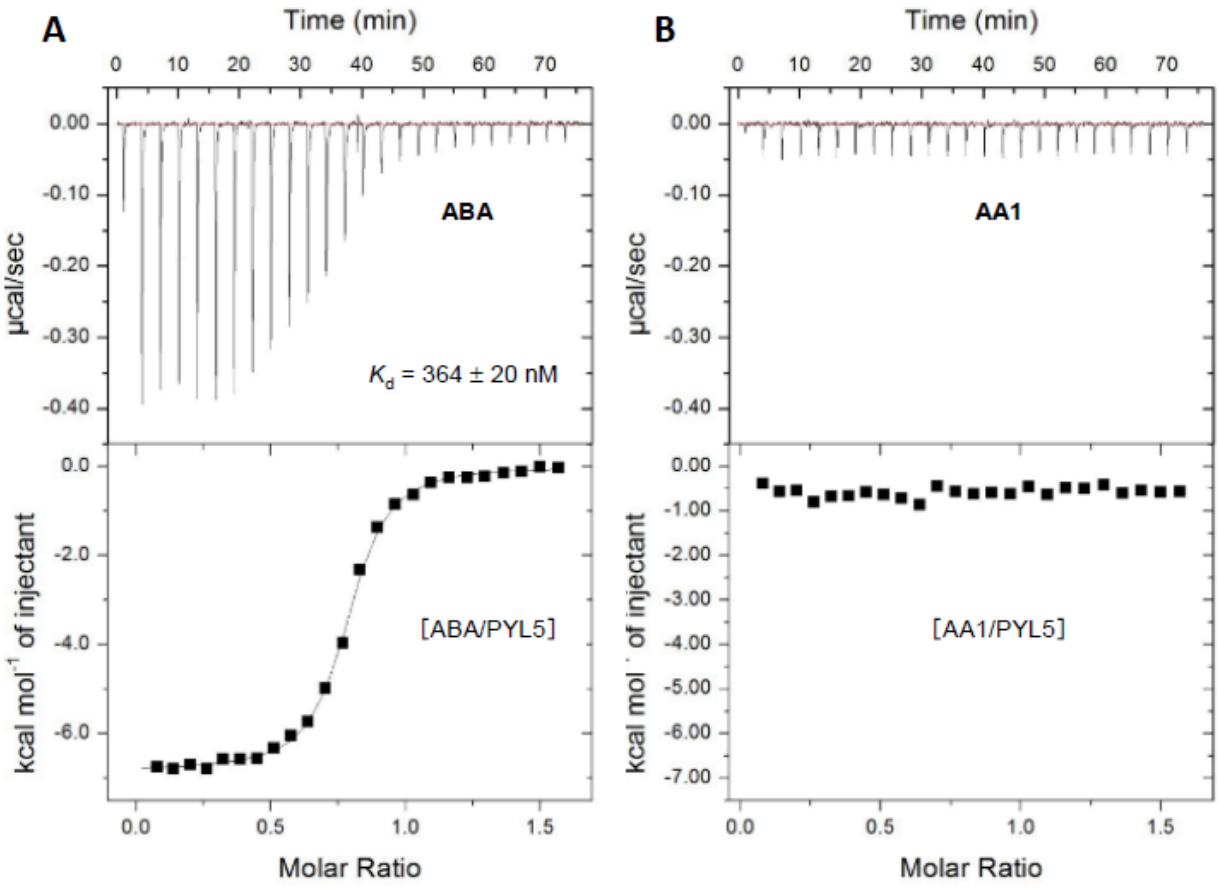

Fig. S10. Isothermal titration calorimetry profiles and thermodynamic data for ABA/AA1-PYL5 binding experiments (**A and B**). (Top two panels) Raw data for 25 sequential injections of 1.25 µL of 0.5 mM ABA (left top) or AA1 (right top) stock solution into cells containing 50 µM 6×His-tagged PYL5 in 0.1 M phosphate buffer, pH 8.0. Injections were performed over a period of 5 sec. with 3 min intervals between injections. (Bottom two panels) Plot of heat evolved (kcal) per mole of ABA (left bottom) or AA1 (right bottom) dilution, against the molar ratio of ABA or AA1 to PYL5. Data were fitted using the software's 'one set of sites' and the solid line represents the best fit.

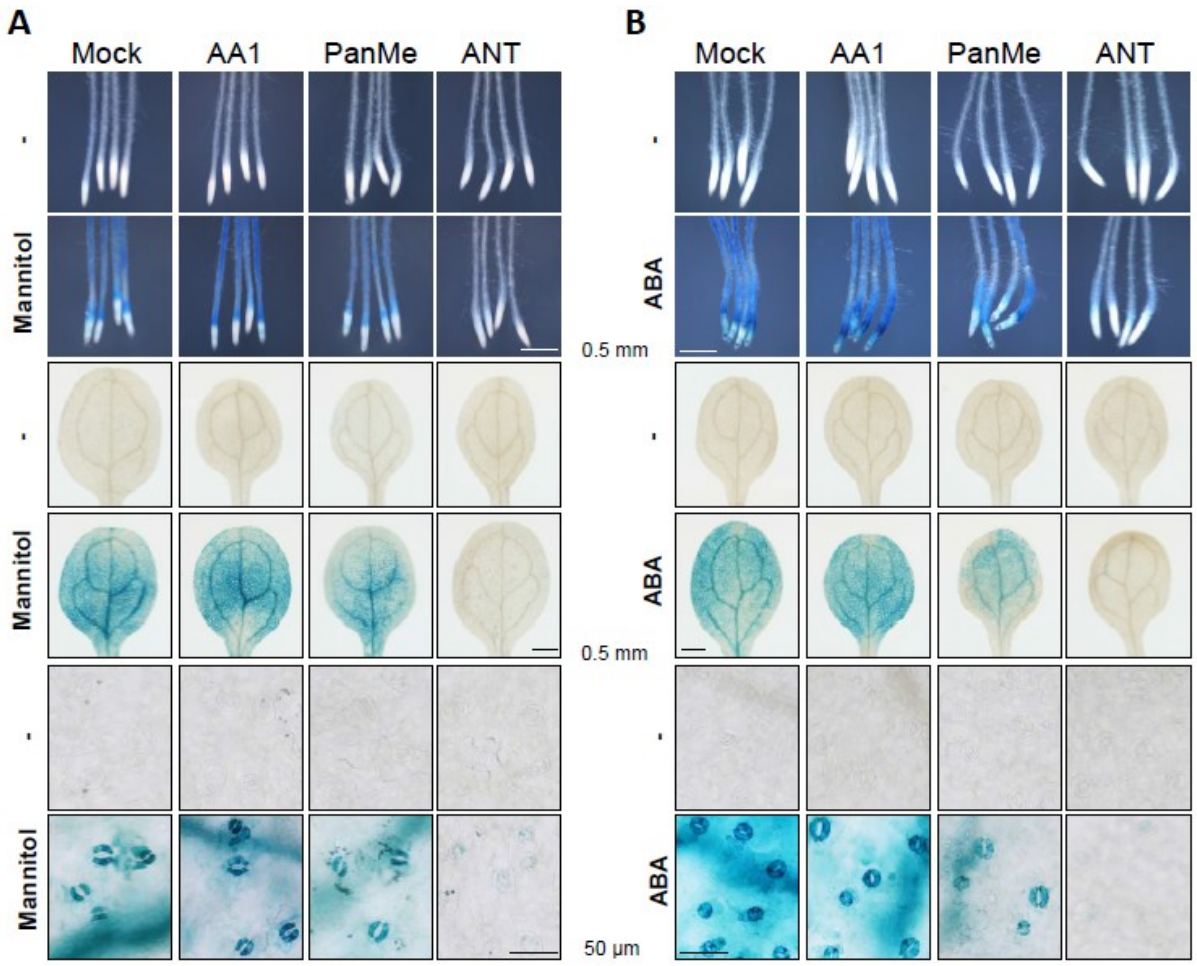

Fig. S11. Spatial expression pattern of *MAPKKK18* after treatment with osmotic stress or exogenous ABA in presence of different antagonists. (A) Five-day-old seedlings of *MAPKKK18p::GUS* transgenic *Arabidopsis* were incubated in 400 mM mannitol solution containing ABA antagonists (2.5 µM) for 6 h at 22°C in light conditions. Scale bars = 0.5 mm (root and leaf) and 50 µm (epidermis). **(B)** Five-day-old seedlings of promoter-*MAPKKK18::GUS* transgenic *Arabidopsis* were incubated in a chemical solution (each 2.5 µM & equimolar concentration of ABA) for 6 h at 22°C in light conditions. Scale bars = 0.5 mm (root and leaf) and 50 µm (epidermis). The leaf data shown in the middle panels are identical to that shown in Fig. 5C.

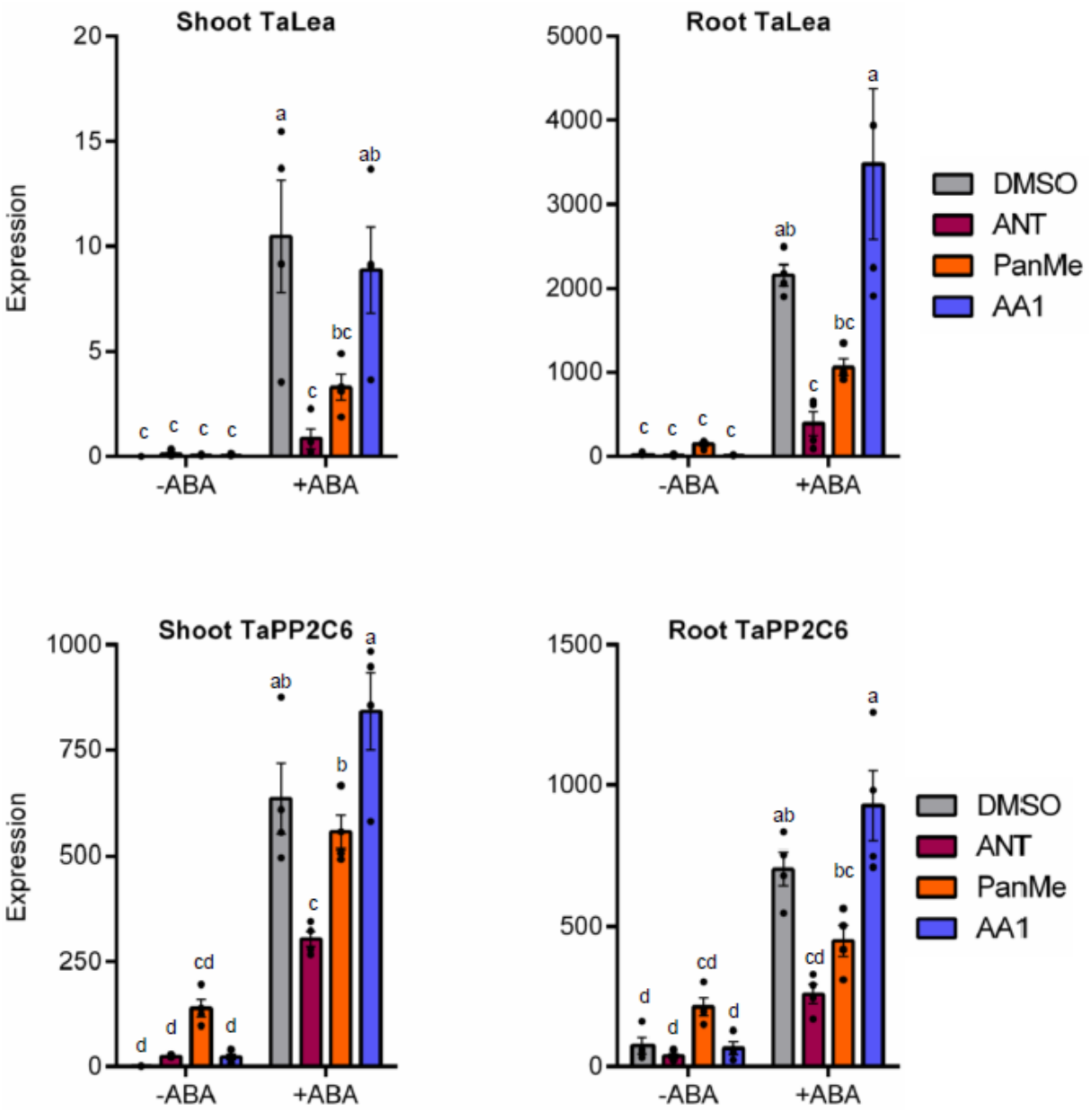

Fig. S12. ANT reduces ABA mediated transcriptional responses in wheat. Comparison of transcript levels for *TaLea* **(A)** and TaPP2C6 **(B)** after treatment with individual antagonists (5 µM) or in co-application with ABA (5 µM) in 7-day-old wheat seedlings (samples prepared 12 hours post-application). Letters indicate different significance levels as determined by using the Tukey's hsd test (n = 4 biological replicates); error bars show s. e. m. Black circles indicate individual data points.

A

ET_{50} *(hours)*

	Barley	
	Morex	Palmella
Mock	32 ± 1.6	>108
ANT	34 ± 4.9	78 ± 0.7

	Tomato
	UC82
Mock	135 ± 3.7
ANT	106 ± 4.0

	Arabidopsis	
	22 ºC	37 ºC
Mock	33 ± 0.4	41 ± 0.3
Fluridone	32 ± 0.3	29 ± 0.7
ANT	30 ± 0.1	32 ± 0.4

B

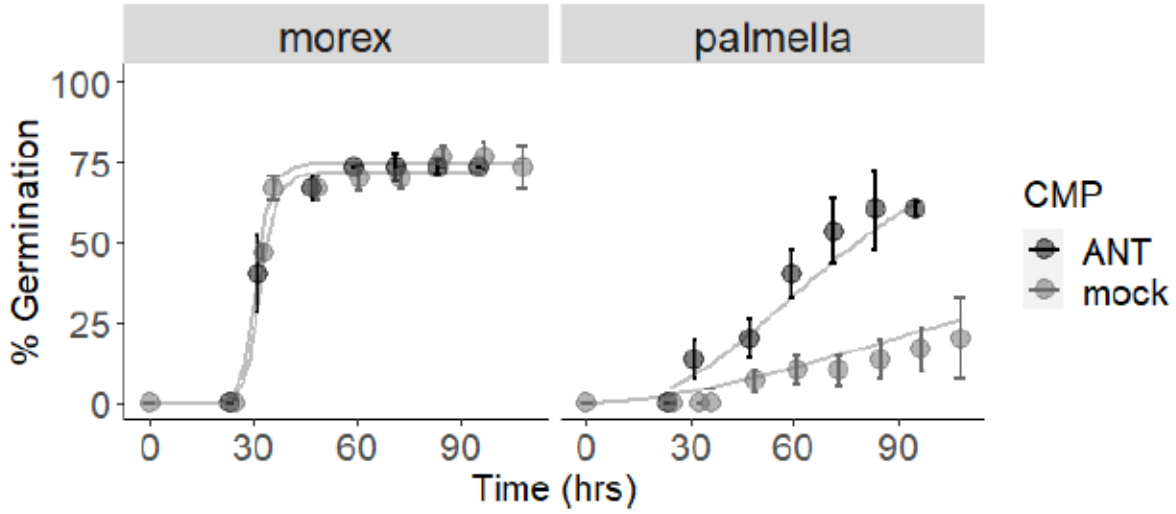

Fig. S13. ANT accelerates germination in multiple species. (A) Seed germination was monitored over time for seeds plated on ½ MS, 0.7% agar plates containing DMSO (mock-treated) or 100 µM ANT (barley), 25 µM ANT(tomato), and 30 µM ANT (Arabidopsis) Time-response data were fit to a log-logistic model using the drc package to infer ET_{50} values(time required to reach 50% germination). Time response data used for inferring the ET_{50} values shown are shown in Fig 5E & F.(B) Effects of ANT on barley are landrace dependent. Palmella data shown here is identical to that shown in Fig. 5E.

Supplementary Table 1. Data collection and refinement statistics

	PYL10 (25-183):**4a**	PYL10 (25-183):**4o/ANT**
Data collection		
Space group	C 1 2 1	C 1 2 1
Cell dimensions		
a, b, c (Å)	59.55, 64.39, 44.60	59.75, 64.39, 44.57
α, β, γ (°)	90, 108.8, 90	90, 109.1, 90
Resolution (Å)	50-1.77 (1.83-1.77)	50-1.80 (1.86-1.80)
Total Reflections	105,525 (7,916)	104,858 (6,927)
Unique Reflections	15,495 (1,467)	14,845 (1,429)
R_{merge}	0.046 (0.383)	0.051 (0.373)
R_{meas}	0.049 (0.423)	0.055 (0.416)
R_{pim}	0.019 (0.175)	0.020 (0.181)
CC1/2	0.999 (0.916)	1.000 (0.912)
CC*	1.000 (0.978)	1.000 (0.977)
I / σI	22.7 (2.8)	25.3 (2.6)
Completeness (%)	97.0 (84.8)	97.0 (86.8)
Redundancy	6.8 (5.4)	7.1 (4.8)
Refinement		
Resolution (Å)	42.43-1.77 (1.83-1.77)	42.46-1.80 (1.86-1.80)
No. reflections	15,099 (1,310)	14,462 (1,290)
R_{cryst} / R_{free}	0.159/0.204	0.161/0.206
No. atoms	1443	1462
Protein	1224	1202
Ligand/ion	50	58
Water	169	202
B-factors		
Protein	31.0	20.2
Ligand/ion	32.6	23.1
Water	40.3	28.0
R.m.s. deviations		
Bond lengths (Å)	0.005	0.006
Bond angles (°)	0.750	0.820
Ramachandran Stats		
Favored	98.0%	98.0%
Allowed	2.0%	2.0%

Analytical data.

Methyl (4-amino-3,5-dibromophenyl)acetate (1a)
^{1}H-NMR (700 MHz; DMSO-d_6): δ 7.35 (s, 2H), 5.27 (s, 2H), 3.61 (s, 3H), 3.56 (s, 2H), 2.51 (t, *J* = 1.8 Hz, 3H). ^{13}C NMR (176 MHz; DMSO): δ 172.1, 142.1, 133.2, 125.1, 107.8, 52.2, 38.3.

Methyl (4-amino-3,5-dicyclopropylphenyl)acetate (1b)
^{1}H-NMR (700 MHz; DMSO-d_6): δ 6.62 (s, 2H), 4.76 (s, 2H), 3.57 (s, 3H), 3.41 (s, 2H), 1.68-1.66 (m, 2H), 0.88-0.85 (m, 4H), 0.47-0.44 (m, 4H). ^{13}C NMR (176 MHz; DMSO): δ 172.8, 145.8, 126.1, 125.4, 121.3, 115.0, 51.9, 11.8, 6.0.

(4-Amino-3,5-dicyclopropylphenyl)acetic acid (1c)
^{1}H-NMR (700 MHz; DMSO-d_6): δ 6.62 (s, 2H), 3.30 (s, 3H), 1.67 (tt, *J* = 8.3, 5.4 Hz, 2H), 0.88-0.85 (m, 4H), 0.46-0.44 (m, 4H). ^{13}C NMR (176 MHz; DMSO): δ 173.9, 145.6, 126.2, 125.3, 122.0, 11.8, 6.0.

(4-Azido-3,5-dicyclopropylphenyl)acetic acid (1d)
^{1}H-NMR (700 MHz; DMSO-d_6): δ 6.75 (s, 2H), 3.46 (s, 2H), 2.12-2.09 (m, 2H), 0.99-0.96 (m, 4H), 0.68-0.66 (m, 4H). ^{13}C NMR (176 MHz; DMSO): δ 173.0, 136.8, 136.6, 133.2, 125.4, 12.1, 8.4.

Methyl 1-{[(4-azido-3,5-dicyclopropylphenyl)methyl]carbonylamino}cyclohexanecarboxylate (2a)
^{1}H-NMR (700 MHz; DMSO-d_6): δ 8.15 (s, 1H), 6.76 (s, 2H), 3.52 (s, 3H), 3.36 (s, 2H), 2.11 (tt, *J* = 8.4, 5.3 Hz, 2H), 1.90 (d, *J* = 13.4 Hz, 2H), 1.63 (td, *J* = 12.6, 3.3 Hz, 2H), 1.50 (ddt, *J* = 21.8, 13.5, 4.3 Hz, 3H), 1.44-1.39 (m, 2H), 1.25-1.18 (m, 1H), 1.00-0.97 (m, 4H), 0.67-0.65 (m, 4H). ^{13}C NMR (176 MHz; DMSO): δ 174.8, 170.2, 136.54, 136.50, 134.7, 124.7, 58.4, 52.1, 42.0, 32.2, 25.3, 21.4, 12.0, 8.4.

1-{[(4-Azido-3,5-dicyclopropylphenyl)methyl]carbonylamino}cyclohexanecarboxylic acid.(2b)
^{1}H-NMR (700 MHz; DMSO-d_6): δ 8.00 (s, 1H), 6.77 (s, 2H), 2.10 (tt, *J* = 8.8, 4.7 Hz, 2H), 1.94 (d, *J* = 13.3 Hz, 2H), 1.61 (td, *J* = 12.7, 2.8 Hz, 2H), 1.53-1.47 (m, 3H), 1.40 (q, *J* = 12.4 Hz, 2H), 1.21 (dt, *J* = 18.9, 8.9 Hz, 1H), 0.99-0.96 (m, 4H), 0.66 (q, *J* = 5.2 Hz, 4H). ^{13}C NMR (176 MHz; DMSO): δ 176.0, 170.0, 136.52, 136.42, 134.9, 124.7, 58.2, 42.2, 32.1, 25.4, 21.5, 12.0, 8.4.

***N*-2-Propynyl-2-quinoxalinecarboxamide (3a)** ^{1}H-NMR (700 MHz; DMSO-d_6): δ 9.48-9.45 (m, 2H), 8.22-8.20 (m, 2H), 8.01 (ddt, *J* = 5.9, 4.0, 1.9 Hz, 2H), 4.15 (dd, *J* = 5.9, 2.5 Hz, 2H), 3.15 (t, *J* = 2.5 Hz, 1H). ^{13}C NMR (176 MHz; DMSO): δ 163.5, 144.5, 144.1, 143.5, 140.3, 132.5, 131.8, 129.9, 129.6, 81.4, 73.4, 28.9.

***N*-2-Propynyl-4-bromo-2-furamide (3b)** ^{1}H-NMR (700 MHz; DMSO-d_6): δ 8.70 (t, *J* = 5.4 Hz, 1H), 8.27 (s, 1H), 6.94 (s, 1H), 4.01 (dd, *J* = 5.6, 2.5 Hz, 2H), 3.15 (t, *J* = 2.5 Hz, 1H). ^{13}C NMR (176 MHz; DMSO): δ 160.5, 147.8, 125.1, 123.3, 111.0, 81.4, 73.6, 28.4.

***N*-2-Propynyl-6-methyl-2-pyridinecarboxamide (3c)** ^{1}H-NMR (700 MHz; DMSO-d_6): δ 8.96 (t, *J* = 5.7 Hz, 1H), 7.86 (dt, *J* = 20.0, 9.2 Hz, 2H), 7.47 (d, *J* = 7.6 Hz, 1H), 4.08 (dd, *J* = 6.1, 2.3 Hz, 2H), 3.10-3.09 (m, 1H), 2.56 (s, 3H). ^{13}C NMR (176 MHz; DMSO): δ 164.2, 157.7, 149.4, 138.3, 126.6, 119.5, 81.7, 73.1, 28.7, 24.3.

***N*-2-Propynyl-2-quinolinecarboxamide (3d)** ^{1}H-NMR (700 MHz; DMSO-d_6): δ 9.29 (t, *J* = 5.9 Hz, 1H), 8.58 (d, *J* = 8.5 Hz, 1H), 8.16 (dd, *J* = 11.0, 8.6 Hz, 2H), 8.09 (d, *J* = 8.2 Hz, 1H), 7.89 (dd, *J* = 8.2, 7.1 Hz, 1H), 7.73 (t, *J* = 7.5 Hz, 1H), 4.15 (dd, *J* = 6.0, 2.5 Hz, 2H), 3.14 (t, *J* = 2.4 Hz, 1H). ^{13}C NMR (176 MHz; DMSO): δ 164.4, 150.2, 146.5, 138.4, 131.0, 129.6, 129.3, 128.64, 128.57, 119.1, 81.7, 73.2, 28.9.

***N*-2-Propynyl-2-naphthamide (3e)** ^{1}H-NMR (700 MHz; DMSO-d_6): δ 9.10 (t, *J* = 5.4 Hz, 1H), 8.48 (s, 1H), 8.04-7.94 (m, 4H), 7.64-7.59 (m, 2H), 4.13 (dd, *J* = 5.5, 2.5 Hz, 2H), 3.15 (t, *J* = 2.5 Hz, 1H). ^{13}C NMR (176 MHz; DMSO): δ 166.4, 134.7, 132.6, 131.6, 129.3, 128.4, 128.16, 128.14, 128.07, 127.2, 124.5, 81.8, 73.4, 29.1.

***N*-2-Propynyl-2,2-difluoro-2*H*-1,3-benzodioxole-4-carboxamide (3f)** ^{1}H-NMR (700 MHz; DMSO-d_6): δ 8.87 (t, *J* = 5.3 Hz, 1H), 7.57 (dd, *J* = 8.0, 1.0 Hz, 1H), 7.51 (dd, *J* = 8.1, 0.9 Hz, 1H), 7.30 (t, *J* = 8.1 Hz, 1H), 4.07 (dd, *J* = 5.6, 2.5 Hz, 2H), 3.16 (t, *J* = 2.5 Hz, 1H). ^{13}C NMR (176 MHz; DMSO): δ 162.2, 143.7, 141.1, 133.1, 131.6, 130.2, 124.8, 123.9, 118.7, 113.1, 81.2, 73.6, 29.0.

***N*-2-Propynyl-5-bromo-2-furamide (3g)** ^{1}H-NMR (700 MHz; DMSO-d_6): δ 8.88 (t, *J* = 5.6 Hz, 1H), 7.18 (d, *J* = 3.6 Hz, 1H), 6.76 (d, *J* = 3.6 Hz, 1H), 3.99 (dd, *J* = 5.8, 2.5 Hz, 2H), 3.12 (t, *J* = 2.5 Hz, 1H). ^{13}C NMR (176 MHz; DMSO): δ 156.8, 149.7, 125.2, 116.7, 114.5, 81.4, 73.4, 28.3.

***N*-2-Propynyl-5-bromo-3-thenamide (3h)** ^{1}H-NMR (700 MHz; DMSO-d_6): δ 8.80 (t, *J* = 4.7 Hz, 1H), 8.15 (s, 1H), 7.59 (s, 1H), 4.02 (dd, *J* = 5.4, 2.2 Hz, 2H), 3.13 (s, 1H). ^{13}C NMR (176 MHz; DMSO): δ 160.9, 137.8, 131.9, 129.8, 112.5, 81.5, 73.5, 39.88, 39.76, 39.65, 28.7.

***N*-2-Propynyl-5-chloro-2-thenamide (3i)** ^{1}H-NMR (700 MHz; DMSO-d_6): δ 9.05 (t, *J* = 5.4 Hz, 1H), 7.66 (d, *J* = 4.1 Hz, 1H), 7.20 (d, *J* = 4.1 Hz, 1H), 4.03 (dd, *J* = 5.6, 2.5 Hz, 2H), 3.17 (t, *J* = 2.5 Hz, 1H). ^{13}C NMR (176 MHz; DMSO): δ 160.3, 138.8, 133.7, 128.83, 128.64, 81.2, 73.8, 28.8.

***N*-2-Propynyl-3-chloro-2-thenamide (3j)** ^{1}H-NMR (700 MHz; DMSO-d_6): δ 8.51 (t, *J* = 5.1 Hz, 1H), 7.86 (d, *J* = 5.3 Hz, 1H), 7.16 (d, *J* = 5.3 Hz, 1H), 4.03 (dd, *J* = 5.7, 2.5 Hz, 2H), 3.14 (t, *J* = 2.5 Hz, 1H). ^{13}C NMR (176 MHz; DMSO): δ 160.1, 131.5, 130.3, 129.7, 124.6, 81.3, 73.5, 29.2.

***N*-2-Propynyl-5-methyl-2-furamide (3k)** ^{1}H-NMR (700 MHz; DMSO-d_6): δ 8.62 (t, *J* = 5.5 Hz, 1H), 7.03 (d, *J* = 3.4 Hz, 1H), 6.25-6.24 (m, 1H), 3.98 (dd, *J* = 5.8, 2.5 Hz, 2H), 3.09 (t, *J* = 2.5 Hz, 1H), 2.33 (s, 3H). ^{13}C NMR (176 MHz; DMSO): δ 157.9, 155.0, 146.4, 115.3, 108.6, 81.7, 73.1, 28.2, 13.9.

***N*-2-Propynyl-2-bromo-1,3-thiazole-5-carboxamide (3l)** ^{1}H-NMR (700 MHz; DMSO-d_6): δ 9.25 (t, *J* = 5.3 Hz, 1H), 8.24 (d, *J* = 7.4 Hz, 1H), 4.05 (dd, *J* = 5.5, 2.5 Hz, 2H), 3.20 (t, *J* = 2.5 Hz, 1H). ^{13}C NMR (176 MHz; DMSO): δ 158.9, 143.8, 140.4, 139.4, 80.8, 74.1, 28.9.

***N*-2-Propynyl-6-bromo-2-pyridinecarboxamide (3m)** ^{1}H-NMR (700 MHz; DMSO-d_6): δ 9.06 (t, *J* = 5.9 Hz, 1H), 8.05 (dd, *J* = 7.6, 0.9 Hz, 1H), 7.95 (t, *J* = 7.7 Hz, 1H), 7.87 (dd,

J = 8.0, 0.9 Hz, 1H), 4.06 (dd, *J* = 5.9, 2.5 Hz, 2H), 3.10 (t, *J* = 2.5 Hz, 1H). ^{13}C NMR (176 MHz; DMSO): δ 162.9, 151.4, 141.5, 140.7, 131.6, 122.1, 81.5, 73.1, 29.0.

***N*-2-Propynyl-6-fluoro-2-quinolinecarboxamide (3n)** ^{1}H-NMR (700 MHz; DMSO-d_6): δ 9.29 (t, *J* = 5.9 Hz, 1H), 8.57 (d, *J* = 8.5 Hz, 1H), 8.21-8.18 (m, 2H), 7.92 (dd, *J* = 9.3, 2.9 Hz, 1H), 7.81 (td, *J* = 8.9, 2.9 Hz, 1H), 4.15 (dd, *J* = 6.0, 2.3 Hz, 2H), 3.13 (t, *J* = 2.4 Hz, 1H). ^{13}C NMR (176 MHz; DMSO): δ 164.2, 161.7, 160.3, 149.90, 149.89, 143.7, 138.00, 137.97, 132.63, 132.58, 130.26, 130.20, 121.41, 121.26, 119.9, 111.76, 111.63, 81.6, 73.3, 28.9.

***N*-2-Propynyl-8-fluoro-2-quinolinecarboxamide (3o)** ^{1}H-NMR (700 MHz; DMSO-d_6): δ 9.17 (t, *J* = 5.9 Hz, 1H), 8.66 (d, *J* = 8.5 Hz, 1H), 8.24 (d, *J* = 8.5 Hz, 1H), 7.94-7.93 (m, 1H), 7.73-7.72 (m, 2H), 4.16 (dd, *J* = 6.0, 2.4 Hz, 2H), 3.14 (t, *J* = 2.5 Hz, 1H). ^{13}C NMR (176 MHz; DMSO): δ 160.07, 158.43, 150.49, 138.53, 138.52, 136.62, 136.55, 130.94, 128.87, 128.82, 128.32, 124.58, 124.56, 120.27, 115.17, 115.07, 81.63, 73.26, 29.07.

***N*-2-Propynyl-7-bromo-2-naphthamide (3p)** ^{1}H-NMR (700 MHz; DMSO-d_6): δ 9.28 (t, *J* = 5.9 Hz, 1H), 8.61 (d, *J* = 8.4 Hz, 1H), 8.30 (d, *J* = 1.8 Hz, 1H), 8.18 (d, *J* = 8.5 Hz, 1H), 8.07 (d, *J* = 8.7 Hz, 1H), 7.87 (dd, *J* = 8.7, 2.0 Hz, 1H), 4.16 (dd, *J* = 6.0, 2.5 Hz, 2H), 3.15 (t, *J* = 2.5 Hz, 1H). ^{13}C NMR (176 MHz; DMSO): δ 164.0, 151.2, 147.0, 138.7, 131.7, 131.4, 130.6, 128.1, 124.2, 119.7, 81.5, 73.4, 29.0.

1-{[(3,5-Dicyclopropyl-4-{4-[(2-quinoxalinylcarbonylamino)methyl]-1*H*-1,2,3-triazol-1-yl}phenyl)methyl]carbonylamino}cyclohexanecarboxylic acid (4a)
^{1}H-NMR (700 MHz; DMSO-d_6): δ 9.55 (t, *J* = 6.0 Hz, 1H), 9.50 (s, 1H), 8.30 (s, 1H), 8.21 (dt, *J* = 7.7, 1.9 Hz, 2H), 8.08 (s, 1H), 8.00 (dq, *J* = 6.8, 3.4 Hz, 2H), 6.80 (s, 2H), 4.77 (d, *J* = 6.0 Hz, 2H), 3.47 (s, 2H), 1.96 (d, *J* = 13.3 Hz, 2H), 1.63 (m, 2H), 1.54-1.48 (m, 3H), 1.44-1.16 (m, 5H), 0.74 (dd, *J* = 8.4, 1.9 Hz, 4H), 0.59-0.58 (m, 4H).^{13}C NMR (176 MHz; DMSO): δ 176.0, 169.8, 163.7, 144.86, 144.81, 144.2, 143.4, 140.37, 140.25, 139.5, 135.4, 132.4, 131.8, 129.9, 129.6, 126.5, 122.8, 58.3, 42.5, 40.9, 40.5, 35.3, 32.1, 25.4, 21.5, 11.1. HRMS $[M+H]^+$ calculated 594.2828, observed 594.2980

1-{[(4-{4-[(4-Bromo-2-furylamino)methyl]-1*H*-1,2,3-triazol-1-yl}-3,5-dicyclopropylphenyl)methyl]carbonylamino}cyclohexanecarboxylic acid (4b)
^{1}H-NMR (700 MHz; DMSO-d_6): δ 8.82 (t, *J* = 5.7 Hz, 1H), 8.28 (d, *J* = 0.9 Hz, 1H), 8.23 (s, 1H), 8.09 (s, 1H), 6.97 (d, *J* = 0.9 Hz, 1H), 6.80 (s, 2H), 4.58 (d, *J* = 5.7 Hz, 2H), 3.47 (s, 2H), 1.97 (d, *J* = 13.3 Hz, 2H), 1.64 (m, 2H), 1.55-1.40 (m, 5H), 1.25-1.17 (m, 1H), 1.25-1.15 (m, 3H), 0.73 (dd, *J* = 8.4, 1.7 Hz, 4H), 0.60-0.59 (m, 4H). ^{13}C NMR (176 MHz, DMSO-*d*6) δ ppm 11.06, 21.52, 25.43, 32.09, 34.67, 40.92, 42.49, 58.30, 111.19, 122.91, 123.16, 125.46, 126.39, 135.44, 139.54, 140.37, 145.01, 147.71, 160.82, 169.79, 175.99. HRMS $[M+H]^+$ calculated 612.1644, observed 612.1663.

1-{[(3,5-Dicyclopropyl-4-{4-[(6-methyl-2-pyridylcarbonylamino)methyl]-1*H*-1,2,3-triazol-1-yl}phenyl)methyl]carbonylamino}cyclohexanecarboxylic acid (4c)

^{1}H-NMR (700 MHz; DMSO-d_6): δ 12.12 (s, 1H), 9.07 (t, *J* = 5.9 Hz, 1H), 8.25 (s, 1H), 8.09 (s, 1H), 7.88 (q, *J* = 7.6 Hz, 2H), 7.47 (d, *J* = 6.9 Hz, 1H), 6.80 (s, 2H), 4.69 (d, *J* = 6.0 Hz, 2H), 3.47 (s, 2H), 1.97 (d, *J* = 13.3 Hz, 2H), 1.64 (t, *J* = 12.8 Hz, 2H), 1.55-1.41 (m, 6H), 1.23-1.15 (m, 3H), 0.73 (d, *J* = 8.5 Hz, 4H), 0.59 (d, *J* = 3.2 Hz, 4H). ^{13}C NMR (176 MHz; DMSO): δ 176.0, 169.8, 164.4, 157.6, 149.6, 145.0, 140.4, 139.5, 138.3,

136.5, 135.4, 126.6, 126.3, 124.7, 122.9, 119.5, 58.3, 42.5, 35.0, 32.1, 25.4, 24.3, 21.5, 11.1, 8.4. HRMS $[M+H]^+$ calculated 557.2876, observed 557.2985.

1-{[(3,5-Dicyclopropyl-4-{4-[(2-quinolylcarbonylamino)methyl]-1*H*-1,2,3-triazol-1-yl}phenyl)methyl]carbonylamino}cyclohexanecarboxylic acid (4d)
^{1}H-NMR (700 MHz; DMSO-d_6): δ 9.41 (t, *J* = 0.7 Hz, 1H), 8.59 (t, *J* = 0.6 Hz, 1H), 8.30 (s, 1H), 8.19-8.10 (m, 4H), 7.89 (s, 1H), 7.72 (t, *J* = 7.3 Hz, 1H), 6.80 (s, 2H), 4.78 (d, *J* = 4.8 Hz, 2H), 3.47 (s, 2H), 1.97 (d, *J* = 13.3 Hz, 2H), 1.65-1.61 (m, 3H), 1.54-1.41 (m, 5H), 1.24-1.16 (m, 3H), 0.73 (d, *J* = 8.5 Hz, 4H), 0.59 (d, *J* = 3.3 Hz, 4H). ^{13}C NMR (176 MHz; DMSO): δ 176.0, 169.8, 164.61, 164.58, 164.51, 150.48, 150.44, 146.43, 146.41, 145.1, 140.4, 139.5, 138.35, 138.33, 138.30, 135.4, 130.99, 130.96, 129.7, 128.6, 126.5, 122.9, 119.19, 119.14, 58.3, 42.5, 40.9, 40.5, 35.3, 32.1, 25.4, 21.5, 11.1. HRMS $[M+H]^+$ calculated 593.2876, observed 593.3080

1-{[(3,5-Dicyclopropyl-4-{4-[(2-naphthylamino)methyl]-1*H*-1,2,3-triazol-1-yl}phenyl)methyl]carbonylamino}cyclohexanecarboxylic acid (4e)
H-NMR (700 MHz; DMSO-d_6): δ 9.21 (t, *J* = 5.6 Hz, 1H), 8.50 (s, 1H), 8.29 (s, 1H), 8.09 (s, 1H), 8.03-7.96 (m, 4H), 7.63-7.58 (m, 2H), 6.81 (s, 2H), 4.71 (d, *J* = 5.6 Hz, 2H), 3.48 (s, 3H), 1.97 (d, *J* = 13.4 Hz, 2H), 1.64 (m, 2H), 1.55-1.41 (m, 5H), 1.23-1.17 (m, 3H), 0.73 (dd, *J* = 8.4, 1.7 Hz, 4H), 0.60-0.59 (m, 4H). ^{13}C NMR (176 MHz; DMSO): δ 176.0, 169.8, 166.8, 140.4, 139.5, 135.5, 134.6, 132.6, 132.2, 129.3, 128.3, 128.1, 127.2, 126.4, 124.7, 122.9, 58.3, 42.5, 40.9, 35.5, 32.1, 25.4, 21.5, 11.1. HRMS $[M+H]^+$ calculated 592.2923, observed 592.3123.

1-{[(3,5-Dicyclopropyl-4-{4-[(2,2-difluoro-2*H*-1,3-benzodioxol-4-ylcarbonylamino)methyl]-1*H*-1,2,3-triazol-1-yl}phenyl)methyl]carbonylamino}cyclohexanecarboxylic acid. (4f)
^{1}H-NMR (700 MHz; DMSO-d_6): δ 8.99 (t, *J* = 5.7 Hz, 1H), 8.27 (s, 1H), 8.09 (s, 1H), 7.55 (ddd, *J* = 19.1, 8.1, 1.1 Hz, 2H), 7.30 (t, *J* = 8.1 Hz, 1H), 6.82 (s, 2H), 4.65 (d, *J* = 5.7 Hz, 2H), 3.48 (s, 2H), 1.97 (d, *J* = 13.4 Hz, 2H), 1.64 (m, 2H), 1.55-1.40 (m, 5H), 1.25-1.16 (m, 3H), 0.73 (dd, *J* = 8.4, 1.8 Hz, 4H), 0.60-0.59 (m, 4H). ^{13}C NMR (176 MHz; DMSO): δ 176.0, 169.8, 162.5, 144.8, 143.6, 141.1, 140.3, 139.5, 135.5, 126.5, 125.5, 124.7, 124.0, 123.0, 119.3, 112.9, 58.3, 42.5, 40.5, 35.3, 32.1, 25.4, 21.5, 11.1. HRMS $[M+H]^+$ calculated 622.2477, observed 622.2701.

1-{[(4-{4-[(5-Bromo-2-furylamino)methyl]-1*H*-1,2,3-triazol-1-yl}-3,5-dicyclopropylphenyl)methyl]carbonylamino}cyclohexanecarboxylic acid (4g)
^{1}H-NMR (700 MHz; DMSO-d_6): δ 8.99 (t, *J* = 5.8 Hz, 1H), 8.99 (t, *J* = 5.8 Hz, 1H), 8.23 (s, 1H), 8.23 (s, 1H), 8.09 (s, 1H), 8.09 (s, 1H), 7.19 (d, *J* = 3.5 Hz, 1H), 7.19 (d, *J* = 3.5 Hz, 1H), 6.80 (s, 2H), 6.80 (s, 2H), 6.76 (d, *J* = 3.5 Hz, 1H), 6.76 (d, *J* = 3.5 Hz, 1H), 4.58 (d, *J* = 5.8 Hz, 2H), 4.58 (d, *J* = 5.8 Hz, 2H), 3.47 (s, 2H), 3.47 (s, 2H), 1.98-1.96 (m, 2H), 1.98-1.96 (m, 2H), 1.64-1.61 (m, 2H),1.55-1.40 (m, 5H), 1.25-1.13 (m, 3H), 0.73 (dd, *J* = 8.4, 1.8 Hz, 4H), 0.60 (m, 4H). ^{13}C NMR (176 MHz; DMSO): δ 176.0, 169.8, 157.1, 152.7, 150.0, 140.4, 139.5, 135.4, 126.4, 124.9, 122.9, 116.5, 114.4, 58.3, 42.5, 40.50, 40.43, 34.6, 32.1, 25.4, 21.5, 11.0. HRMS $[M+H]^+$ calculated 612.1644, observed 612.1755.

1-{[(4-{4-[(5-Bromo-3-thenylamino)methyl]-1*H*-1,2,3-triazol-1-yl}-3,5-dicyclopropylphenyl)methyl]carbonylamino}cyclohexanecarboxylic acid (4h)

^{1}H-NMR (700 MHz; DMSO-d_6): δ 12.12 (s, 1H), 8.92 (t, *J* = 5.6 Hz, 1H), 8.24 (s, 1H), 8.16 (s, 1H), 8.09 (s, 1H), 7.62 (s, 1H), 6.80 (s, 2H), 4.60 (d, *J* = 5.6 Hz, 2H), 3.47 (s, 2H), 1.97 (d, *J* = 13.3 Hz, 2H), 1.66-1.62 (m, 2H), 1.55-1.41 (m, 5H), 1.23-1.14 (m, 3H), 0.73 (d, *J* = 8.5 Hz, 4H), 0.60 (d, *J* = 4.2 Hz, 4H). ^{13}C NMR (176 MHz; DMSO): δ 176.0, 169.8, 161.2, 145.1, 140.4, 139.5, 138.2, 135.4, 131.7, 130.0, 126.4, 122.9, 112.4, 58.3, 42.5, 35.0, 32.1, 25.4, 21.5, 11.1. HRMS $[M+H]^+$ calculated 628.1416, observed 628.1469.

1-{[(4-{4-[(5-Chloro-2-thenylamino)methyl]-1*H*-1,2,3-triazol-1-yl}-3,5-dicyclopropylphenyl)methyl]carbonylamino}cyclohexanecarboxylic acid (4i)
^{1}H-NMR (700 MHz; DMSO-d_6): δ 9.17 (t, *J* = 5.7 Hz, 1H), 8.26 (s, 1H), 8.09 (s, 1H), 7.69 (d, *J* = 4.1 Hz, 1H), 7.19 (d, *J* = 4.0 Hz, 1H), 6.80 (s, 2H), 4.60 (d, *J* = 5.7 Hz, 2H), 3.47 (s, 2H), 1.97 (d, *J* = 13.2 Hz, 2H), 1.64-1.60 (m, 2H), 1.55-1.41 (m, 5H), 1.25-1.14 (m, 3H), 0.72 (dd, *J* = 8.4, 1.8 Hz, 4H), 0.60 (m, 4H). ^{13}C NMR (176 MHz; DMSO): δ 176.0, 169.8, 160.5, 144.8, 140.3, 139.52, 139.36, 135.4, 133.4, 128.68, 128.56, 126.5, 122.9, 58.3, 42.5, 35.1, 32.1, 25.4, 21.5, 11.1. HRMS $[M+H]^+$ calculated 582.1941, observed 582.2079.

1-{[(4-{4-[(3-Chloro-2-thenylamino)methyl]-1*H*-1,2,3-triazol-1-yl}-3,5-dicyclopropylphenyl)methyl]carbonylamino}cyclohexanecarboxylic acid (4j)
^{1}H-NMR (700 MHz; DMSO-d_6): δ 8.65 (t, *J* = 5.7 Hz, 1H), 8.22 (s, 1H), 8.09 (s, 1H), 7.84 (d, *J* = 5.2 Hz, 1H), 7.15 (d, *J* = 5.2 Hz, 1H), 6.82 (s, 2H), 4.63 (d, *J* = 5.7 Hz, 2H), 3.48 (s, 2H), 1.97 (d, *J* = 13.3 Hz, 2H), 1.64-1.61 (m, 2H), 1.55-1.41 (m, 5H), 1.25-1.16 (m, 3H), 0.73 (dd, *J* = 8.4, 1.8 Hz, 4H), 0.59-0.60 (m, 4H). ^{13}C NMR (176 MHz; DMSO): δ 176.0, 169.8, 160.3, 144.8, 140.3, 139.5, 135.5, 132.0, 130.0, 129.6, 126.4, 124.2, 123.0, 58.3, 42.5, 35.5, 32.1, 25.4, 21.5, 11.1. HRMS $[M+H]^+$ calculated 582.1941, observed 582.2103

1-{[(3,5-Dicyclopropyl-4-{4-[(5-methyl-2-furylamino)methyl]-1*H*-1,2,3-triazol-1-yl}phenyl)methyl]carbonylamino}cyclohexanecarboxylic acid (4k)
^{1}H-NMR (700 MHz; DMSO-d_6): δ 8.73 (t, *J* = 5.8 Hz, 1H), 8.19 (s, 1H), 8.09 (s, 1H), 7.03 (d, *J* = 3.3 Hz, 1H), 6.80 (s, 2H), 6.24 (dd, *J* = 3.3, 0.9 Hz, 1H), 4.57 (d, *J* = 5.8 Hz, 2H), 3.47 (s, 2H), 2.33 (s, 3H), 1.97 (d, *J* = 13.3 Hz, 2H), 1.64-1.61 (m, 2H), 1.55-1.41 (m, 5H), 1.25-1.13 (m, 3H), 0.73 (dd, *J* = 8.4, 1.8 Hz, 4H), 0.60 (m, 4H). ^{13}C NMR (176 MHz; DMSO): δ 181.9, 176.0, 169.8, 158.2, 154.7, 146.7, 140.4, 139.5, 135.4, 126.3, 122.8, 115.1, 108.6, 58.3, 42.5, 40.5, 34.5, 32.1, 25.4, 21.5, 13.9, 11.0. HRMS $[M+H]^+$ calculated 546.2716, observed 546.2851.

1-{[(4-{4-[(2-Bromo-1,3-thiazol-5-ylcarbonylamino)methyl]-1*H*-1,2,3-triazol-1-yl}-3,5-dicyclopropylphenyl)methyl]carbonylamino}cyclohexanecarboxylic acid (4l)

^{1}H-NMR (700 MHz; DMSO-d_6): δ 9.38 (t, *J* = 5.7 Hz, 1H), 8.29 (s, 1H), 8.27 (s, 1H), 8.09 (s, 1H), 6.81 (s, 2H), 4.62 (d, *J* = 5.7 Hz, 2H), 3.47 (s, 2H), 1.97 (d, *J* = 13.4 Hz, 2H), 1.64-1.61 (m, 2H), 1.55-1.40 (m, 5H), 1.25-1.14 (m, 3H), 0.73 (dd, *J* = 8.4, 1.7 Hz, 4H), 0.60 (m, 4H). ^{13}C NMR (176 MHz; DMSO): δ 176.0, 169.8, 159.1, 144.5, 143.7, 140.35, 140.18, 139.9, 139.5, 135.4, 126.6, 122.9, 58.3, 42.5, 40.50, 40.44, 35.1, 32.1, 25.4, 21.5, 11.1. HRMS $[M+H]^+$ calculated 629.1368, observed 629.1422.

1-{[(4-{4-[(6-Bromo-2-pyridylcarbonylamino)methyl]-1*H*-1,2,3-triazol-1-yl}-3,5-dicyclopropylphenyl)methyl]carbonylamino}cyclohexanecarboxylic acid. (4m)

^{1}H-NMR (700 MHz; DMSO-d_6): δ 9.15 (t, *J* = 6.0 Hz, 1H), 8.24 (s, 1H), 8.09-8.06 (m, 2H), 7.96 (t, *J* = 7.8 Hz, 1H), 7.87 (dd, *J* = 7.9, 0.8 Hz, 1H), 6.82 (s, 2H), 4.68 (d, *J* = 6.0 Hz, 2H), 3.47 (s, 2H), 1.97 (d, *J* = 13.3 Hz, 2H), 1.65-1.61 (m, 2H 1.55-1.40 (m, 5H), 1.25-1.14 (m, 3H), 0.73 (dd, *J* = 8.4, 1.8 Hz, 4H), 0.59-0.60 (m, 4H). ^{13}C NMR (176 MHz; DMSO): δ 176.0, 169.8, 163.0, 151.7, 144.9, 141.5, 140.7, 140.4, 139.5, 135.4, 131.4, 126.4, 122.9, 122.1, 58.3, 42.5, 35.3, 32.1, 25.4, 21.5, 11.1. HRMS $[M+H]^+$ calculated 623.1804, observed 623.1932.

1-{[(3,5-Dicyclopropyl-4-{4-[(8-fluoro-2-quinolylcarbonylamino)methyl]-1*H*-1,2,3-triazol-1-yl}phenyl)methyl]carbonylamino}cyclohexanecarboxylic acid. (4n)
^{1}H-NMR (700 MHz; DMSO-d_6): δ 9.27 (t, *J* = 5.9 Hz, 1H), 8.67 (d, *J* = 8.6 Hz, 1H), 8.30 (s, 1H), 8.26 (d, *J* = 8.5 Hz, 1H), 8.09 (s, 1H), 7.93 (t, *J* = 4.5 Hz, 1H), 7.72 (t, *J* = 6.1 Hz, 2H), 6.80 (s, 2H), 4.78 (d, *J* = 5.9 Hz, 2H), 3.47 (s, 2H), 1.96 (d, *J* = 13.2 Hz, 2H), 1.65-1.61 (m, 2H), 1.54-1.41 (m, 5H), 1.24-1.16 (m, 3H), 0.73 (dd, *J* = 8.4, 1.8 Hz, 4H), 0.60-0.59 (m, 4H). ^{13}C NMR (176 MHz; DMSO): δ 176.0, 169.8, 164.2, 158.4, 156.9, 150.7, 144.9, 140.4, 139.5, 138.5, 136.6, 135.4, 130.9, 128.78, 128.74, 126.5, 124.56, 124.54, 122.9, 120.3, 115.13, 115.02, 58.3, 42.5, 40.9, 35.3, 32.1, 25.4, 21.5, 11.1. HRMS $[M+H]^+$ calculated 611.2788, observed 611.2778.

1-{[(3,5-Dicyclopropyl-4-{4-[(6-fluoro-2-quinolylcarbonylamino)methyl]-1*H*-1,2,3-triazol-1-yl}phenyl)methyl]carbonylamino}cyclohexanecarboxylic acid. (4o/Antabactin)
^{1}H-NMR (700 MHz; DMSO-d_6): δ 9.39 (t, *J* = 5.8 Hz, 1H), 8.57 (d, *J* = 8.5 Hz, 1H), 8.29 (s, 1H), 8.20 (dd, *J* = 13.8, 6.9 Hz, 2H), 8.09 (s, 1H), 7.92 (dd, *J* = 9.2, 2.2 Hz, 1H), 7.80 (td, *J* = 8.8, 2.5 Hz, 1H), 6.80 (s, 2H), 4.76 (d, *J* = 5.9 Hz, 2H), 3.47 (s, 2H), 1.96 (d, *J* = 13.3 Hz, 2H), 1.65-1.61 (m, 2H), 1.54-1.41 (m, 5H), 1.24-1.16 (m, 3H), 0.73 (dd, *J* = 8.4, 1.8 Hz, 4H), 0.60-0.56 (m, 4H). ^{13}C NMR (176 MHz; DMSO): δ 176.0, 169.8, 164.4, 161.7, 160.3, 150.2, 145.0, 143.7, 140.4, 139.5, 137.9, 135.4, 132.63, 132.57, 126.4, 122.9, 121.36, 121.21, 119.9, 111.75, 111.63, 58.3, 42.5, 40.9, 35.3, 32.1, 25.4, 21.5, 11.1. HRMS $[M+H]^+$ calculated 611.2788, observed 611.2785

1-{[(4-{4-[(7-Bromo-2-quinolylcarbonylamino)methyl]-1*H*-1,2,3-triazol-1-yl}-3,5-dicyclopropylphenyl)methyl]carbonylamino}cyclohexanecarboxylic acid. (4p)
^{1}H-NMR (700 MHz; DMSO-d_6): δ 9.39 (s, 1H), 8.61 (d, *J* = 8.5 Hz, 1H), 8.30 (d, *J* = 7.1 Hz, 2H), 8.21 (d, *J* = 7.9 Hz, 1H), 8.09-8.06 (m, 2H), 7.86 (d, *J* = 8.7 Hz, 1H), 6.80 (s, 2H), 4.77 (d, *J* = 5.9 Hz, 2H), 3.47 (s, 2H), 1.97 (d, *J* = 13.3 Hz, 2H), 1.65-1.61 (m, 2H), 1.54-1.42 (m, 5H), 1.22-1.16 (m, 3H), 0.73 (dd, *J* = 8.4, 1.8 Hz, 4H), 0.60-0.59 (m, 4H). ^{13}C NMR (176 MHz; DMSO): δ 176.0, 169.8, 164.2, 151.4, 147.0, 144.9, 140.4, 139.5, 138.6, 135.4, 131.62, 131.47, 130.6, 128.1, 126.5, 124.2, 122.9, 119.7, 58.3, 42.5, 40.9, 35.3, 32.1, 25.4, 21.5, 11.1.

1-{[(3,5-Dicyclopropyl-4-{4-[(7-ethynyl-2-quinolylcarbonylamino)methyl]-1*H*-1,2,3-triazol-1-yl}phenyl)methyl]carbonylamino}cyclohexanecarboxylic acid. (4q)
^{1}H-NMR (700 MHz; DMSO-d_6): δ 9.40 (t, *J* = 6.0 Hz, 1H), 8.60 (d, *J* = 8.5 Hz, 1H), 8.30 (s, 1H), 8.20 (d, *J* = 8.8 Hz, 2H), 8.11 (d, *J* = 8.8 Hz, 2H), 7.74 (d, *J* = 8.4 Hz, 1H), 6.80 (s, 2H), 4.76 (d, *J* = 6.0 Hz, 2H), 4.51 (s, 1H), 3.47 (s, 2H), 1.96 (d, *J* = 13.3 Hz, 2H), 1.63 (m, 2H), 1.54-1.42 (m, 5H), 1.23-1.16 (m, 3H), 0.73 (dd, *J* = 8.4, 1.8 Hz, 4H), 0.60-0.59 (m, 4H). ^{13}C NMR (176 MHz; DMSO): δ 176.0, 169.8, 164.3, 151.4, 145.9, 144.9,

140.3, 139.5, 138.4, 135.4, 132.9, 132.5, 131.9, 130.8, 129.3, 129.2, 126.5, 124.2, 122.9, 119.9, 83.9, 83.2, 58.3, 42.5, 35.3, 32.1, 25.4, 21.5, 11.1.

1-[({4-[4-({7-[1-(3-{3',6'-Bis(dimethylamino)-3-oxospiro[isobenzofuran-1,9'-xanthen]-5-ylcarbonylamino}propyl)-1*H*-1,2,3-triazol-4-yl]-2-quinolylcarbonylamino}methyl)-1*H*-1,2,3-triazol-1-yl]-3,5-dicyclopropylphenyl}methyl)carbonylamino]cyclohexanecarboxylic acid. (4r/TAMRA-ANT)

^{1}H-NMR (700 MHz; DMSO-d_6): δ 9.40 (t, *J* = 5.2 Hz, 1H), 8.91 (d, *J* = 26.2 Hz, 2H), 8.61-8.57 (m, 2H), 8.47 (s, 1H), 8.30 (s, 1H), 8.24-8.16 (m, 4H), 8.07 (s, 1H), 7.31 (d, *J* = 7.9 Hz, 1H), 6.80 (s, 2H), 6.46 (dt, *J* = 21.1, 11.5 Hz, 6H), 4.78 (d, *J* = 5.2 Hz, 2H), 4.59 (t, *J* = 6.5 Hz, 2H), 3.47-3.44 (m, 4H), 2.94 (s, 12H), 2.26 (t, *J* = 6.5 Hz, 2H), 1.97 (d, *J* = 12.1 Hz, 2H), 1.64-1.61 (m, 3H), 1.53-1.40 (m, 5H), 1.23-1.18 (m, 3H), 0.73 (dd, *J* = 8.4, 1.8 Hz, 4H), 0.60-0.59 (m, 4H). ^{13}C NMR (176 MHz; DMSO): δ 169.7, 168.8, 165.4, 164.5, 155.3, 152.58, 152.41, 151.0, 146.9, 145.9, 144.9, 140.4, 139.6, 138.2, 136.4, 135.4, 135.0, 133.3, 129.4, 128.82, 128.79, 127.3, 126.4, 126.2, 124.66, 124.62, 123.6, 123.3, 122.9, 119.1, 109.4, 106.0, 98.4, 85.2, 48.30, 48.23, 48.15, 48.13, 42.5, 40.5, 37.4, 35.3, 32.1, 29.99, 29.94, 25.4, 21.5, 11.1. HRMS $[M+H]^+$ calculated 1129.5048, observed 1129.5059.

1-[({3,5-Dicyclopropyl-4-[4-(*p*-tolyl)-1*H*-1,2,3-triazol-1-yl]phenyl}methyl)carbonylamino]cyclohexanecarboxylic acid. (T1)

^{1}H-NMR (700 MHz; DMSO-d_6): δ 12.15 (s, 1H), 8.87 (s, 1H), 8.12 (s, 1H), 7.85 (d, *J* = 7.7 Hz, 2H), 7.30 (d, *J* = 7.8 Hz, 2H), 6.85 (s, 2H), 3.50 (s, 2H), 2.35 (s, 3H), 1.98 (d, *J* = 13.2 Hz, 2H), 1.67-1.63 (m, 2H), 1.56-1.42 (m, 5H), 1.27-1.22 (m, 3H), 0.76 (d, *J* = 8.6 Hz, 4H), 0.63 (m, 4H). ^{13}C NMR (176 MHz; DMSO): δ 176.0, 169.8, 146.8, 140.4, 139.7, 137.8, 135.4, 129.9, 128.3, 125.7, 124.5, 123.0, 58.3, 42.5, 32.1, 25.4, 21.53, 21.34, 11.1. HRMS $[M+H]^+$ calculated 500.2742, observed 500.2886.

^{1}H-NMR data for AA1 purchased from Life Chemicals and used in our experiments.

^{1}H-NMR(400 MHz; DMSO-d_6): δ 7.32-7.22 (m, 5H), 5.15 (s, 2H), 3.88 (t, J = 7.2 Hz, 2H), 3.44 (s, 2H), 2.76-2.75 (m, 4H), 2.60 (dd, J = 10.1, 5.9 Hz, 2H), 2.40-2.32 (m, 4H), 2.15 (quintet, J = 7.5 Hz, 2H).

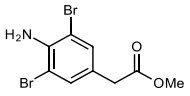
Br
H2N
Br
O
OMe

1a

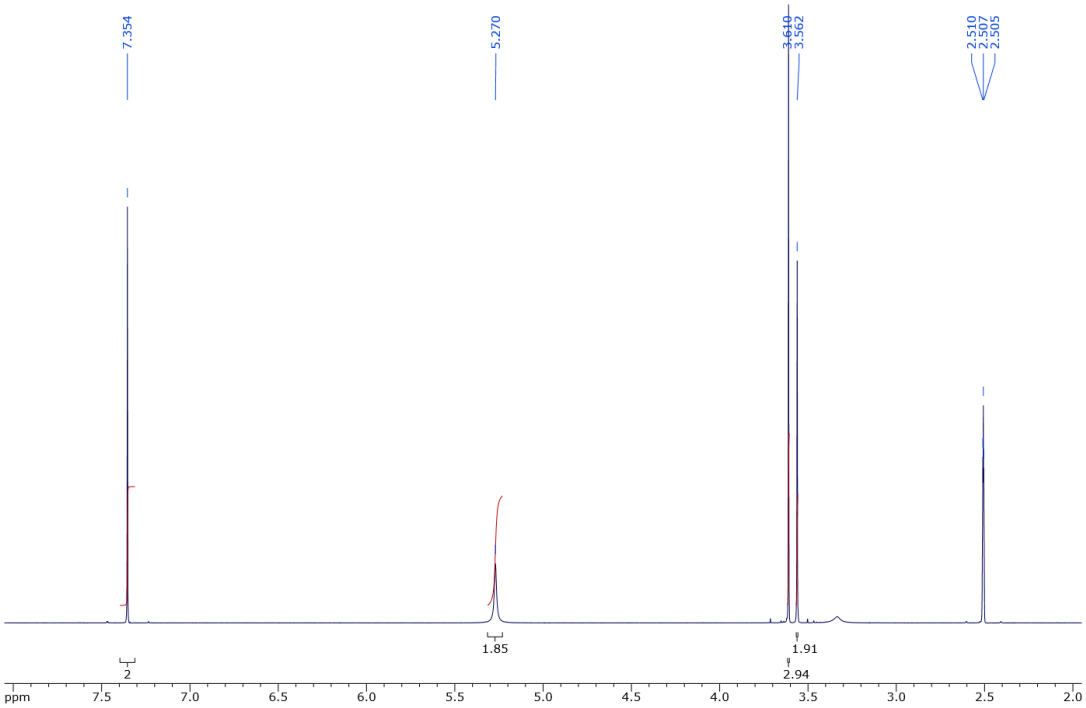
7.354
5.270
3.640
3.562
2.510
2.507
2.505
1.85
1.91
2
2.94
ppm
7.5
7.0
6.5
6.0
5.5
5.0
4.5
4.0
3.5
3.0
2.5
2.0

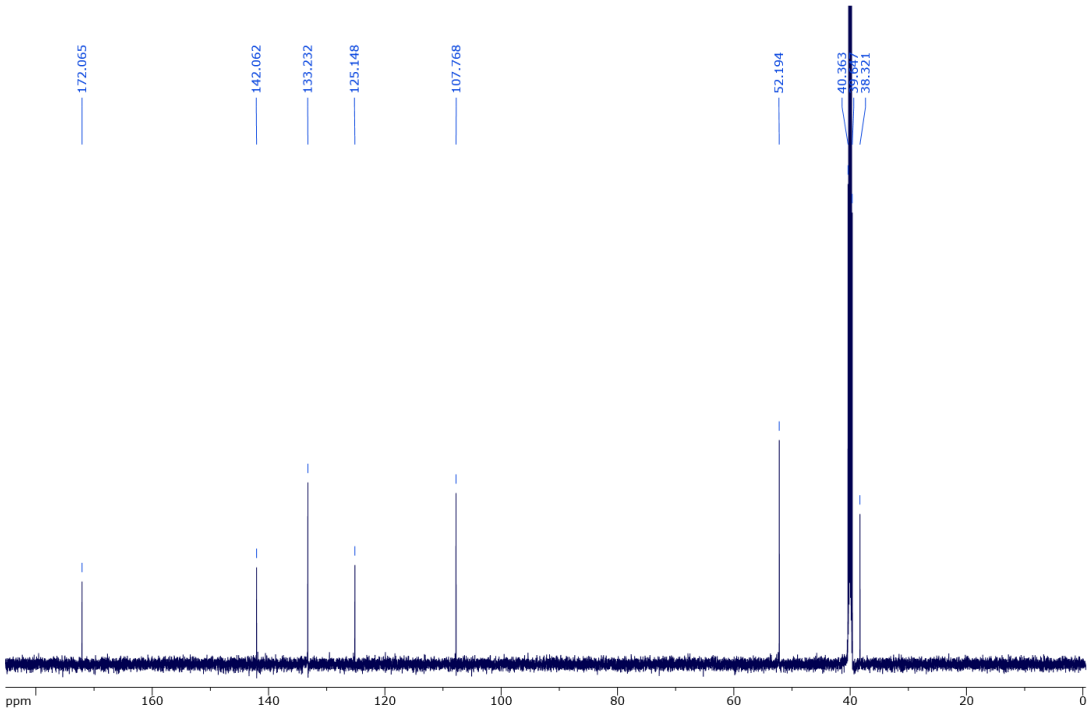
172.065
142.062
133.232
125.148
107.768
52.194
40.363
39.047
38.321
ppm
160
140
120
100
80
60
40
20
0

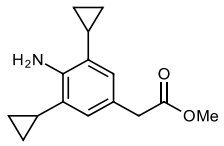
H2N
O
OMe

1b

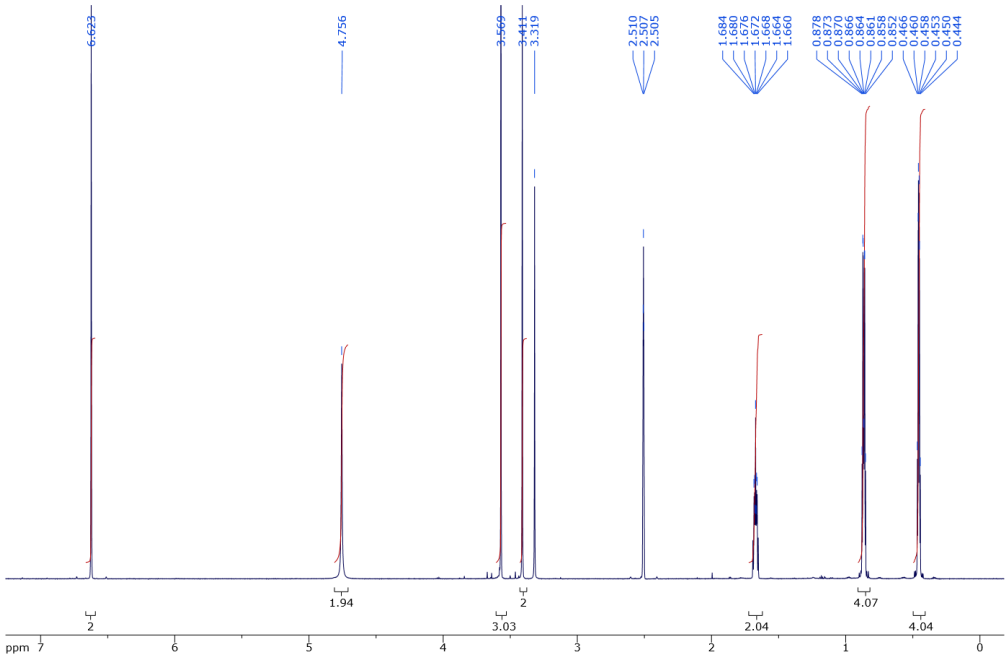
6.623
4.756
3.569
3.441
3.319
2.510
2.507
2.505
1.684
1.680
1.676
1.672
1.668
1.664
1.660
0.878
0.873
0.870
0.866
0.864
0.861
0.858
0.852
0.446
0.460
0.458
0.453
0.450
0.444
1.94
2
3.03
2
2.04
4.07
4.04
ppm

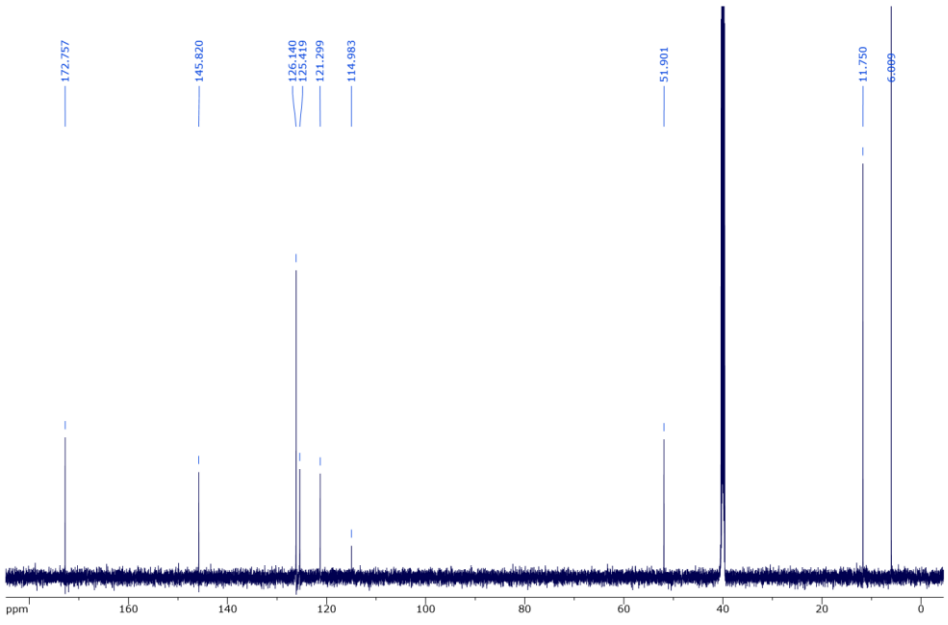
172.757
145.820
126.140
125.419
121.299
114.983
51.901
11.750
6.009
ppm

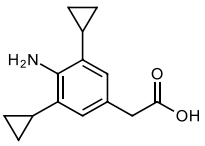
H2N
O
OH

1c

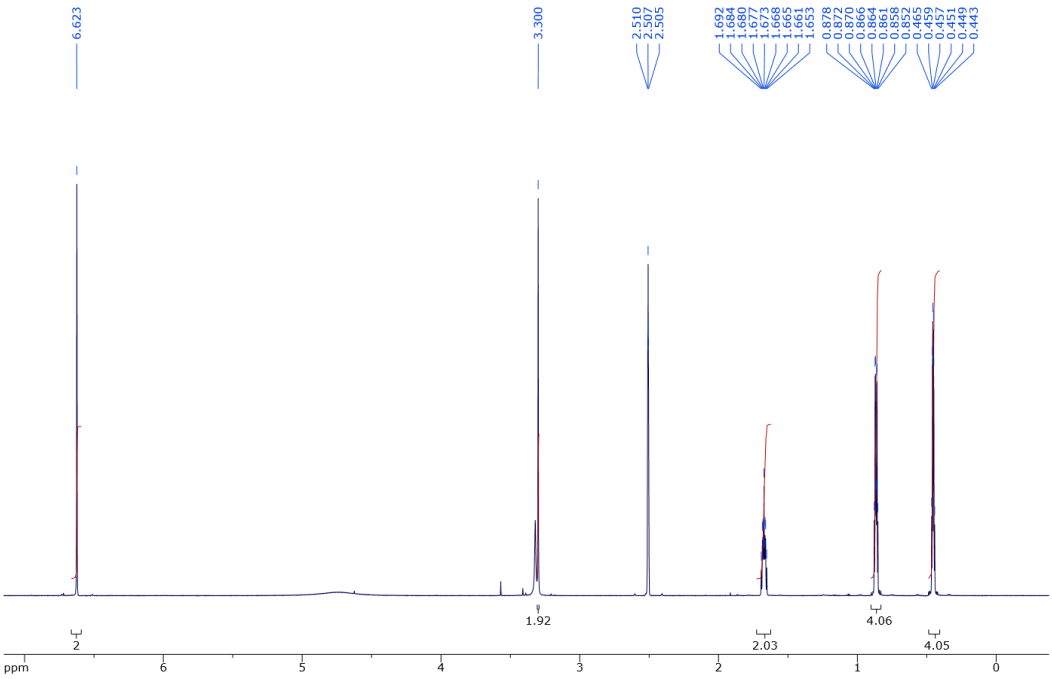
6.623
3.300
2.510
2.507
2.505
1.692
1.684
1.680
1.677
1.673
1.668
1.665
1.661
1.653
0.878
0.872
0.870
0.866
0.864
0.861
0.858
0.852
0.465
0.459
0.457
0.451
0.449
0.443
1.92
4.06
2.03
4.05
2
ppm
6
5
4
3
2
1
0

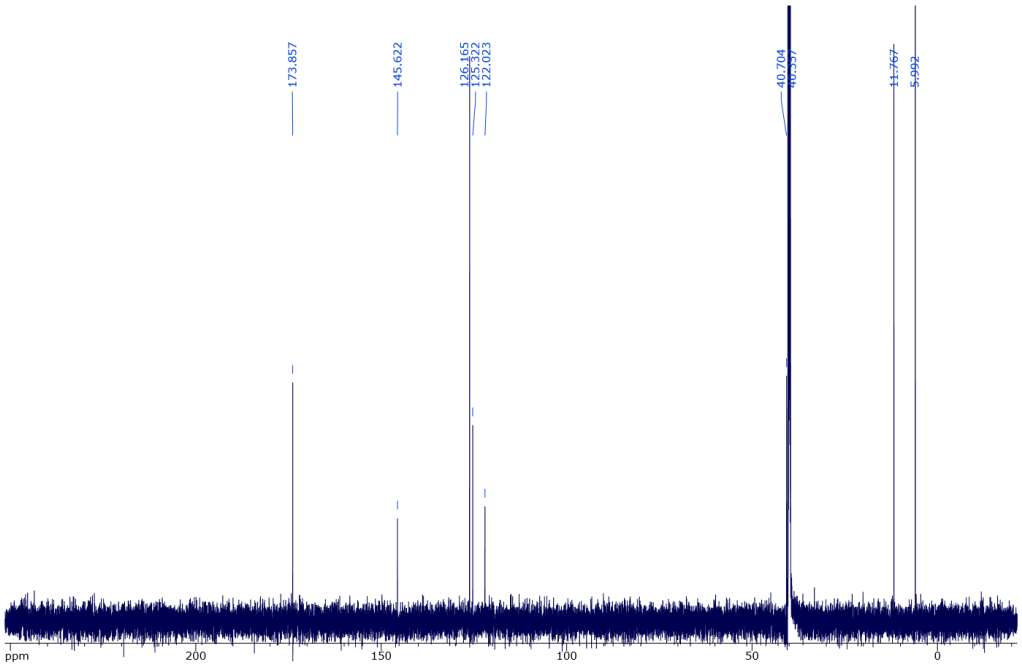
173.857
145.622
126.165
125.322
123.023
122.023
40.704
40.557
11.767
5.992
ppm
200
150
100
50
0

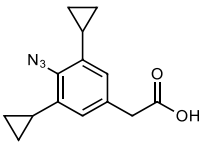
N3
O
OH

1d

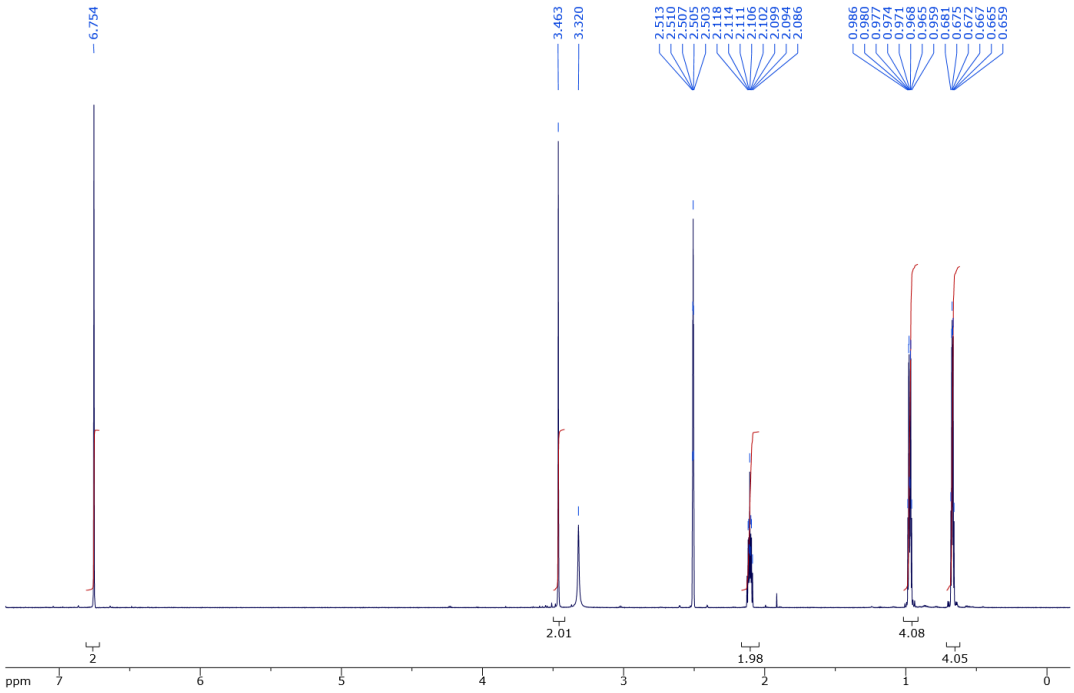
6.754
3.463
3.320
2.513
2.510
2.507
2.505
2.503
2.118
2.114
2.111
2.106
2.102
2.099
2.094
2.086
0.986
0.980
0.977
0.974
0.971
0.968
0.965
0.959
0.681
0.675
0.672
0.667
0.665
0.659
2.01
4.08
2
1.98
4.05
ppm

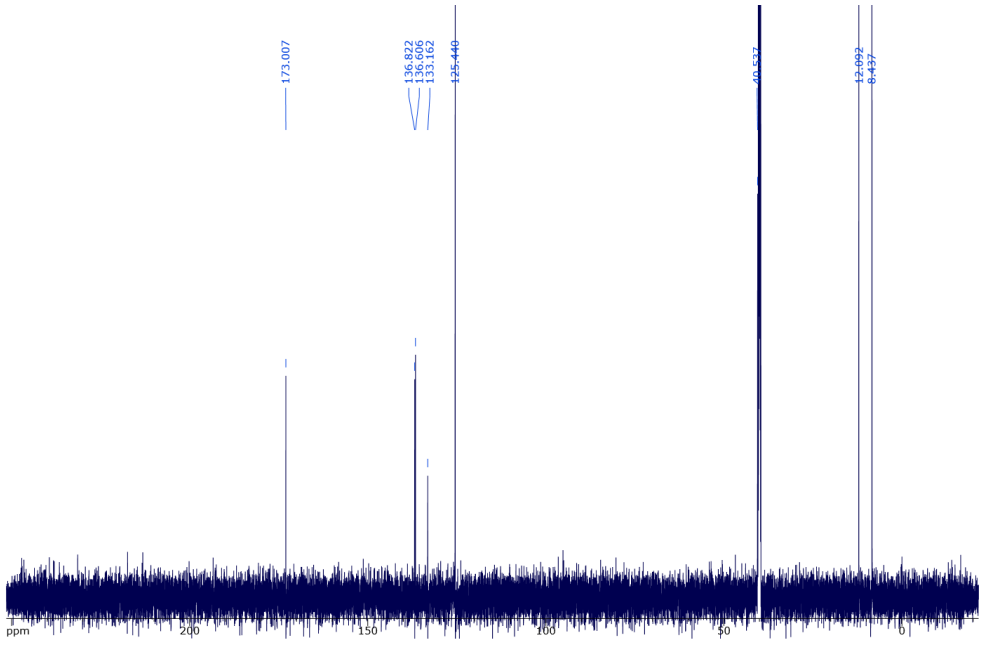
173.007
136.822
136.606
133.162
125.440
40.537
12.992
8.437
ppm

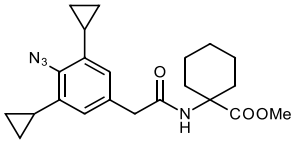
N3
O
N
H
COOMe

2a

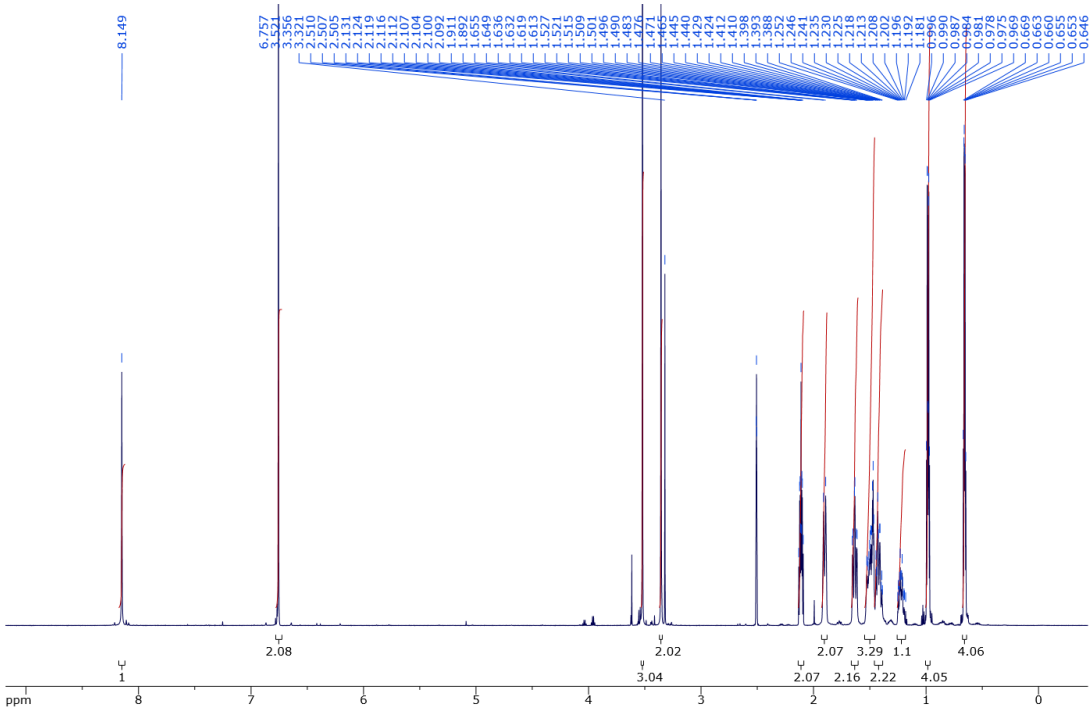
8.149
6.757
3.356
3.321
2.510
2.507
2.505
2.131
2.124
2.119
2.116
2.112
2.107
2.104
2.100
2.092
1.911
1.892
1.655
1.649
1.636
1.632
1.619
1.613
1.527
1.521
1.515
1.509
1.501
1.496
1.490
1.483
1.476
1.471
1.465
1.445
1.440
1.429
1.424
1.412
1.410
1.398
1.393
1.388
1.357
1.246
1.241
1.235
1.230
1.225
1.218
1.213
1.208
1.202
1.196
1.192
1.181
0.996
0.990
0.987
0.984
0.981
0.978
0.975
0.969
0.669
0.663
0.660
0.655
0.653
0.646
2.08
2.02
2.07
3.29
1.1
4.06
1
3.04
2.07
2.16
2.22
4.05
ppm

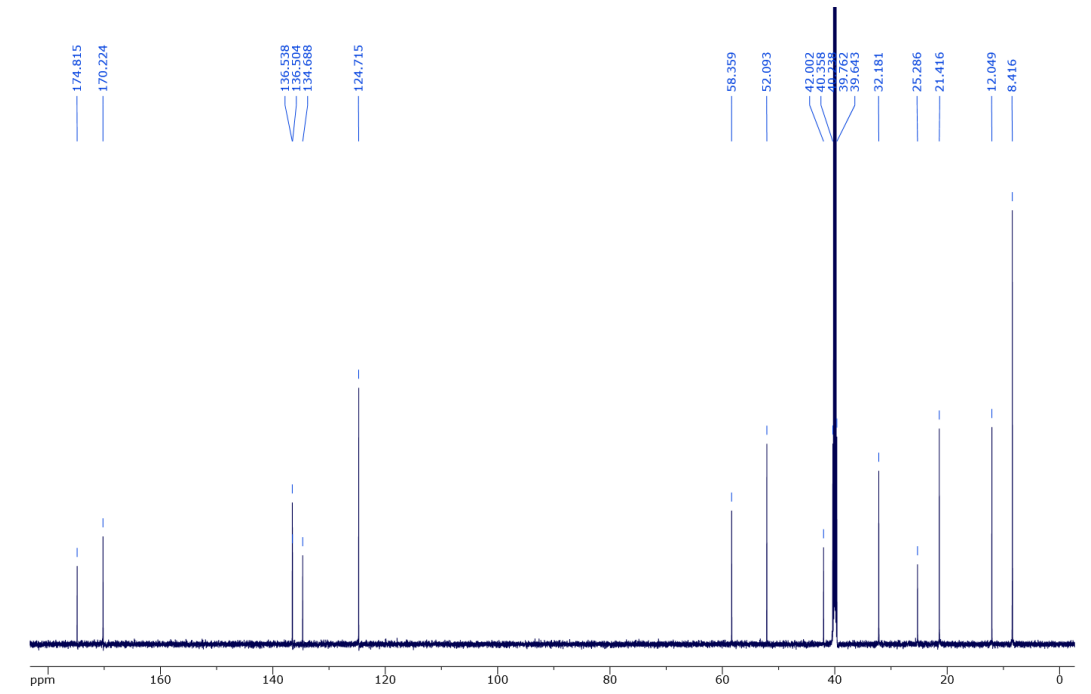
174.815
170.224
136.538
136.504
134.688
124.715
58.359
52.093
42.002
40.398
40.238
39.762
39.643
32.181
25.286
21.416
12.049
8.416
ppm

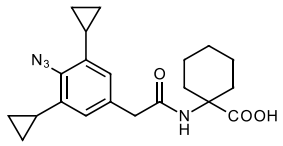
N3
O
N
H
COOH

2b

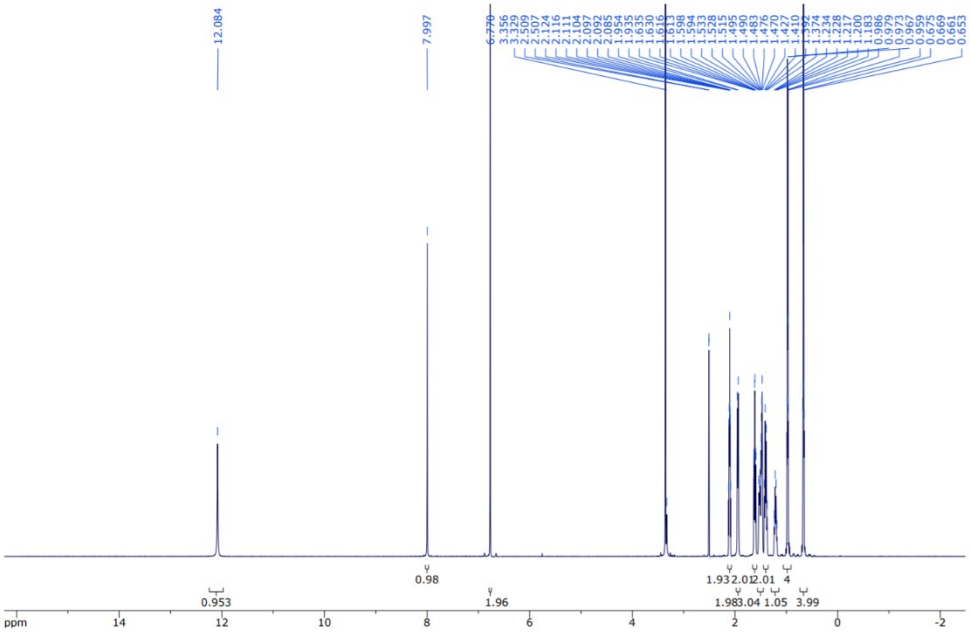
12.084
7.997
6.770
0.953
0.98
1.96
1.93
2.01
2.01
4
1.98
3.04
1.05
3.99
ppm
14
12
10
8
6
4
2
0
-2

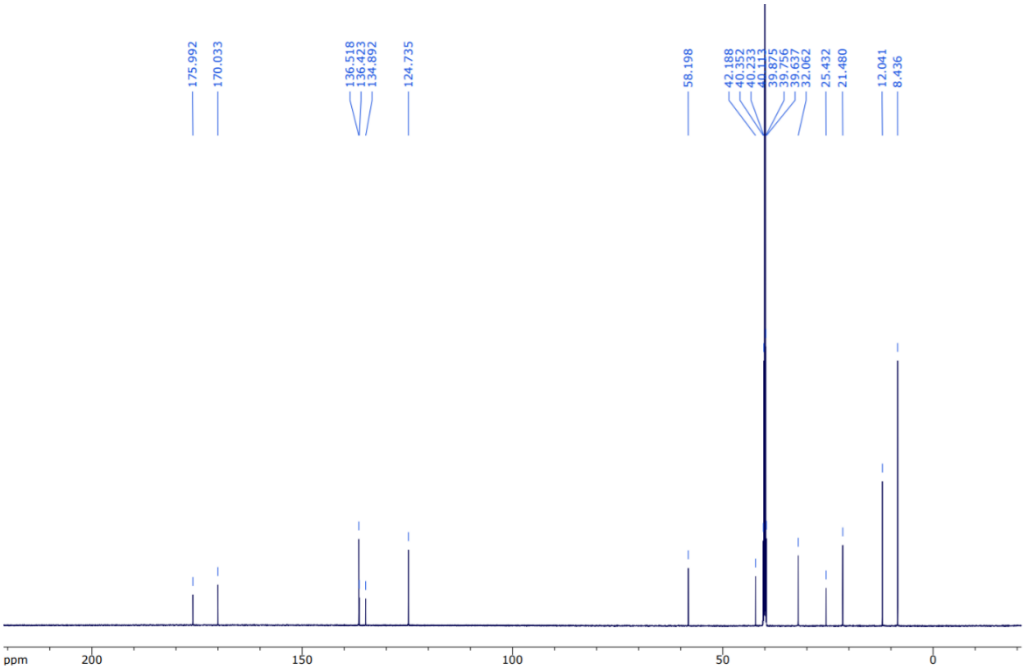
175.992
170.033
136.518
136.423
134.892
124.735
58.198
42.188
40.352
40.233
39.875
39.756
39.637
32.062
25.432
21.480
12.041
8.436
ppm
200
150
100
50
0

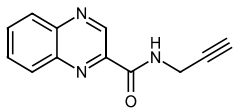

3a

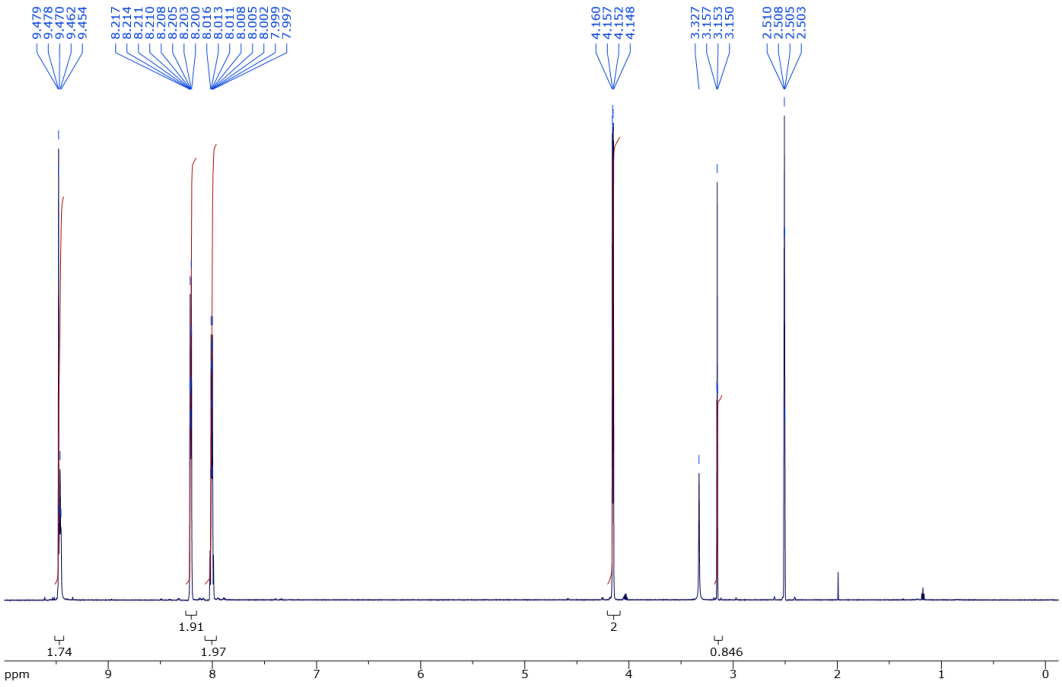
9.479
9.478
9.470
9.462
9.454
8.217
8.214
8.211
8.210
8.208
8.205
8.203
8.200
8.015
8.011
8.008
8.005
8.002
7.999
7.997
4.160
4.157
4.152
4.148
3.327
3.157
3.153
3.150
2.510
2.508
2.505
2.503
1.74
1.91
1.97
2
0.846
ppm

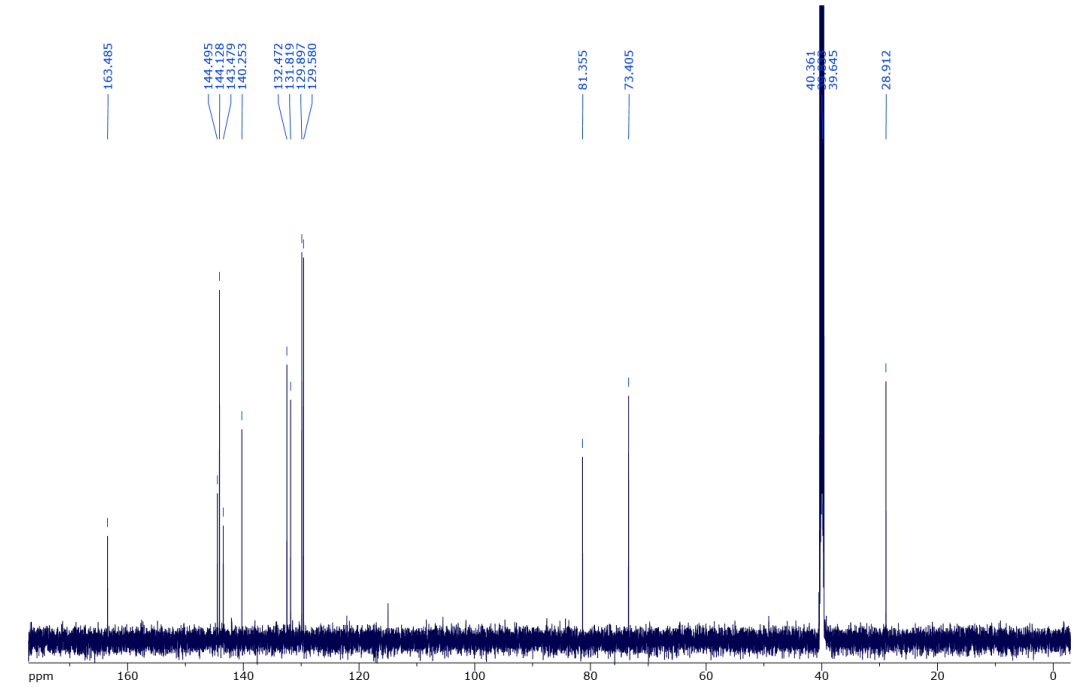
163.485
144.495
144.138
143.479
140.253
132.472
131.819
129.897
129.580
81.355
73.405
40.361
39.645
28.912
ppm

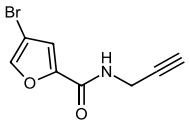
Br
O
H
N
O

3b

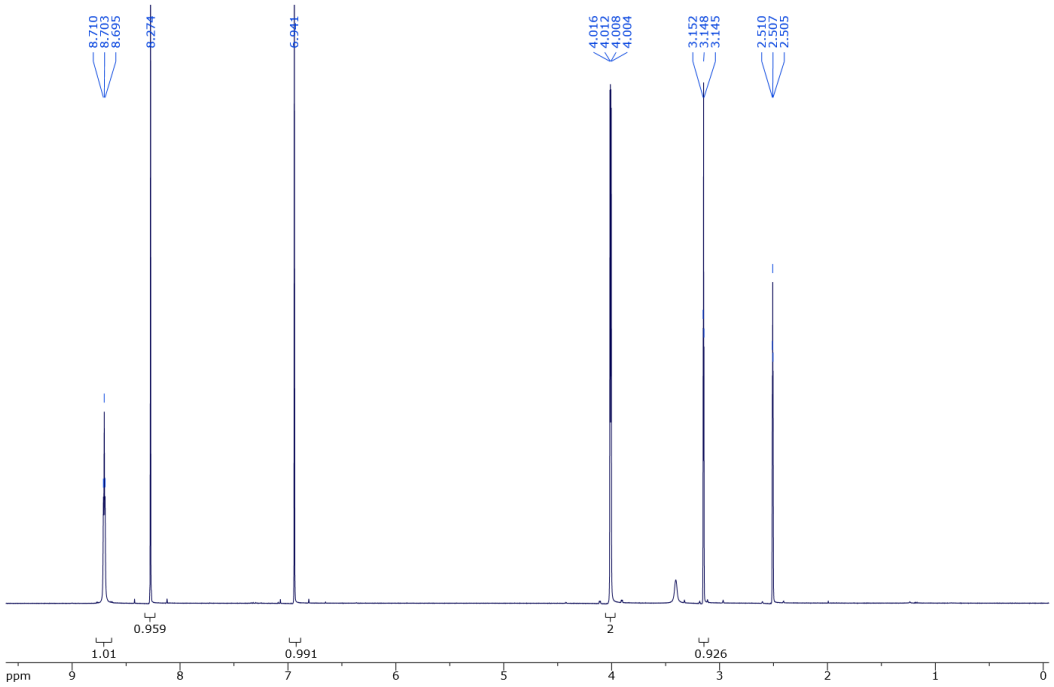
8.710
8.703
8.695
7.274
6.941
4.016
4.012
4.008
4.004
3.152
3.148
3.145
2.510
2.507
2.505
0.959
2
1.01
0.991
0.926
ppm

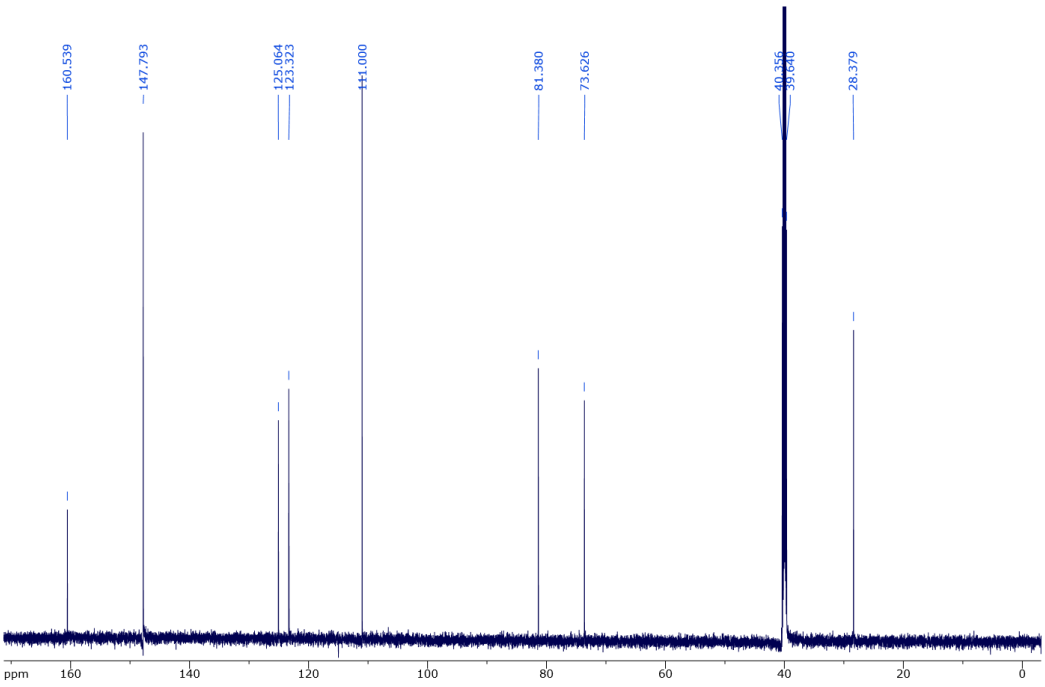
160.539
147.793
125.064
123.323
111.000
81.380
73.626
40.356
39.740
28.379
ppm

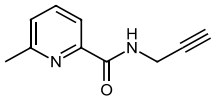

3c

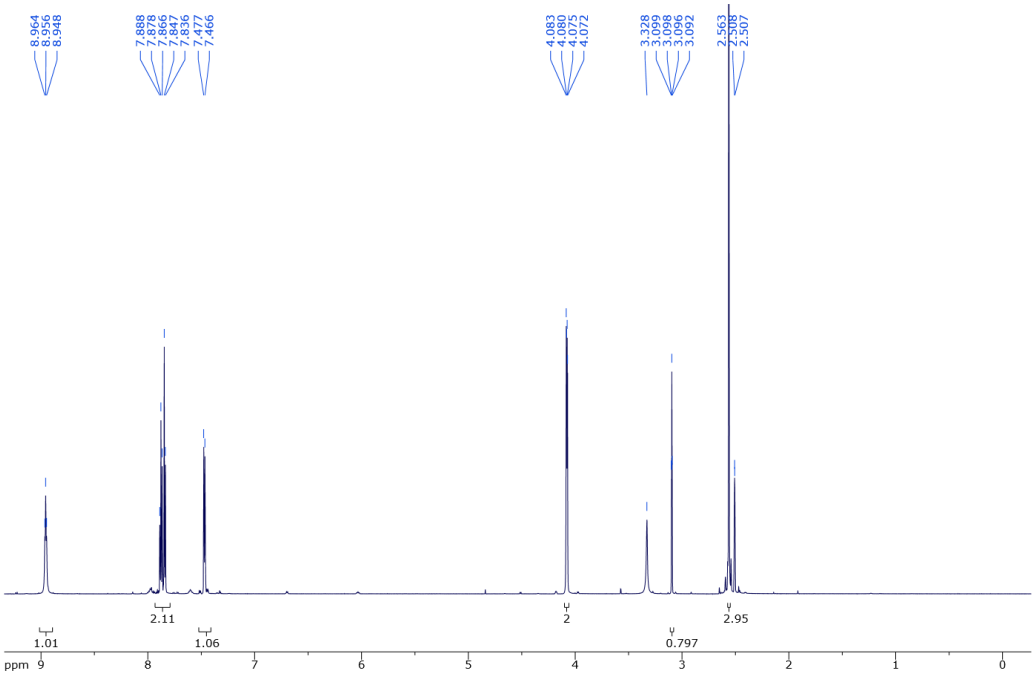
8.964
8.956
8.948
7.888
7.878
7.866
7.847
7.836
7.477
7.466
4.083
4.080
4.075
4.072
3.328
3.099
3.098
3.096
3.092
2.563
2.508
2.507
1.01
2.11
1.06
2
0.797
2.95
ppm 9 8 7 6 5 4 3 2 1 0

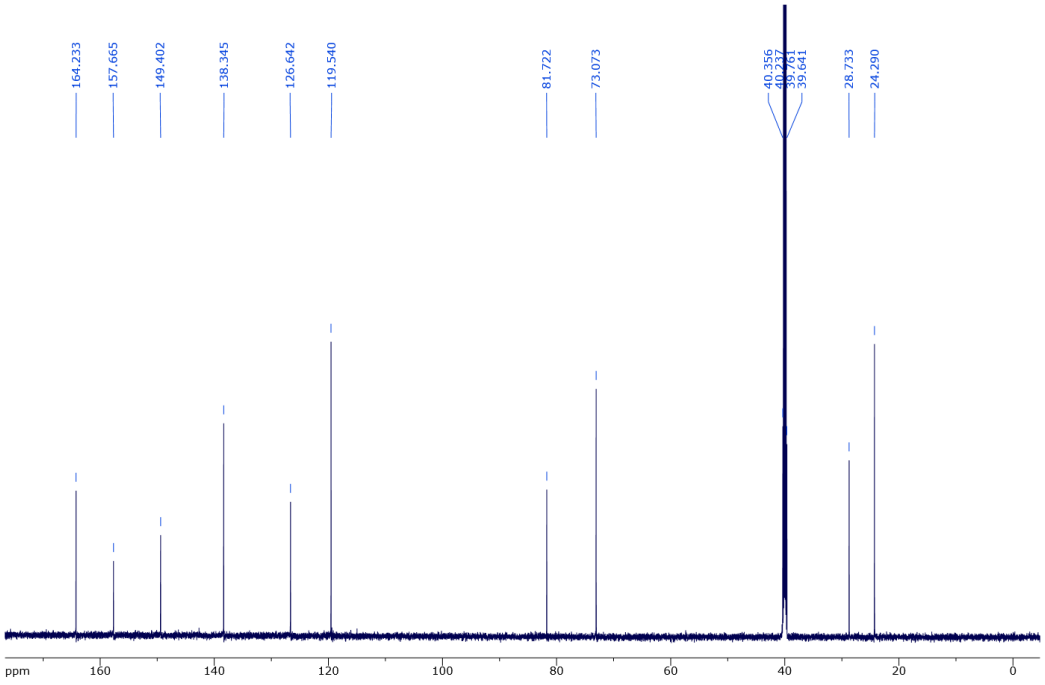
164.233
157.665
149.402
138.345
126.642
119.540
81.722
73.073
40.356
40.237
39.761
39.641
28.733
24.290
ppm 160 140 120 100 80 60 40 20 0

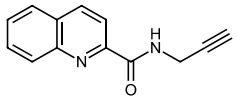

3d

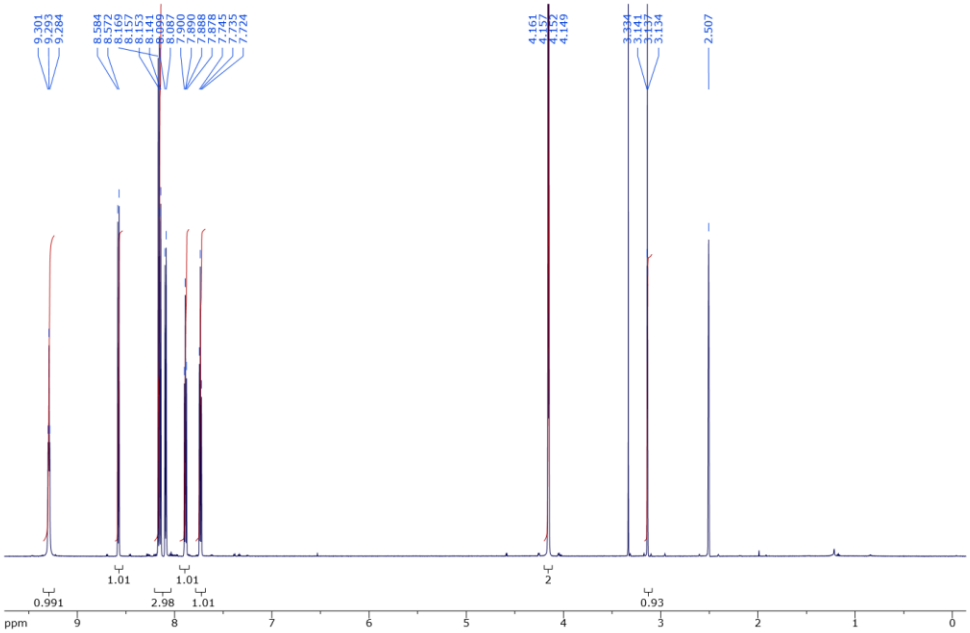
9.301
9.293
9.284
8.584
8.572
8.169
8.157
8.153
8.141
8.087
7.900
7.890
7.888
7.878
7.745
7.735
7.724
4.161
4.157
4.149
3.334
3.141
3.137
3.134
2.507
1.01
1.01
2
0.991
2.98
1.01
0.93
ppm

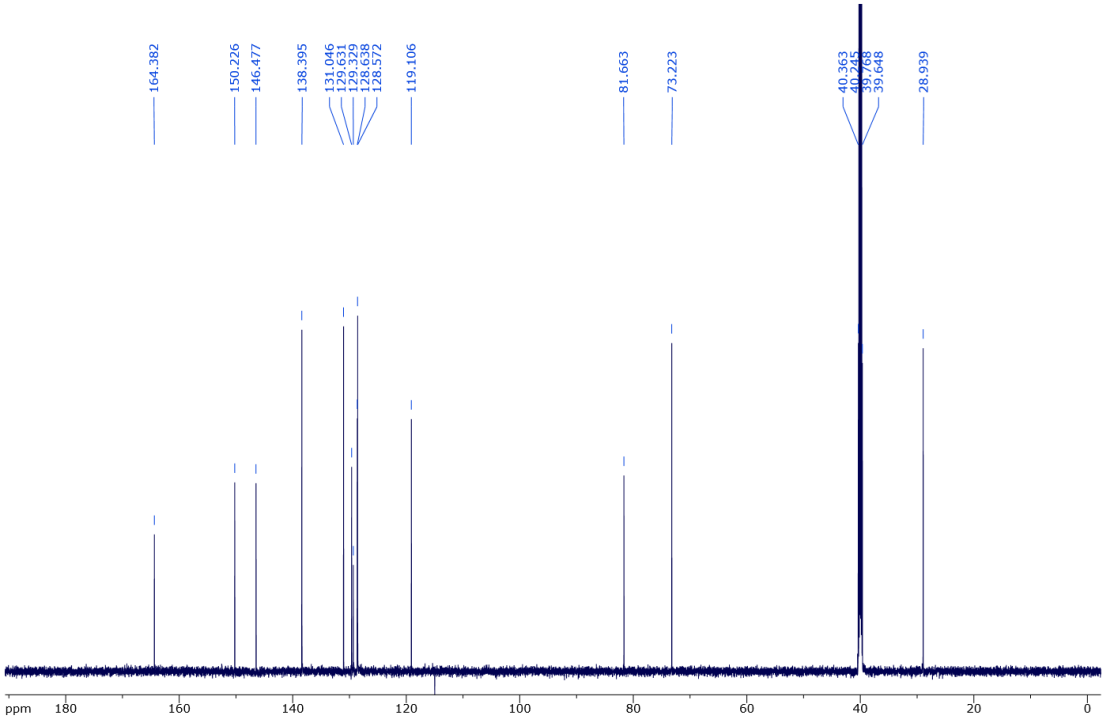
164.382
150.226
146.477
138.395
131.046
129.431
129.324
128.638
128.572
119.106
81.663
73.223
40.363
40.245
39.768
39.648
28.939
ppm

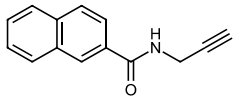

3e

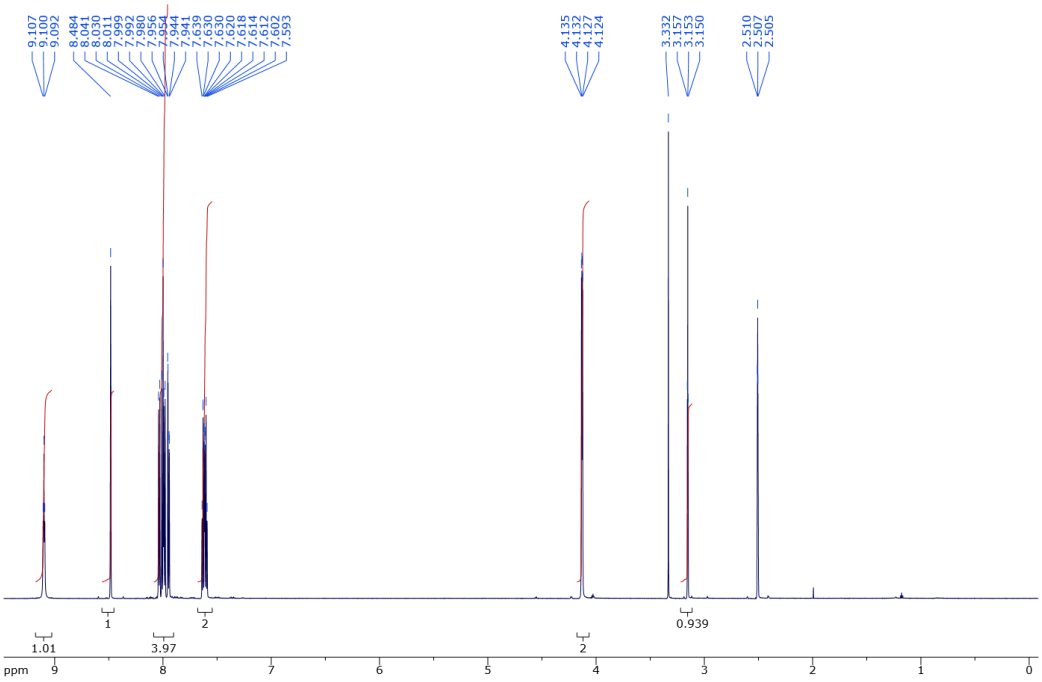
9.107
9.100
9.092
8.484
8.041
8.030
8.011
7.999
7.992
7.980
7.956
7.954
7.944
7.941
7.639
7.630
7.620
7.618
7.614
7.612
7.600
7.593
4.135
4.132
4.127
4.124
3.332
3.157
3.153
3.150
2.510
2.507
2.505
1.01
1
3.97
2
2
0.939
ppm

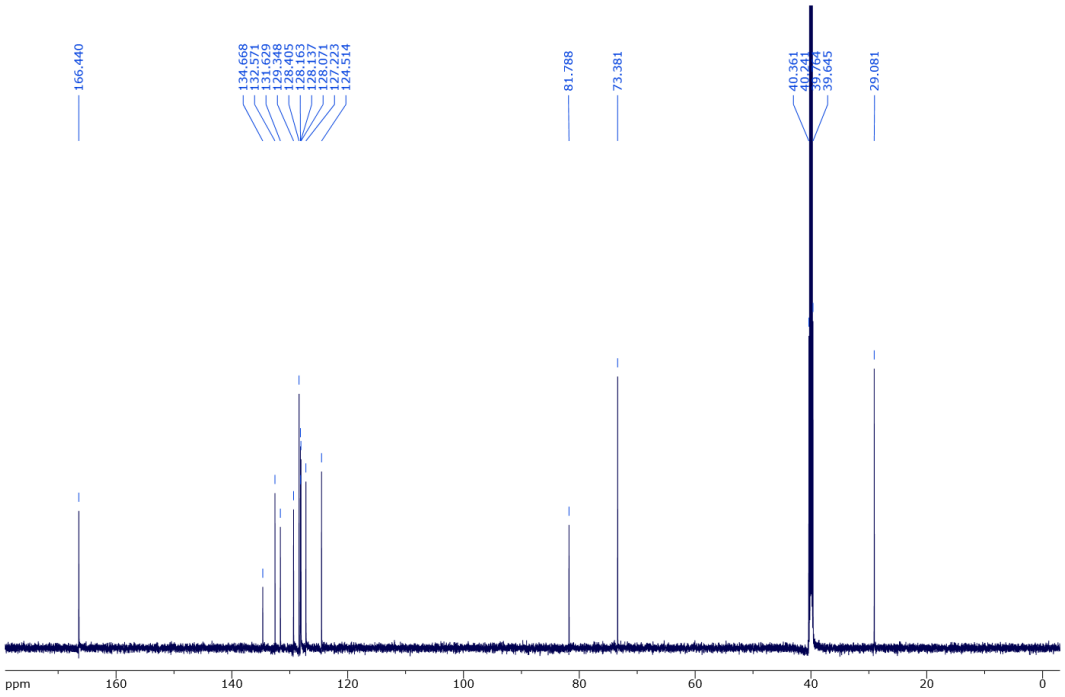
166.440
134.668
132.571
131.609
129.348
128.405
128.163
128.137
127.071
125.221
124.514
81.788
73.381
40.361
40.241
39.764
39.645
29.081
ppm

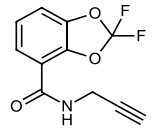

3f

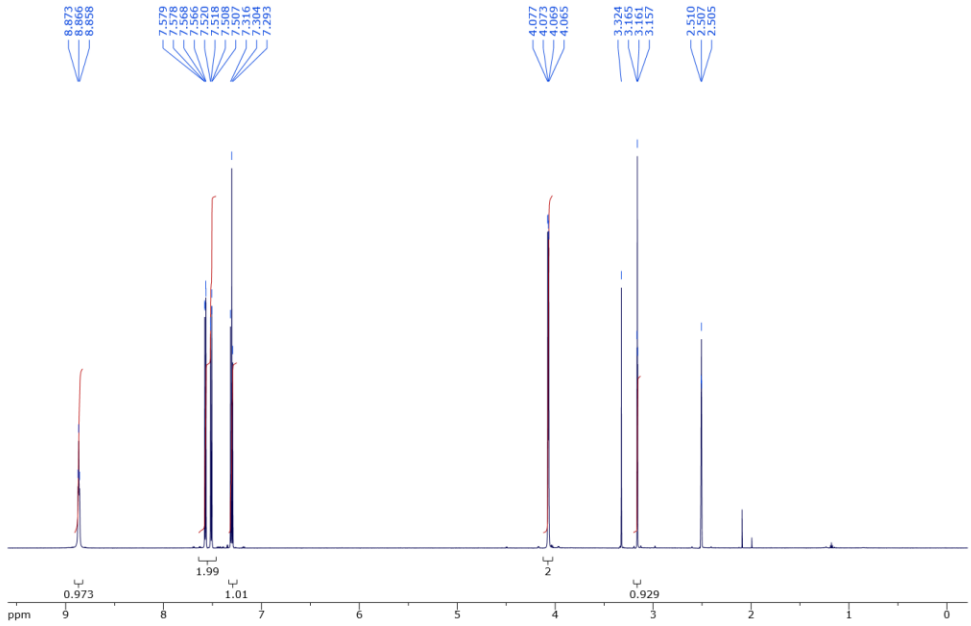
8.873
8.866
8.858
7.579
7.578
7.568
7.566
7.520
7.518
7.508
7.507
7.316
7.304
7.293
4.077
4.073
4.069
4.065
3.324
3.165
3.161
3.157
2.510
2.507
2.505
1.99
1.01
2
0.973
0.929
ppm

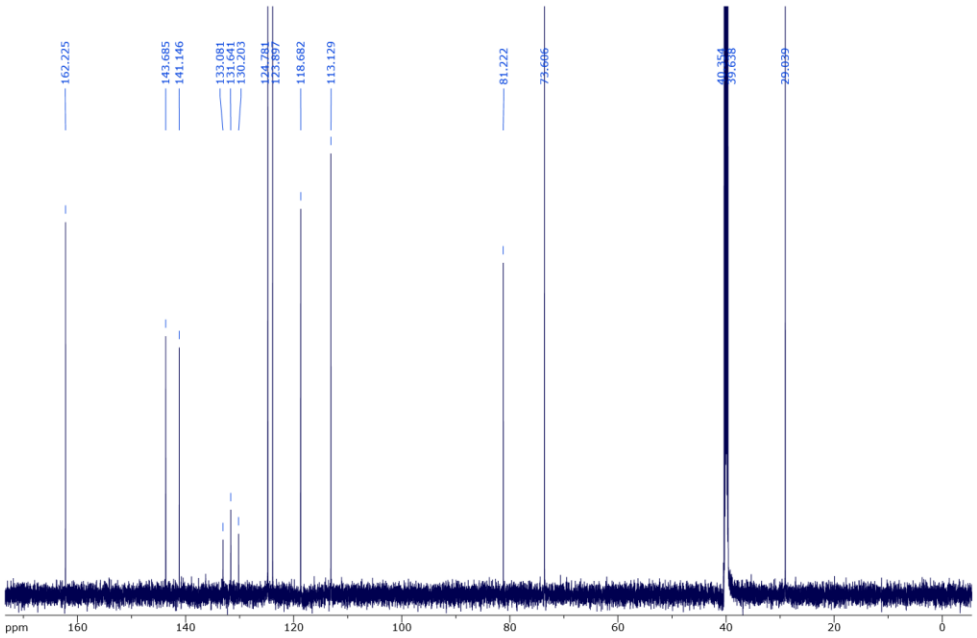
162.225
143.685
141.146
133.081
131.641
130.203
124.781
123.897
118.682
113.129
81.222
73.606
40.354
39.638
29.039
ppm

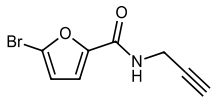
Br
O
O
N
H

3g

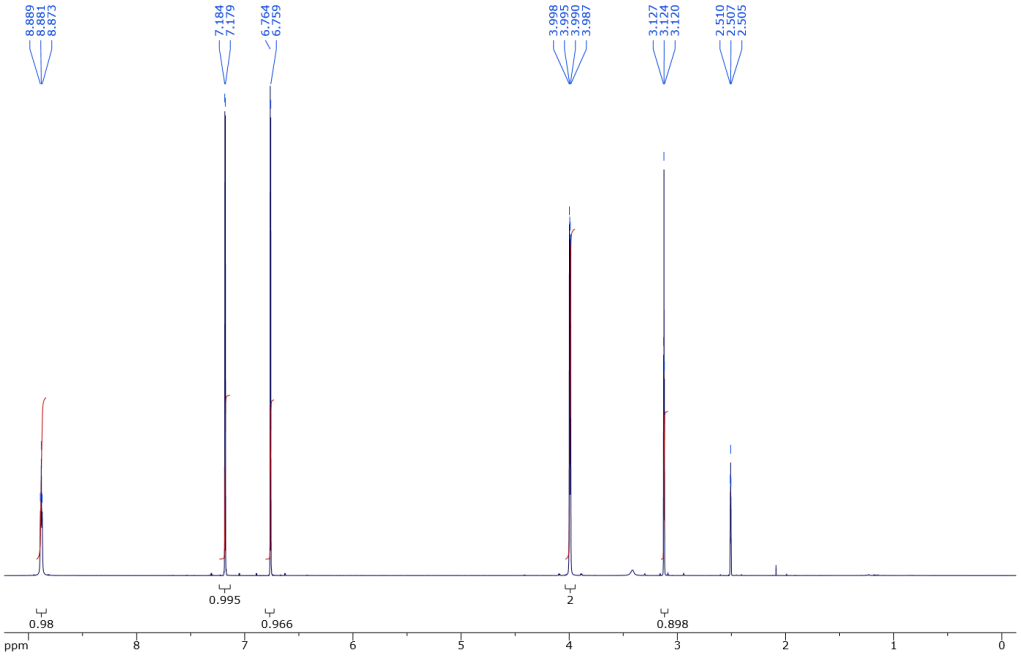
8.889
8.881
8.873
7.184
7.179
6.764
6.759
3.998
3.995
3.990
3.987
3.127
3.124
3.120
2.510
2.507
2.505
0.98
0.995
0.966
2
0.898
ppm

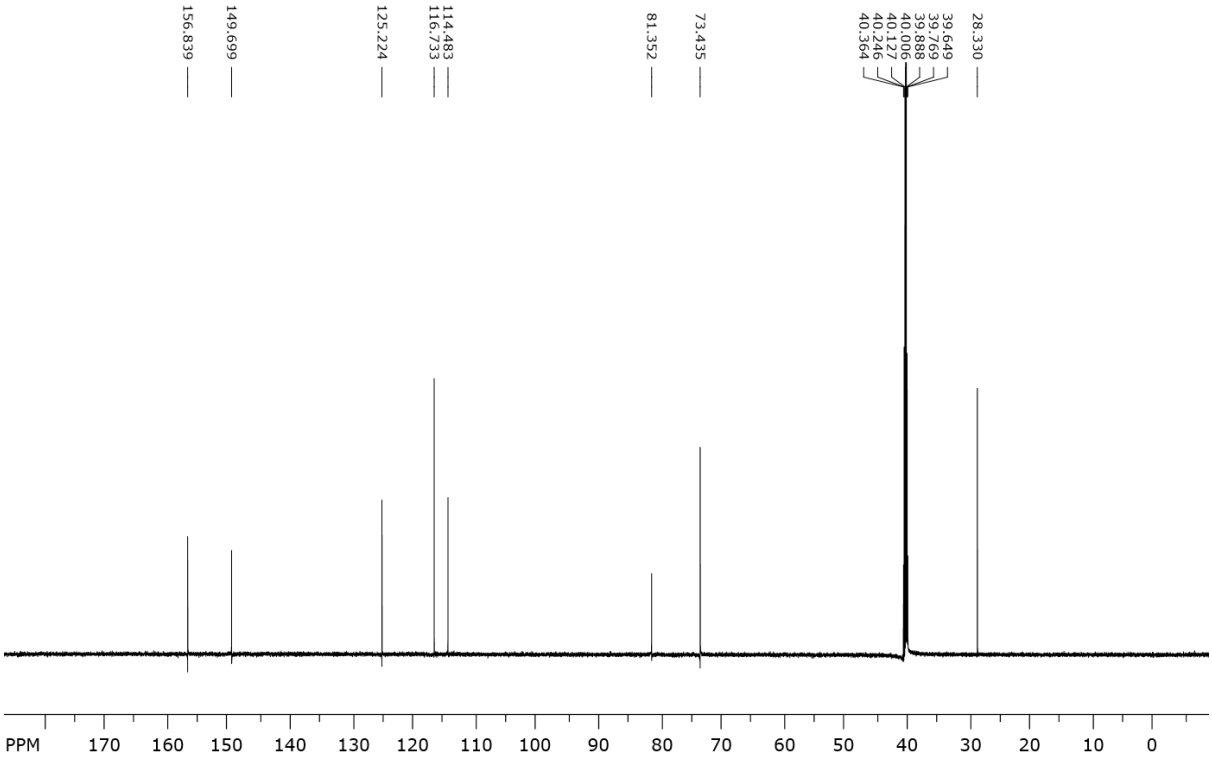
156.839
149.699
125.224
114.483
116.733
81.352
73.435
40.364
40.246
40.127
40.006
39.888
39.769
39.649
28.330
PPM

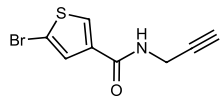
S
Br
H
N
O

3h

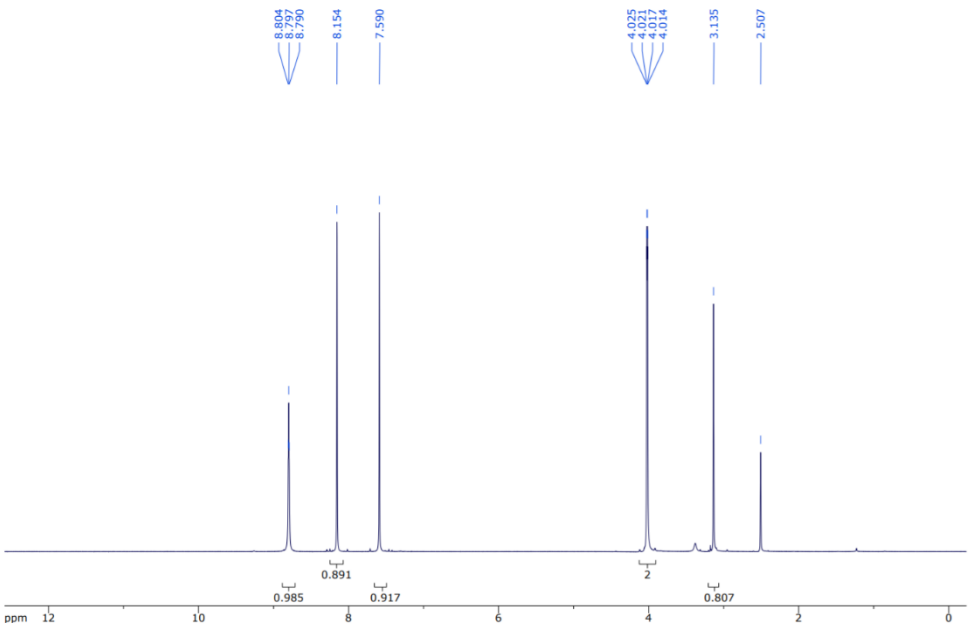
8.804
8.797
8.790
8.154
7.590
4.025
4.021
4.017
4.014
3.135
2.507
0.985
0.891
0.917
2
0.807
ppm
12
10
8
6
4
2
0

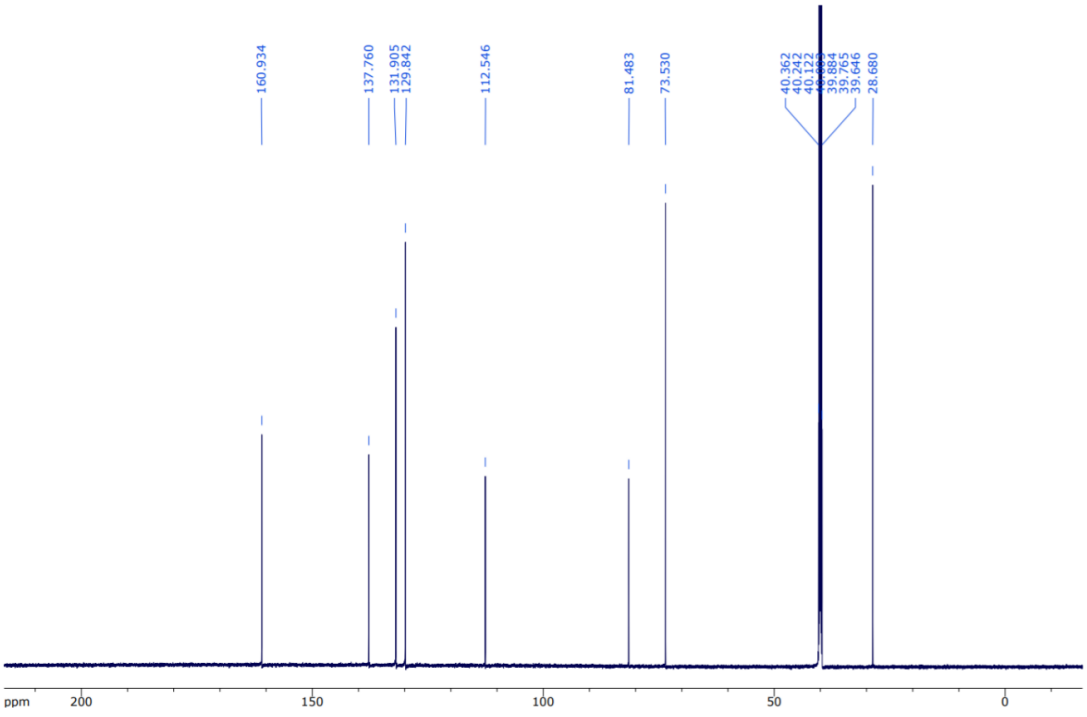
160.934
137.760
131.905
129.842
112.546
81.483
73.530
40.362
40.242
40.122
39.884
39.765
39.646
28.680
ppm
200
150
100
50
0

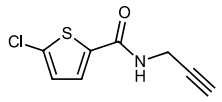
Cl
S
O
N
H

3i

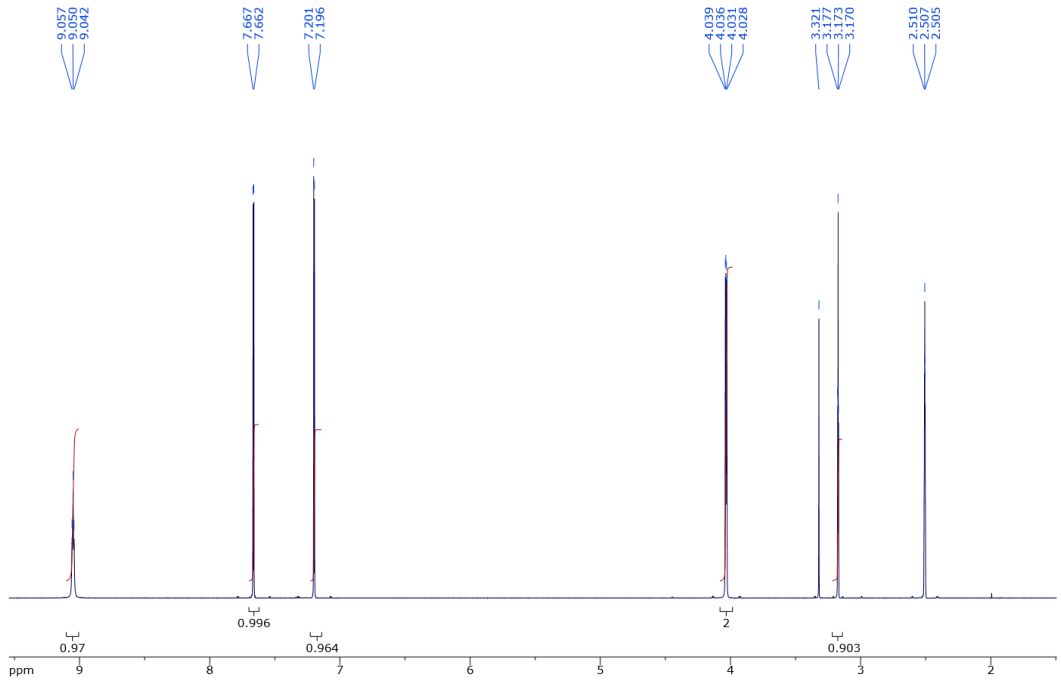
9.057
9.050
9.042
7.667
7.662
7.201
7.196
4.039
4.036
4.031
4.028
3.321
3.177
3.173
3.170
2.510
2.507
2.505
0.996
2
0.97
0.964
0.903
ppm
9
8
7
6
5
4
3
2

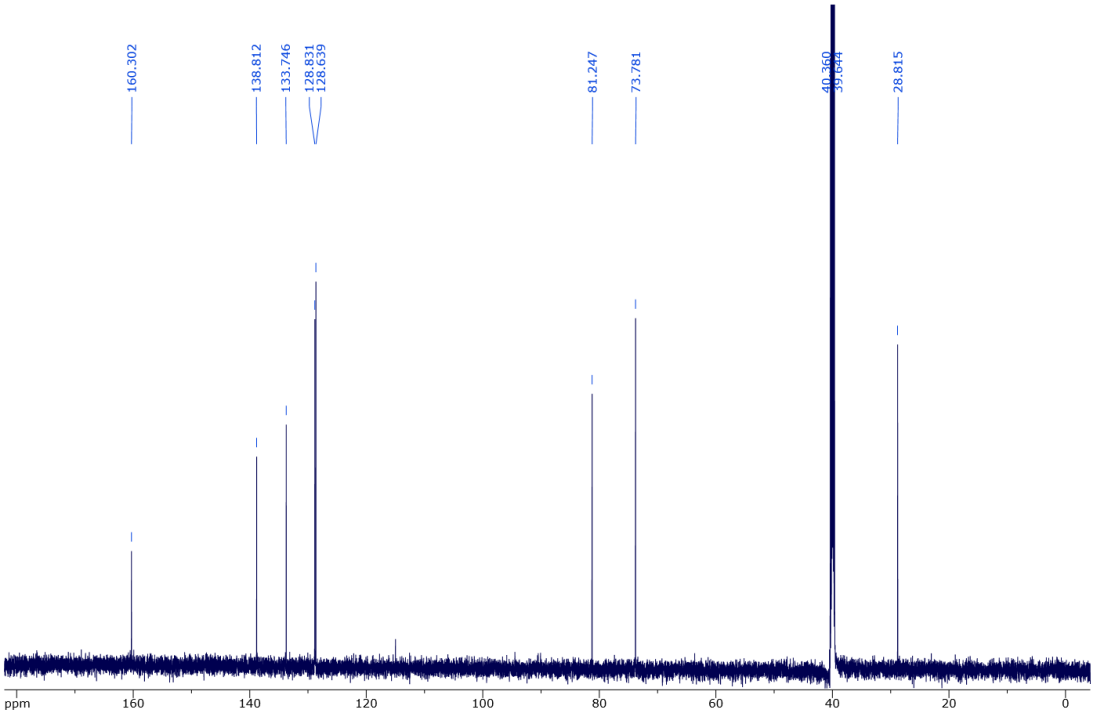
160.302
138.812
133.746
128.831
128.639
81.247
73.781
40.350
39.644
28.815
ppm
160
140
120
100
80
60
40
20
0

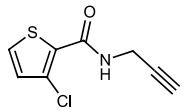
O
S
N
H
Cl

3j

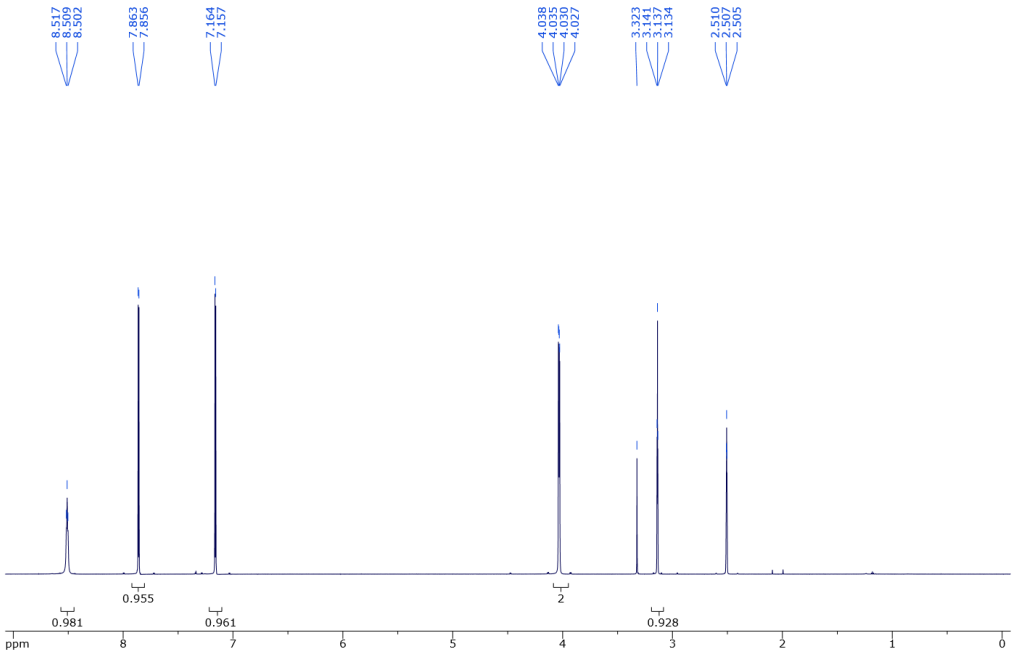
8.517
8.509
8.502
7.863
7.856
7.164
7.157
4.038
4.035
4.030
4.027
3.323
3.141
3.137
3.134
2.510
2.507
2.505
0.981
0.955
0.961
2
0.928
ppm
8
7
6
5
4
3
2
1
0

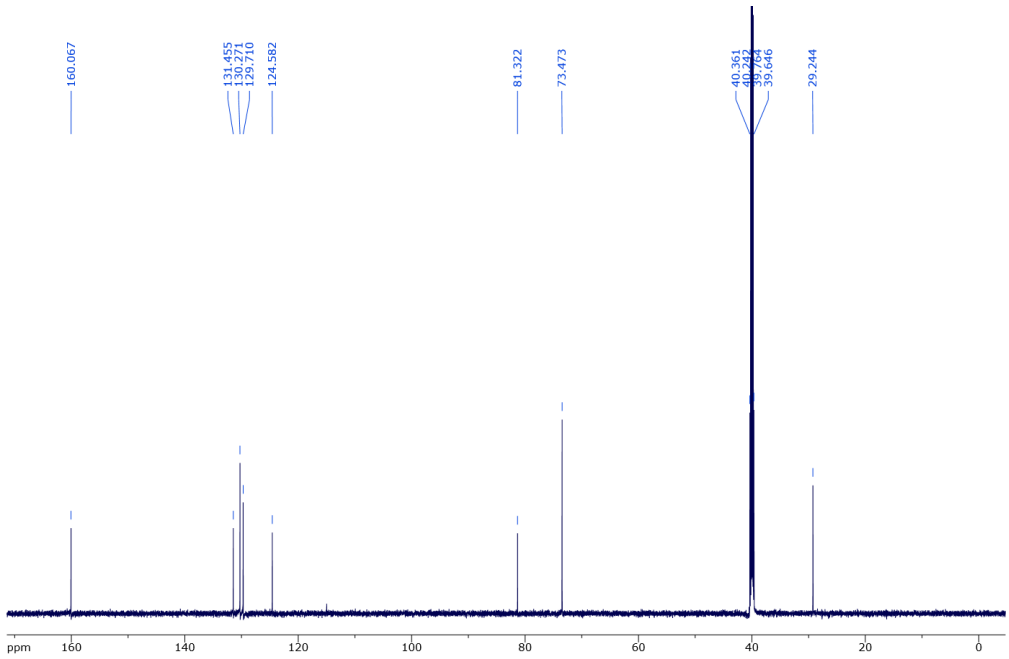
160.067
131.455
130.271
129.710
124.582
81.322
73.473
40.361
40.242
40.124
39.646
29.244
ppm
160
140
120
100
80
60
40
20
0

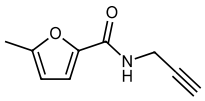

3k

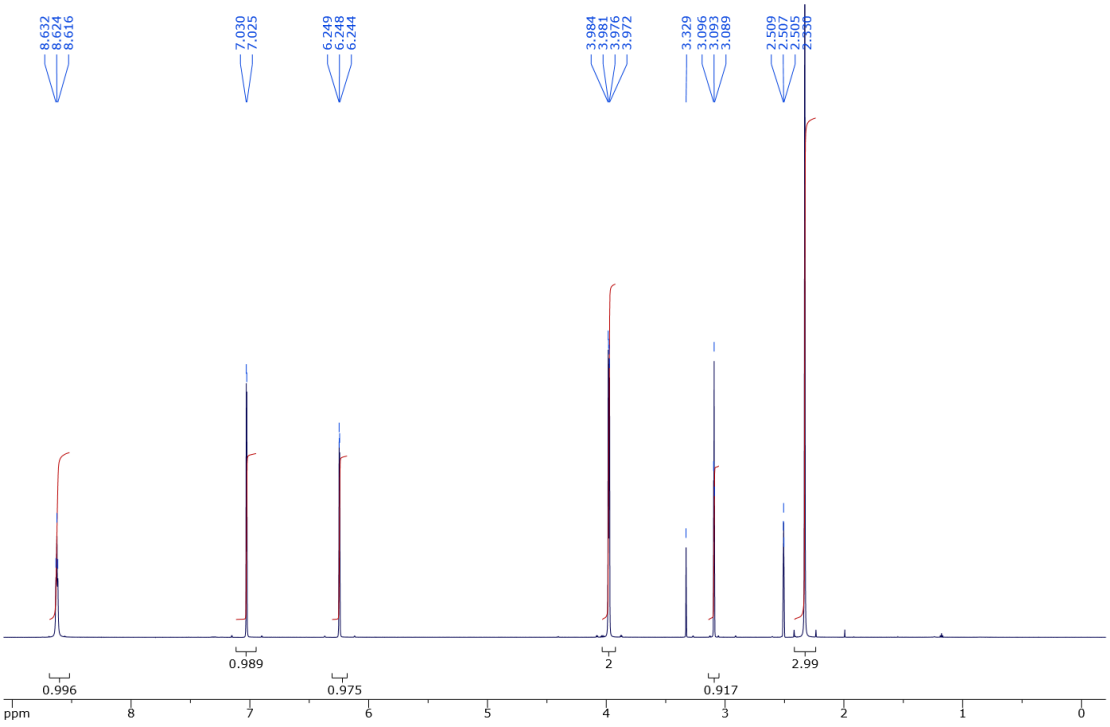
8.632
8.624
8.616
7.030
7.025
6.249
6.248
6.244
3.984
3.981
3.976
3.972
3.329
3.096
3.093
3.089
2.509
2.507
2.505
2.330
0.996
0.989
0.975
2
0.917
2.99
ppm

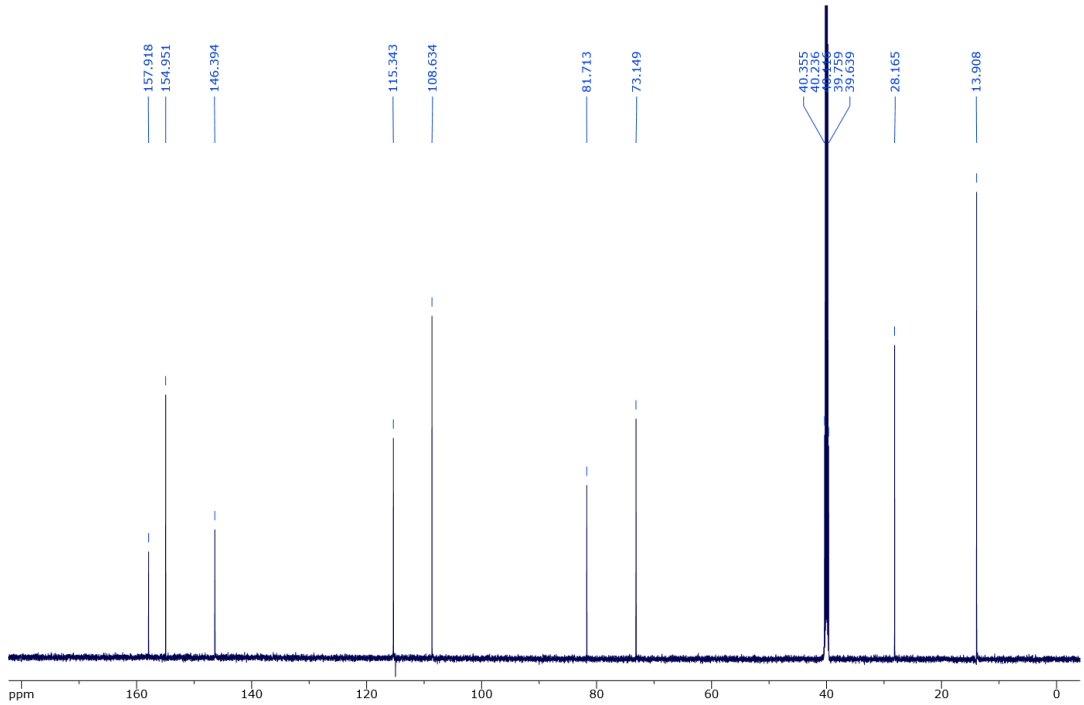
157.918
154.951
146.394
115.343
108.634
81.713
73.149
40.355
40.236
39.739
39.639
28.165
13.908
ppm

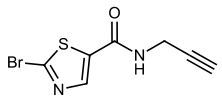
O
S
Br
N
N
H

3l

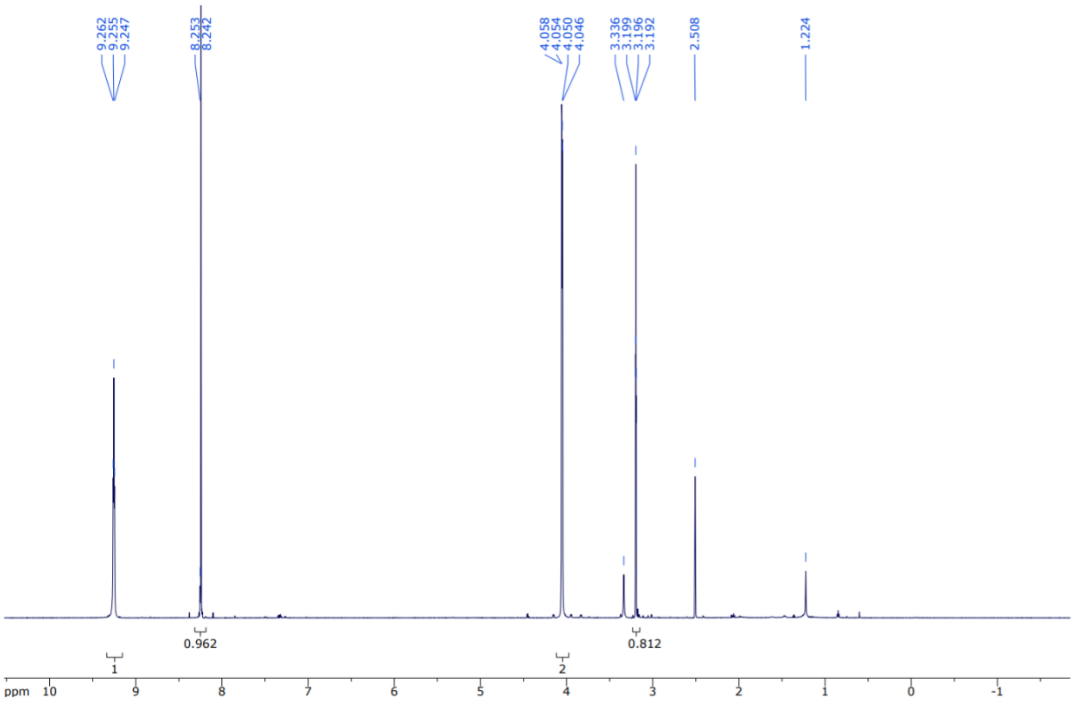
9.262
9.255
9.247
8.253
8.242
4.058
4.054
4.050
4.046
3.336
3.199
3.196
3.192
2.508
1.224
0.962
0.812
1
2
ppm 10
9
8
7
6
5
4
3
2
1
0
-1

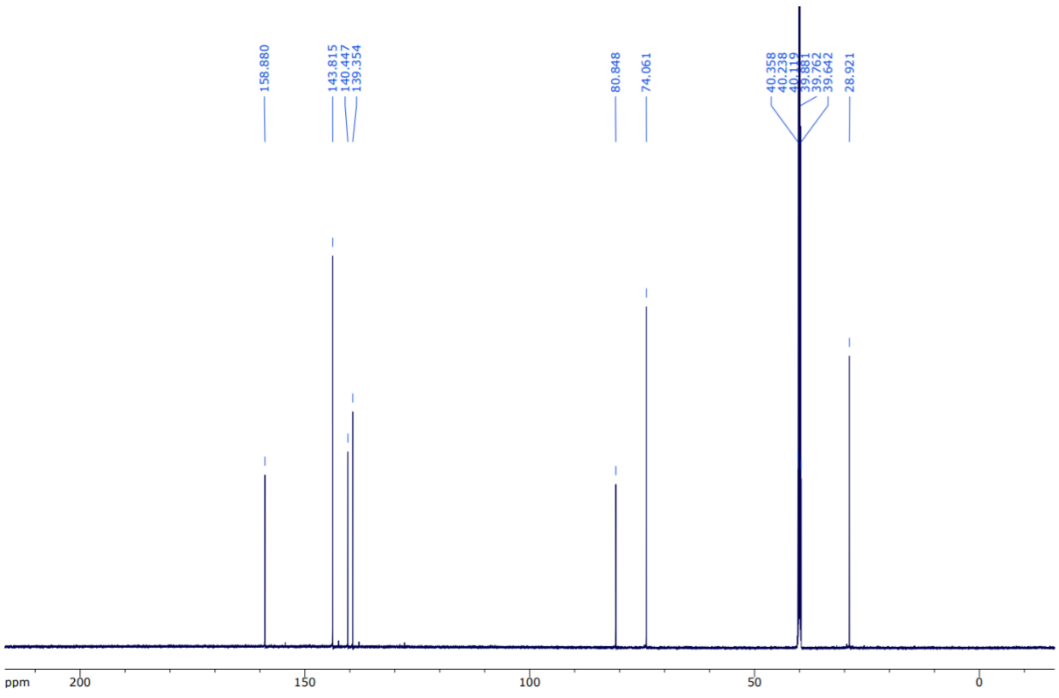
158.880
143.815
140.447
139.354
80.848
74.061
40.358
40.238
40.119
39.881
39.762
39.642
28.921
ppm 200
150
100
50
0

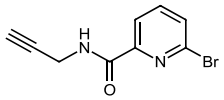
H
N
O
N
Br

3m

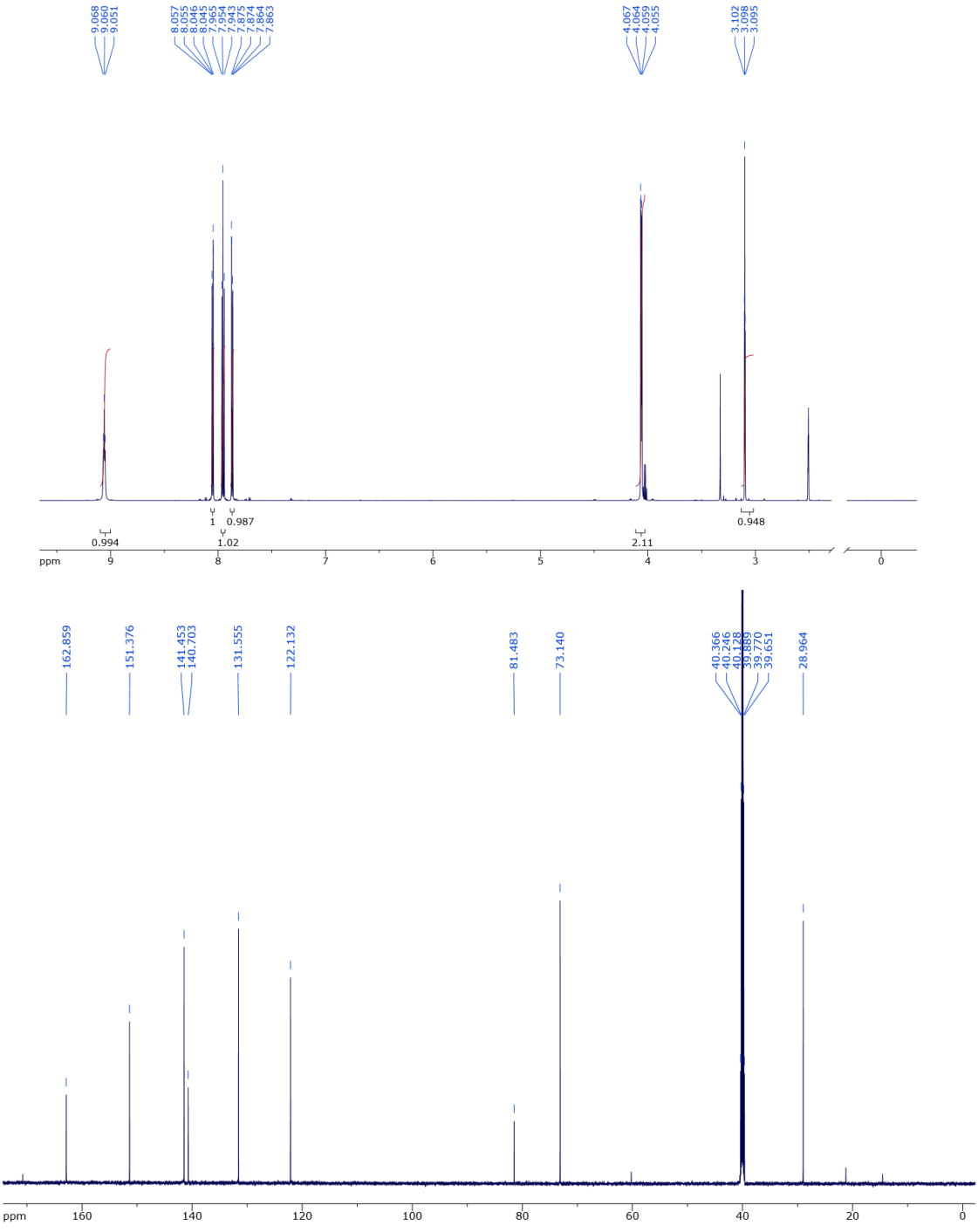
9.068
9.060
9.051
8.057
8.055
8.046
8.045
7.955
7.954
7.943
7.875
7.874
7.864
7.863
4.067
4.064
4.059
4.055
3.102
3.098
3.095
0.994
1
0.987
1.02
2.11
0.948
ppm
9
8
7
6
5
4
3
0
162.859
151.376
141.453
140.703
131.555
122.132
81.483
73.140
40.366
40.246
40.126
39.889
39.770
39.651
28.964
ppm
160
140
120
100
80
60
40
20
0

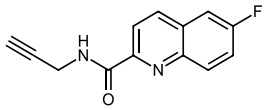
F
H
N
N
O

3o


9.294
9.286
9.278
8.573
8.561
8.212
8.204
8.198
8.195
8.191
8.183
7.930
7.926
7.917
7.912
7.825
7.821
7.813
7.809
7.800
7.796
4.151
4.148
4.142
4.139
3.325
3.138
3.135
3.131
2.508
2.506

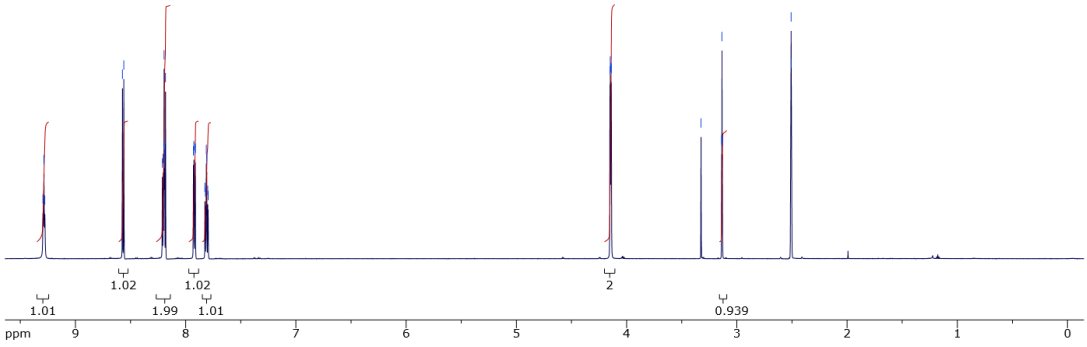
1.02
1.02
2
1.01
1.99
1.01
0.939
ppm
9
8
7
6
5
4
3
2
1
0

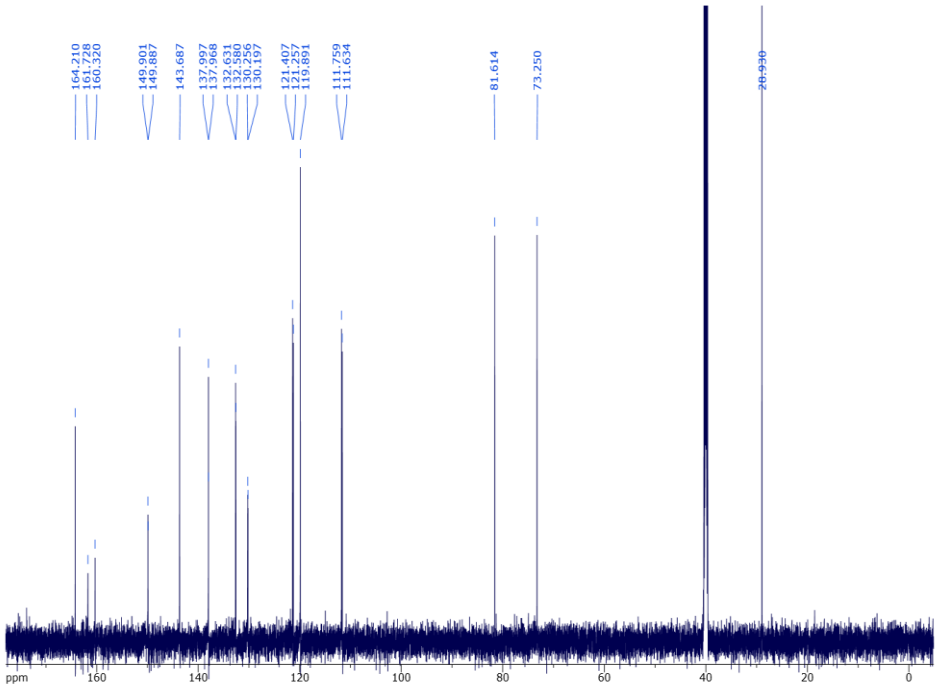
164.210
161.728
160.320
149.901
149.887
143.687
137.997
137.968
132.631
132.580
130.255
130.197
121.407
121.257
119.891
111.759
111.634
81.614
73.250
20.930
ppm
160
140
120
100
80
60
40
20
0

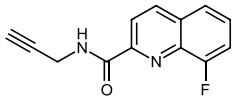

3n

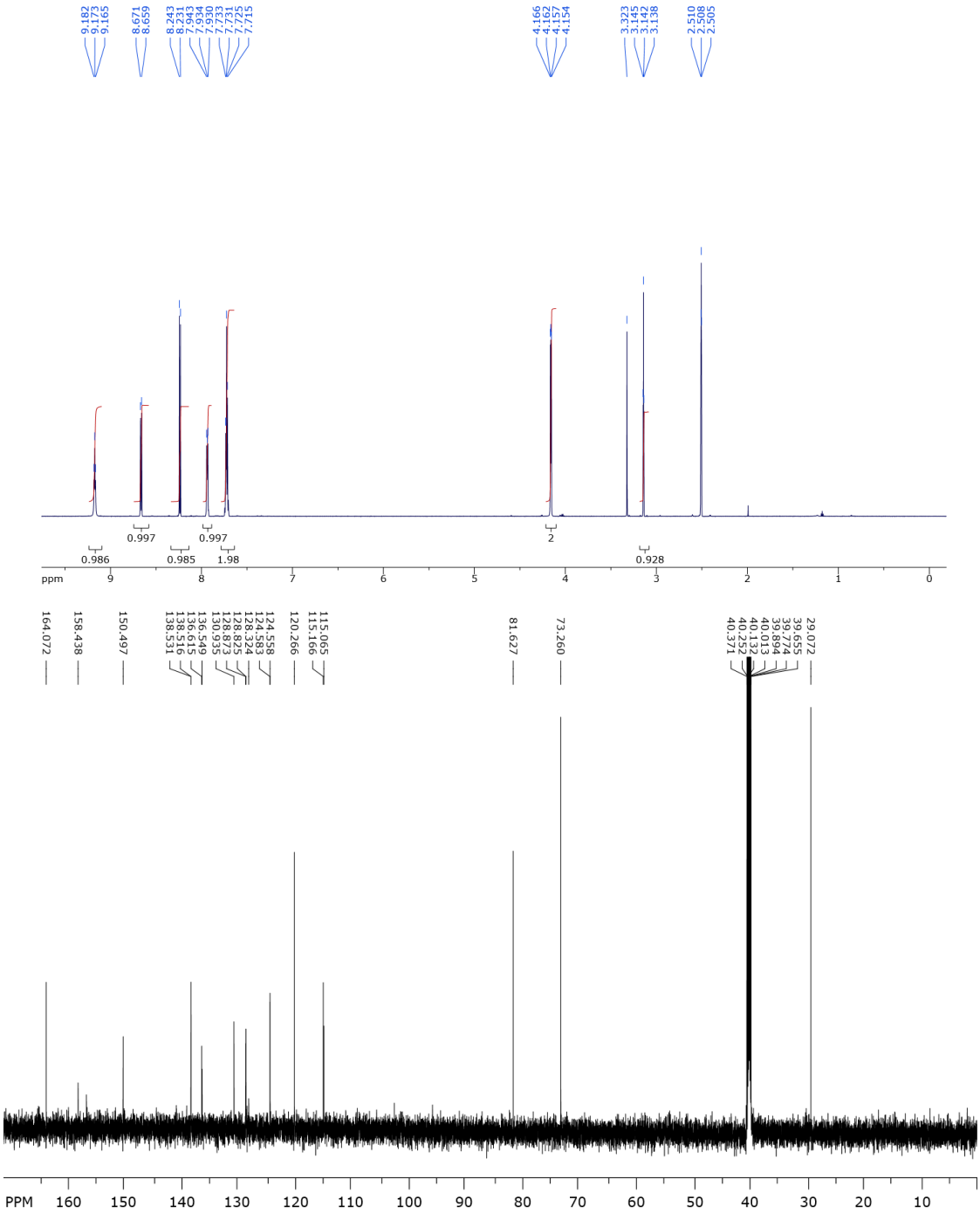
9.182
9.173
9.165
8.671
8.659
8.243
8.231
7.943
7.934
7.930
7.733
7.731
7.725
7.715
4.166
4.162
4.157
4.154
3.323
3.145
3.142
3.138
2.510
2.508
2.505
0.997
0.997
2
0.986
0.985
1.98
0.928
ppm
9
8
7
6
5
4
3
2
1
0
164.072
158.438
150.497
138.531
138.516
136.615
136.549
130.935
128.873
128.825
128.324
124.583
124.558
120.266
115.166
115.065
81.627
73.260
40.371
40.252
40.132
40.013
39.894
39.774
39.655
29.072
PPM
160
150
140
130
120
110
100
90
80
70
60
50
40
30
20
10

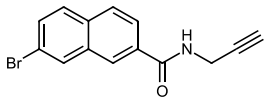
Br
H
N
O

3p

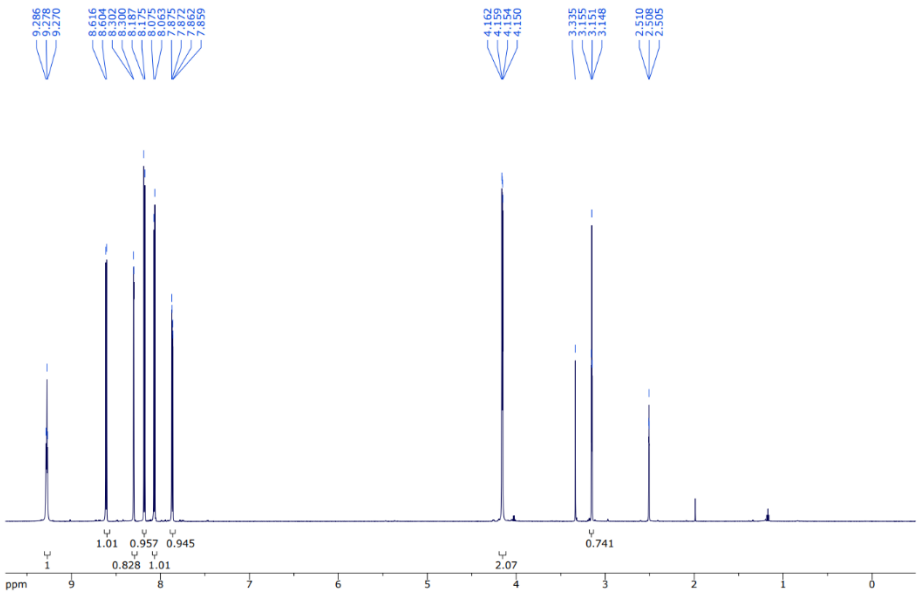
9.286
9.278
9.270
8.616
8.604
8.302
8.300
8.187
8.175
8.075
8.063
7.875
7.872
7.862
7.859
4.162
4.159
4.154
4.150
3.335
3.155
3.151
3.148
2.510
2.508
2.505
1.01
0.957
0.945
0.828
1.01
0.741
2.07
ppm

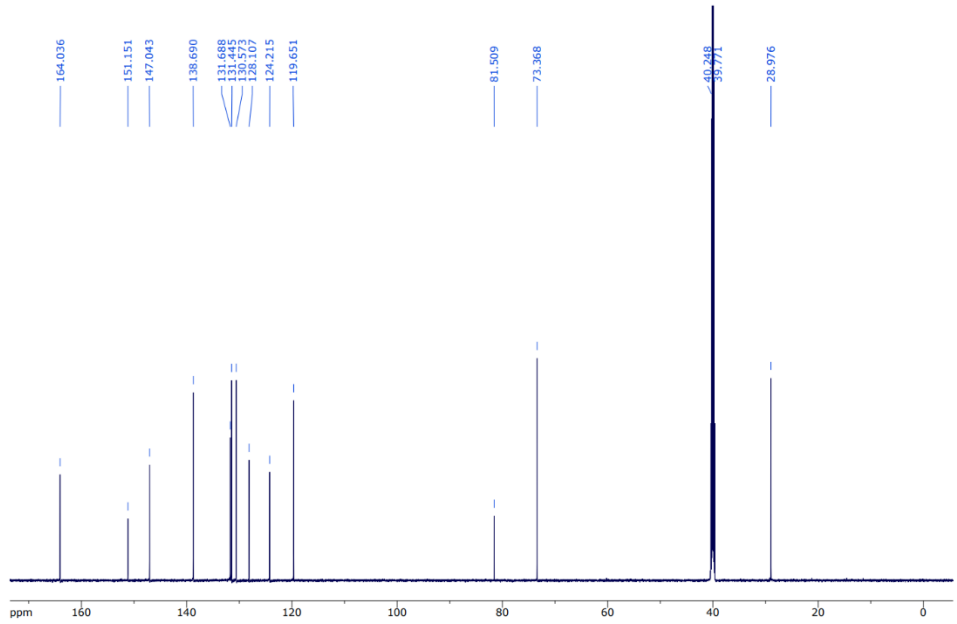
164.036
151.151
147.043
138.690
131.688
131.445
130.573
128.107
124.215
119.651
81.509
73.368
40.248
39.771
28.976
ppm

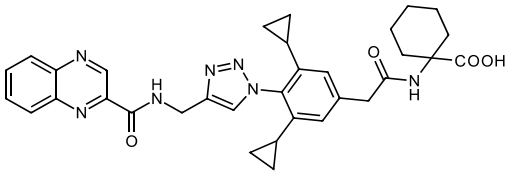

4a

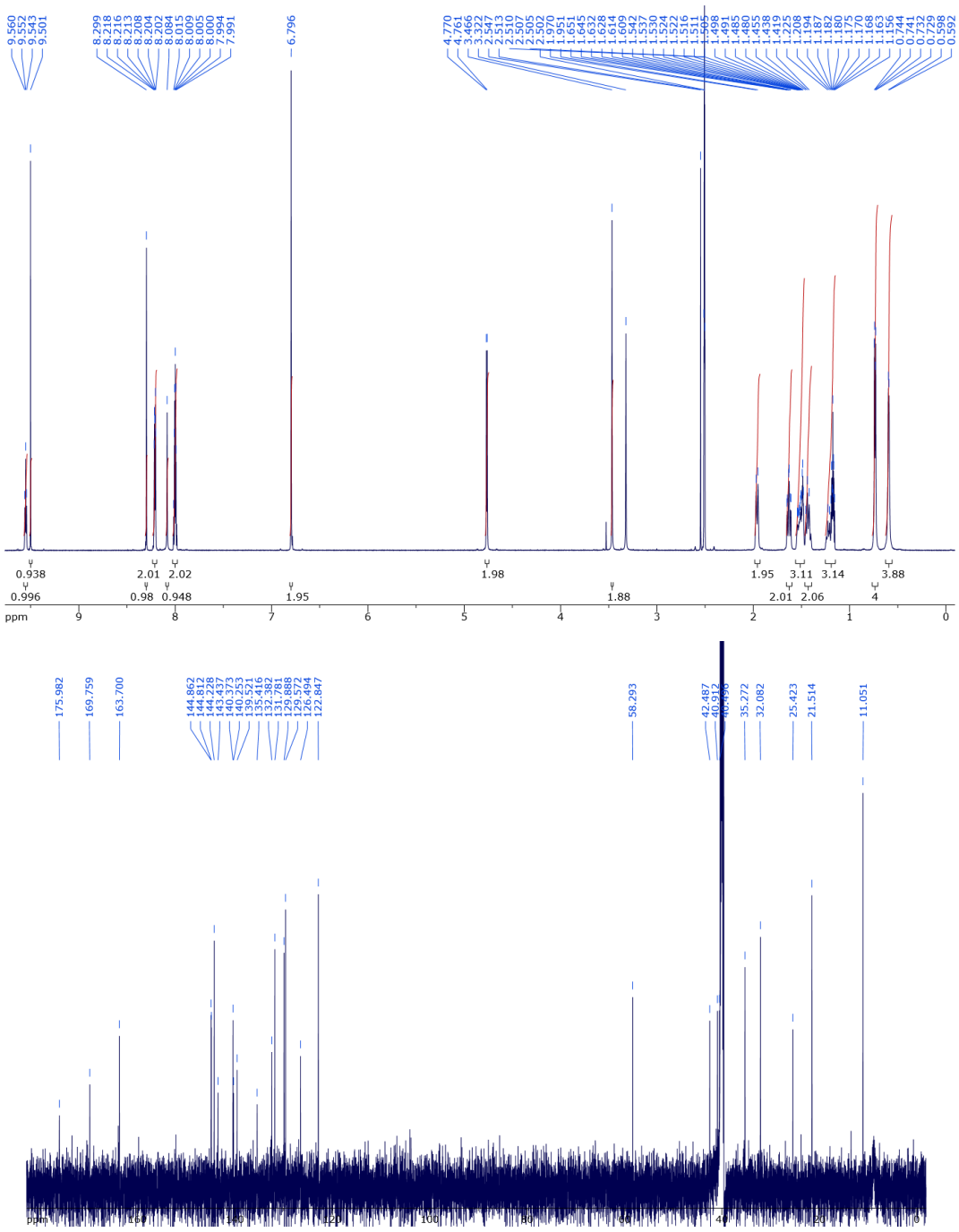

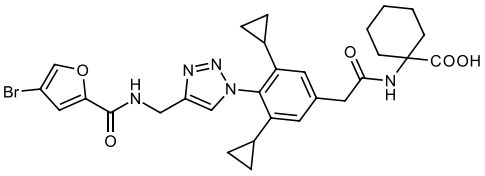
Br
O
O
H
N
N
N
O
N
H
COOH

4b

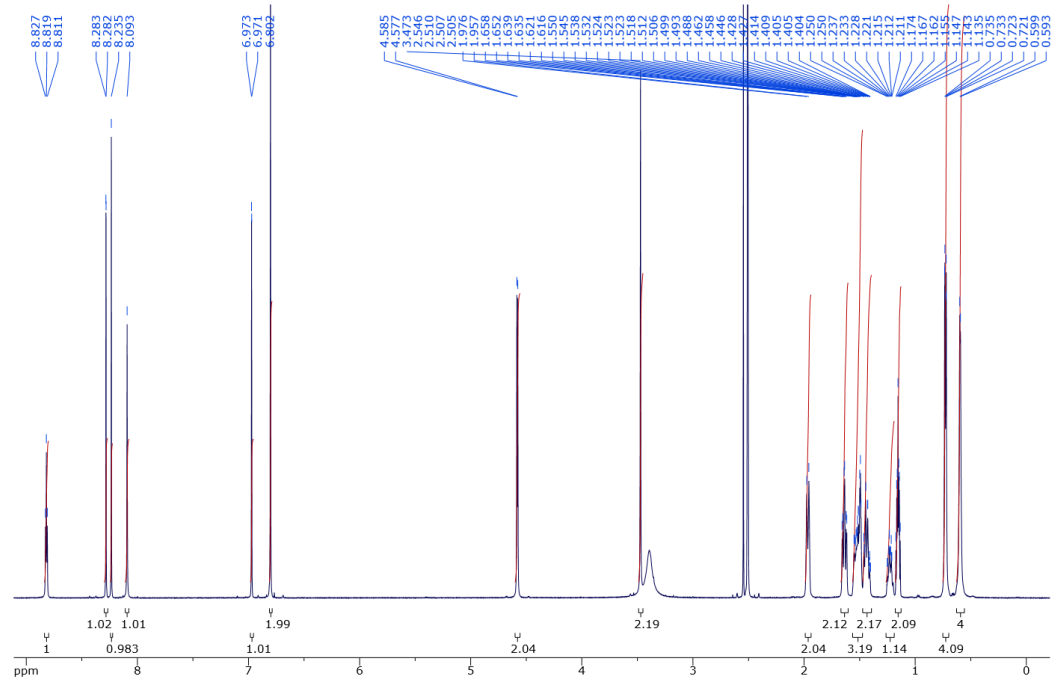
8.827
8.819
8.811
8.283
8.282
8.235
8.093
6.973
6.971
6.882
4.585
4.577
4.477
2.546
2.510
2.507
2.505
1.976
1.957
1.658
1.652
1.639
1.635
1.621
1.616
1.550
1.545
1.538
1.532
1.524
1.523
1.518
1.512
1.506
1.499
1.493
1.488
1.462
1.458
1.446
1.428
1.422
1.414
1.409
1.405
1.405
1.404
1.250
1.250
1.237
1.233
1.228
1.221
1.215
1.212
1.211
1.174
1.167
1.162
1.155
1.147
1.143
1.135
0.735
0.733
0.733
0.723
0.721
0.599
0.593
1.02
1.01
1.99
2.19
2.12
2.17
2.09
4
1
0.983
1.01
2.04
2.04
3.19
1.14
4.09
ppm

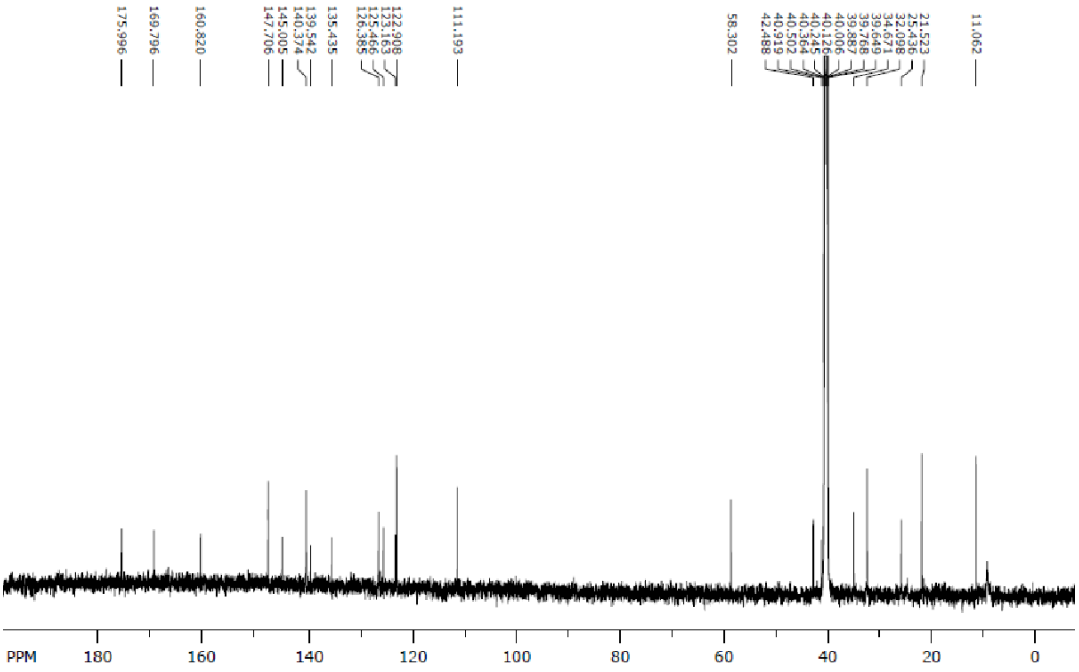
175.996
169.796
160.820
147.706
145.005
140.374
139.542
135.435
126.385
125.466
123.163
122.908
111.193
58.302
42.488
40.919
40.502
40.364
40.126
40.090
39.887
39.649
39.411
32.098
21.523
11.092
PPM

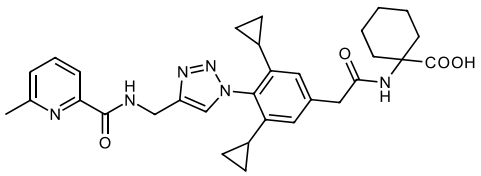
COOH

4c

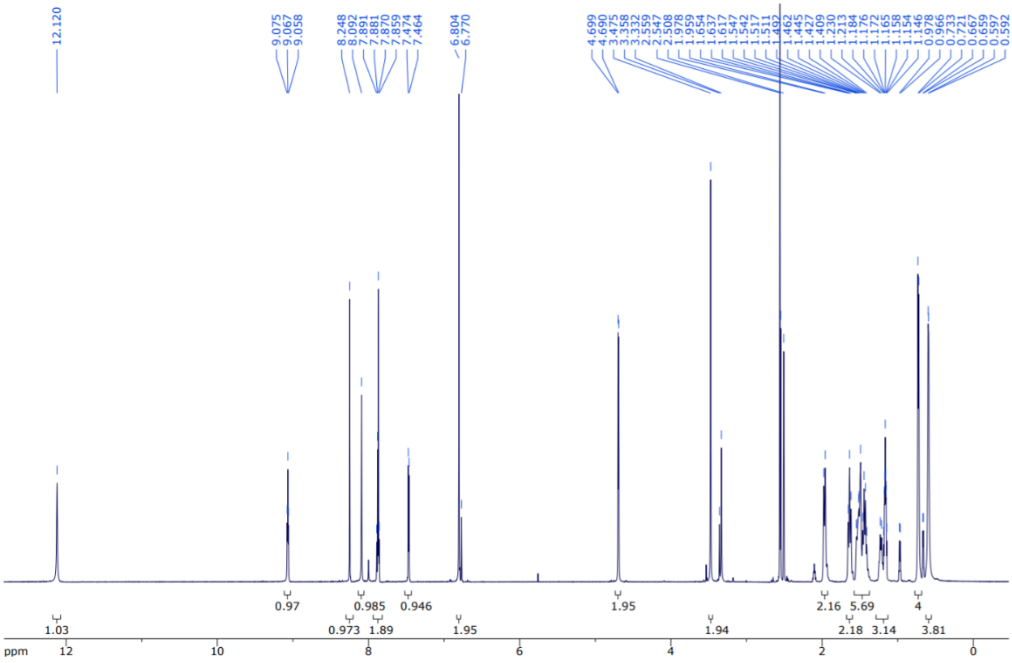
12.120
9.075
9.067
9.058
8.248
8.092
7.891
7.881
7.870
7.859
7.474
7.464
6.804
6.770
4.699
4.690
3.475
3.358
3.332
3.319
2.547
2.508
1.978
1.969
1.654
1.637
1.617
1.547
1.542
1.517
1.511
1.482
1.442
1.445
1.427
1.409
1.230
1.231
1.184
1.176
1.172
1.165
1.158
1.154
1.146
0.978
0.966
0.733
0.721
0.667
0.659
0.597
0.592
0.97
0.985
0.946
1.95
2.16
5.69
4
1.03
0.973
1.89
1.95
1.94
2.18
3.14
3.81
ppm
12
10
8
6
4
2
0

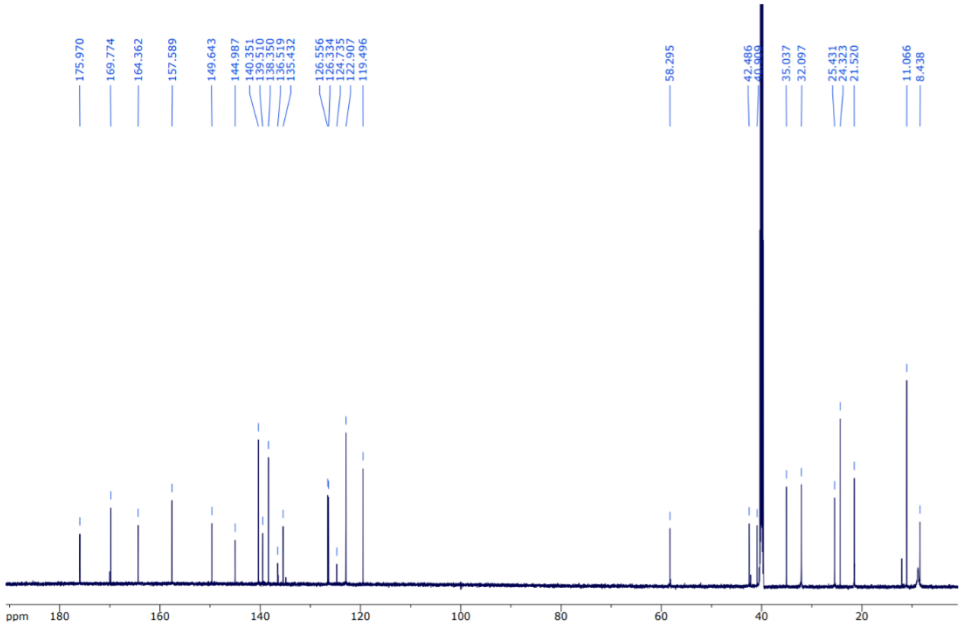
175.970
169.774
164.362
157.589
149.643
144.987
140.351
139.510
138.350
136.519
135.432
126.556
126.334
124.735
122.907
119.496
58.295
42.486
40.909
35.037
32.097
25.431
24.323
21.520
11.066
8.438
ppm
180
160
140
120
100
80
60
40
20

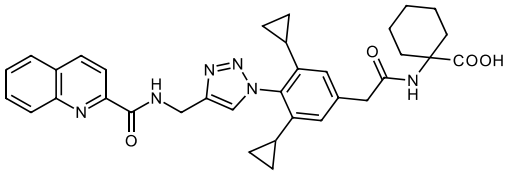
COOH
O
N
H
N
N
N
O
N
H
O

4d

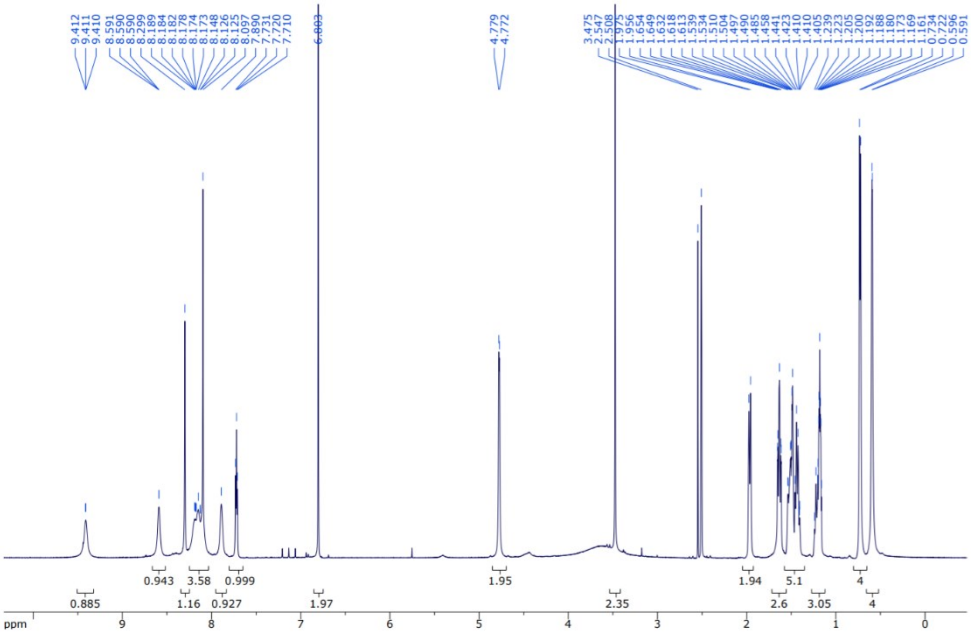
9.412
9.411
9.410
8.591
8.590
8.589
8.184
8.182
8.178
8.174
8.173
8.148
8.126
8.125
8.097
7.890
7.731
7.730
7.710
6.603
4.779
4.772
3.475
3.467
2.508
1.975
1.656
1.654
1.649
1.632
1.618
1.613
1.539
1.534
1.510
1.504
1.497
1.490
1.485
1.458
1.441
1.423
1.410
1.410
1.405
1.239
1.233
1.205
1.200
1.192
1.188
1.180
1.173
1.169
1.161
0.734
0.722
0.596
0.591
0.943
3.58
0.999
1.95
1.94
5.1
4
0.885
1.16
0.927
1.97
2.35
2.6
3.05
4
ppm
9
8
7
6
5
4
3
2
1
0

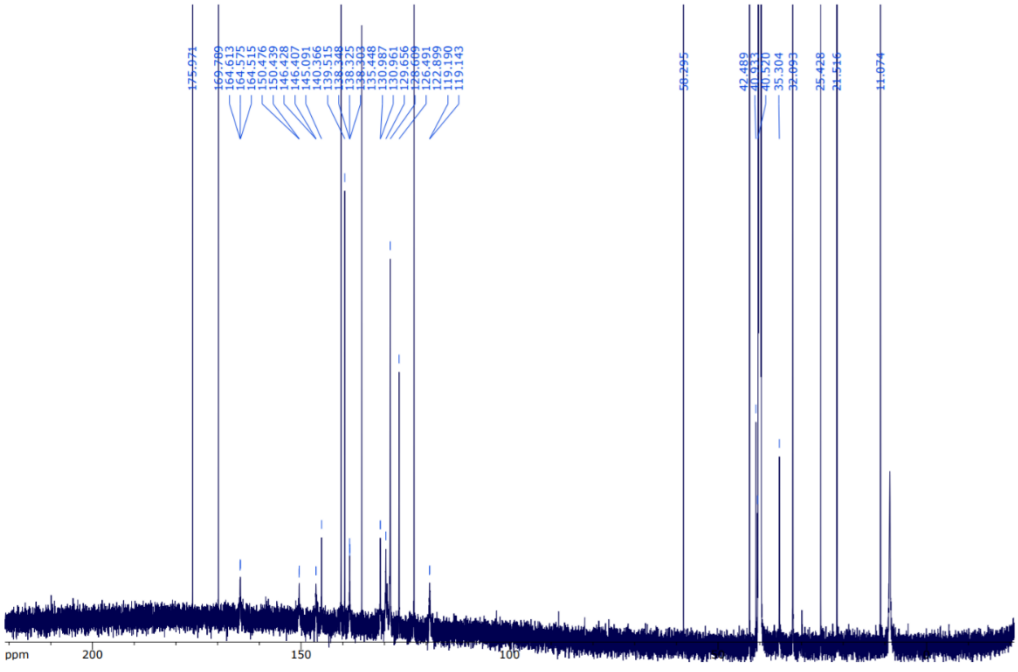
175.971
169.709
164.673
164.515
150.476
150.439
146.428
146.407
145.091
140.366
138.325
138.303
135.448
131.987
130.961
129.656
128.609
126.891
125.890
119.190
119.143
50.295
42.489
40.611
40.520
35.304
32.093
25.428
21.516
11.074
ppm
200
150
100

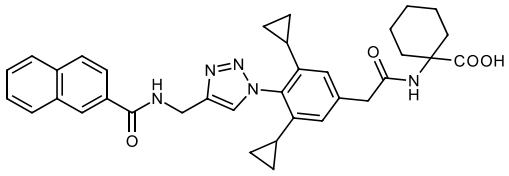
COOH
O
N
H
N
N
N
H
O

4e

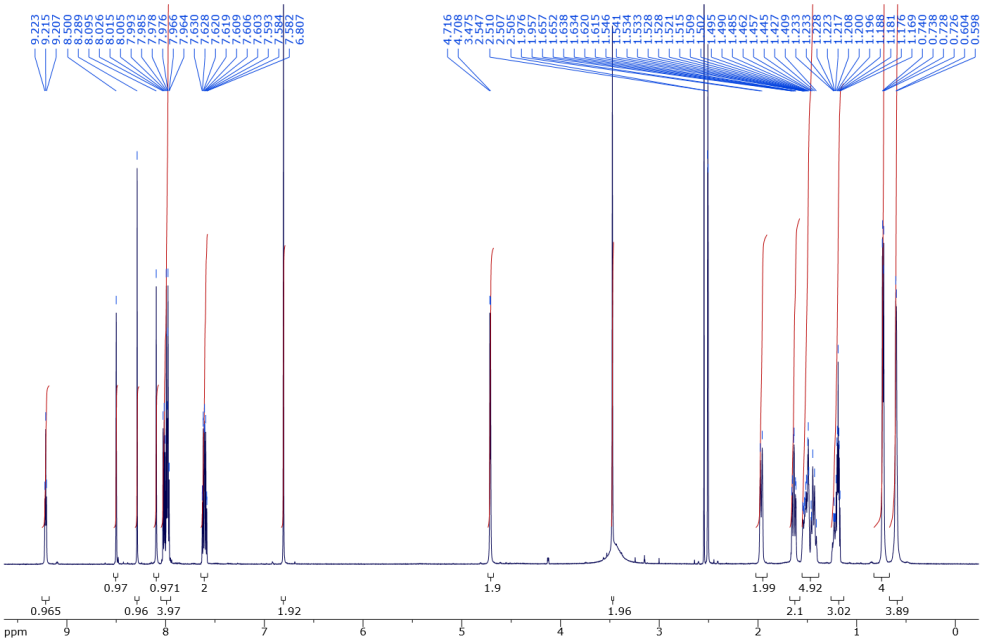
9.223
9.215
9.207
8.500
8.489
8.095
8.026
8.015
8.005
7.993
7.985
7.978
7.976
7.966
7.964
7.630
7.628
7.620
7.619
7.609
7.606
7.603
7.593
7.584
7.582
6.807
4.716
4.708
3.475
2.547
2.510
2.507
2.505
1.976
1.957
1.657
1.652
1.638
1.634
1.630
1.615
1.546
1.541
1.534
1.533
1.528
1.528
1.521
1.515
1.509
1.502
1.495
1.488
1.480
1.485
1.462
1.457
1.445
1.427
1.409
1.233
1.231
1.228
1.223
1.217
1.208
1.200
1.196
1.188
1.181
1.176
1.169
0.740
0.738
0.728
0.726
0.604
0.598
0.97
0.971
2
1.9
1.99
4.92
4
0.965
0.96
3.97
1.92
1.96
2.1
3.02
3.89
ppm

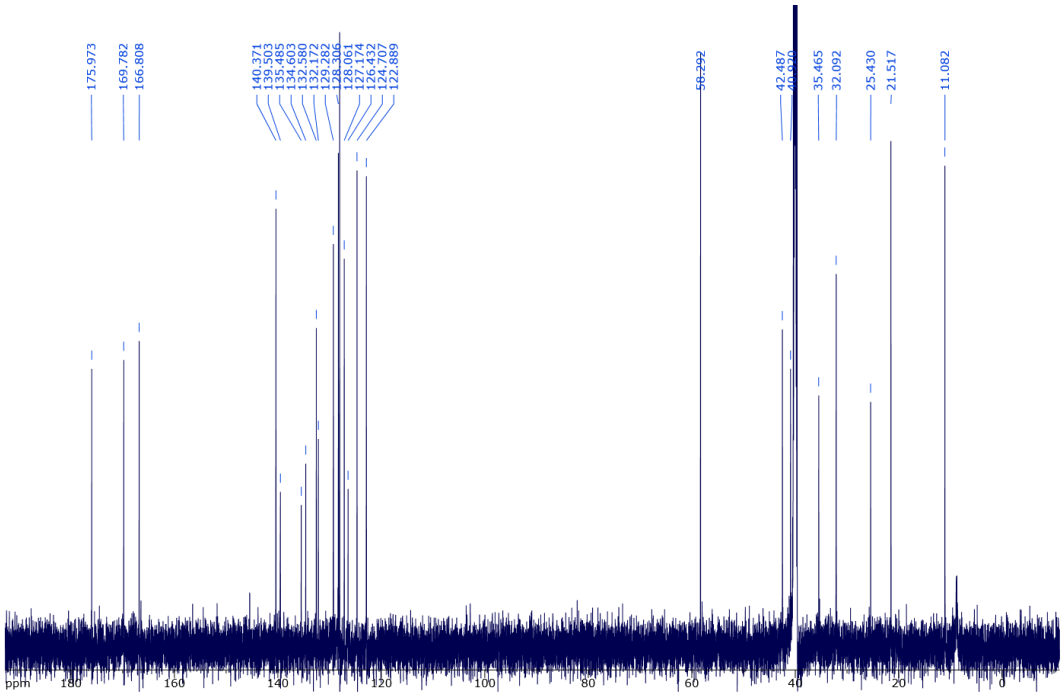
175.973
169.782
166.808
140.371
139.403
135.465
134.603
132.580
132.172
129.282
128.836
128.061
127.174
126.432
124.707
122.889
58.292
42.487
40.920
35.465
32.092
25.430
21.517
11.082
ppm

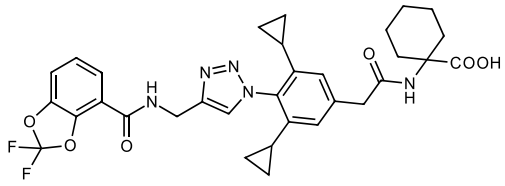
COOH
O
N
H
N
N
N
H
O
O
O
F
F

4f

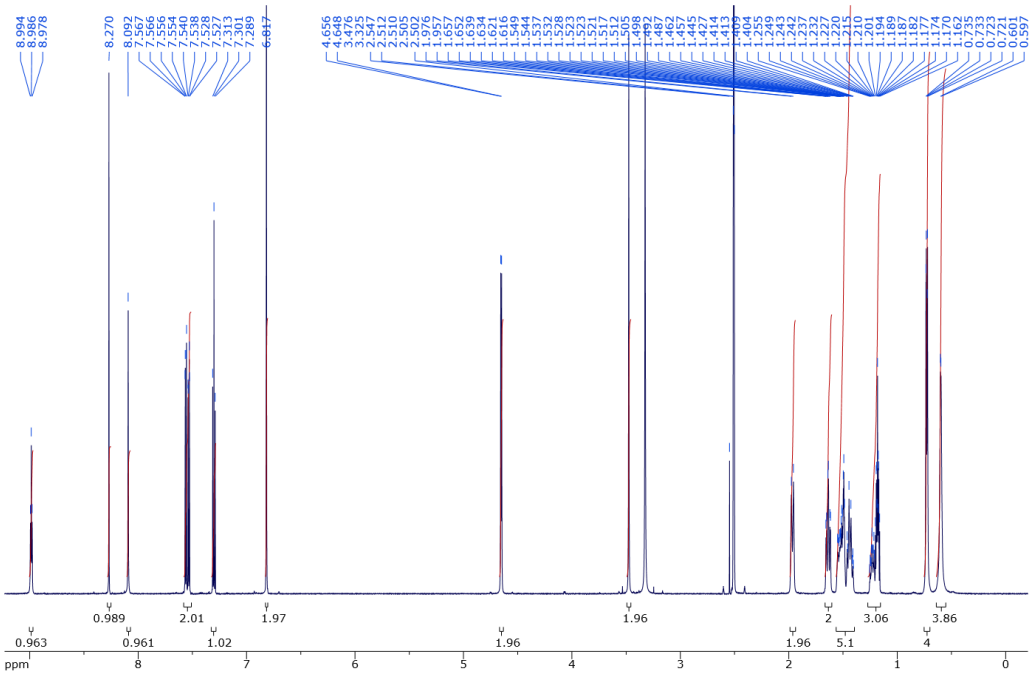
8.994
8.986
8.978
8.270
8.092
7.567
7.566
7.556
7.554
7.540
7.538
7.528
7.527
7.311
7.310
7.289
6.817
4.656
4.648
4.476
3.325
2.547
2.512
2.510
2.505
2.502
1.976
1.657
1.652
1.639
1.634
1.621
1.616
1.549
1.544
1.537
1.532
1.528
1.523
1.521
1.517
1.512
1.505
1.498
1.492
1.488
1.462
1.457
1.445
1.427
1.414
1.413
1.405
1.404
1.255
1.249
1.243
1.242
1.237
1.232
1.227
1.220
1.215
1.210
1.201
1.194
1.189
1.187
1.182
1.177
1.174
1.170
1.162
0.735
0.733
0.723
0.721
0.601
0.597
0.989
2.01
1.97
1.96
2
3.06
3.86
0.963
0.961
1.02
1.96
1.96
5.1
4
ppm

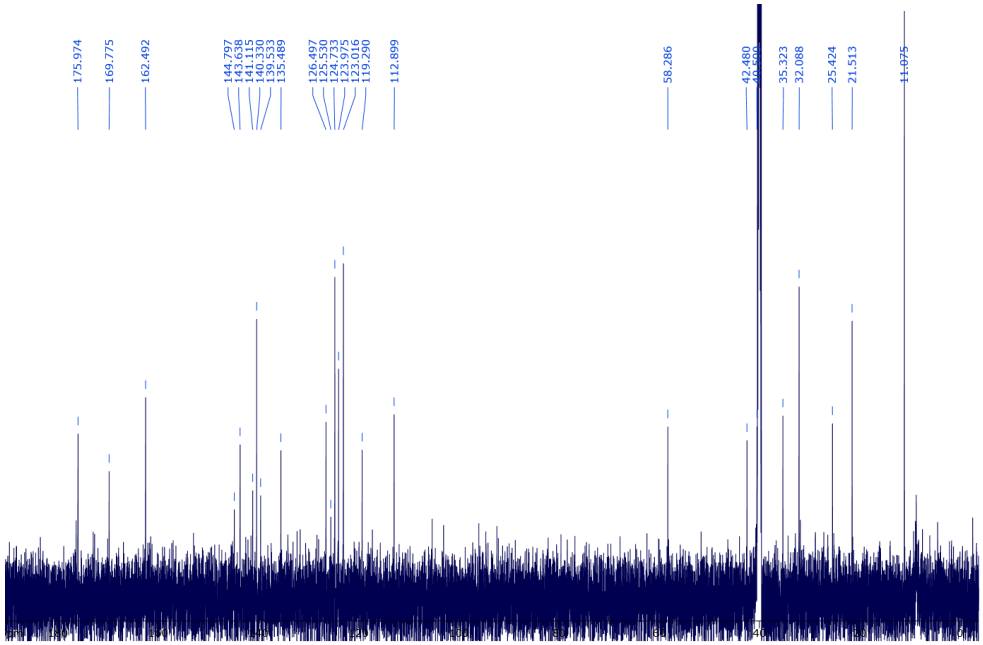
175.974
169.775
162.492
144.797
143.638
141.115
140.780
139.533
135.489
126.497
125.530
124.733
124.575
123.016
119.290
112.899
58.286
42.480
40.500
35.323
32.088
25.424
21.513
11.075

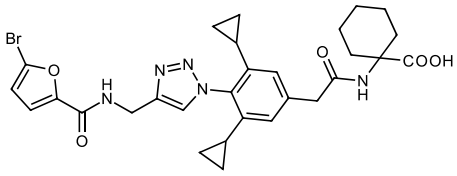
Br
O
H
N
O
N=N
N
O
N
H
COOH

4g

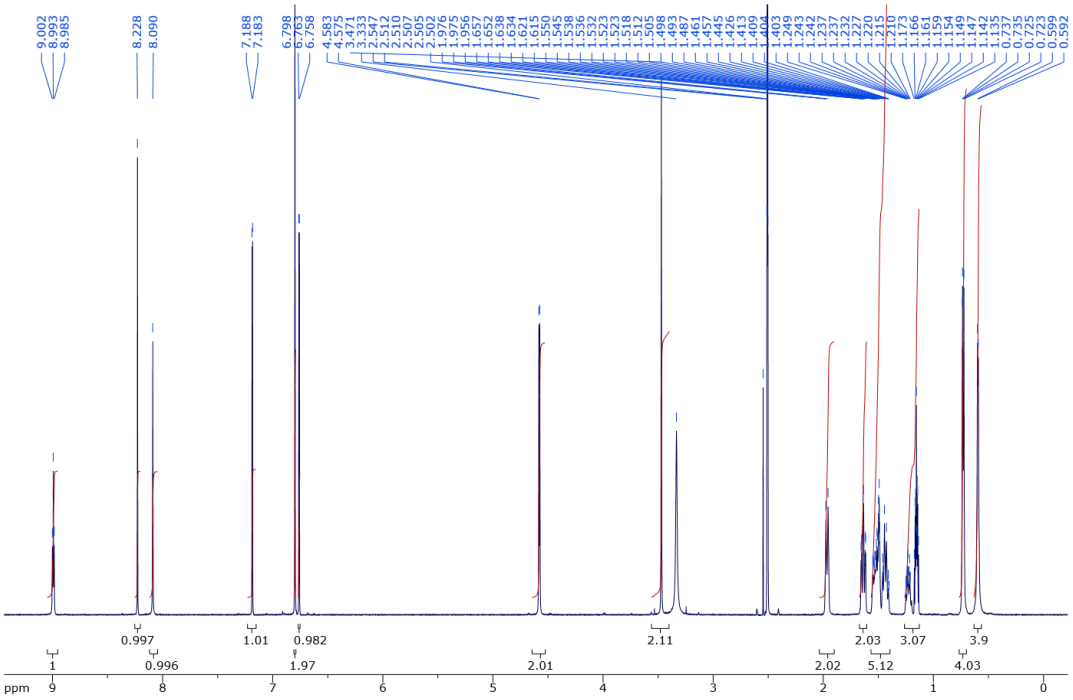
9.002
8.993
8.985
8.228
8.090
7.188
7.183
6.798
6.763
6.758
4.583
4.575
3.471
3.333
2.547
2.512
2.510
2.507
2.505
2.502
2.076
1.975
1.956
1.657
1.652
1.638
1.634
1.621
1.615
1.550
1.545
1.538
1.536
1.532
1.523
1.523
1.518
1.512
1.505
1.498
1.493
1.487
1.461
1.457
1.445
1.426
1.413
1.409
1.404
1.403
1.249
1.243
1.242
1.237
1.237
1.232
1.227
1.220
1.215
1.173
1.166
1.161
1.159
1.154
1.149
1.147
1.142
1.135
0.737
0.735
0.725
0.723
0.599
0.592
0.997
1.01
0.982
2.11
2.03
3.07
3.9
1
0.996
1.97
2.01
2.02
5.12
4.03
ppm
9
8
7
6
5
4
3
2
1
0

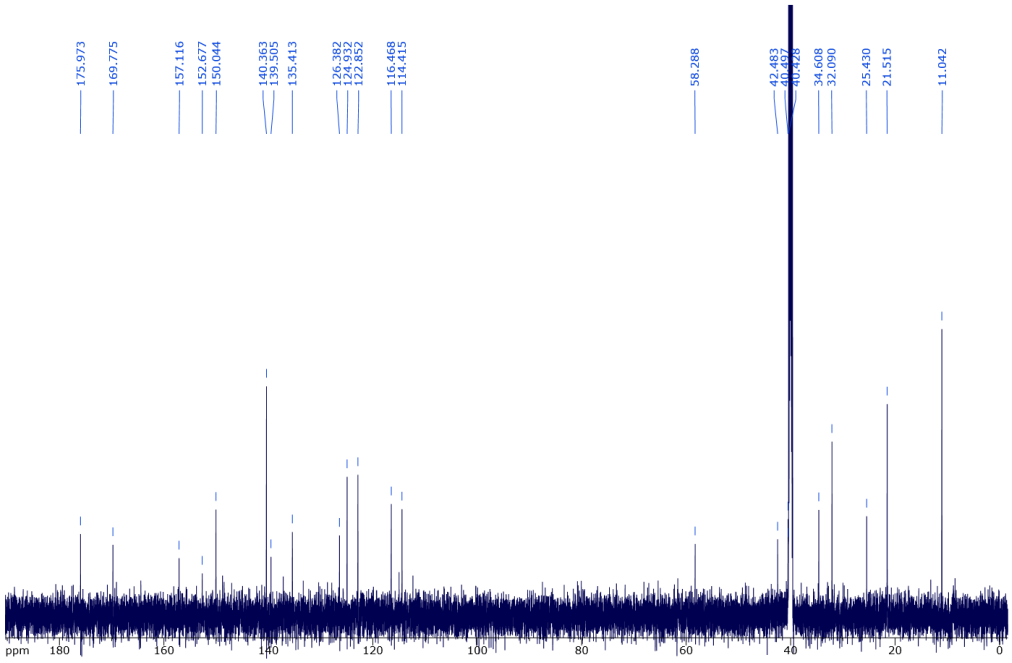
175.973
169.775
157.116
152.677
150.044
140.363
139.505
135.413
126.382
124.932
122.852
116.468
114.415
58.288
42.483
42.457
40.428
34.608
32.090
25.430
21.515
11.042
ppm
180
160
140
120
100
80
60
40
20
0

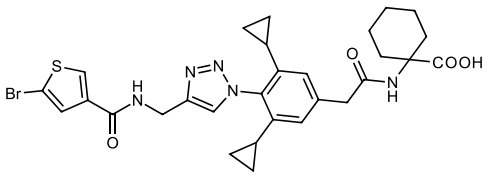
Br
S
O
H
N
N=N
N
O
N
H
COOH

4h

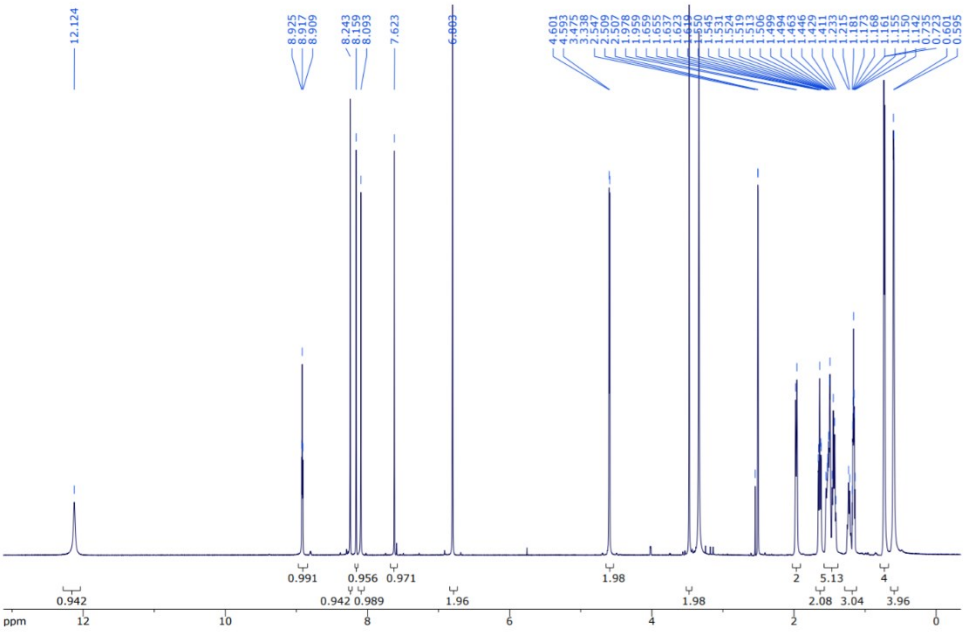
12.124
8.925
8.917
8.909
8.243
8.159
8.093
7.623
6.883
4.601
4.573
4.475
3.338
2.547
2.509
2.507
1.978
1.959
1.659
1.655
1.637
1.623
1.618
1.550
1.545
1.531
1.514
1.519
1.513
1.506
1.499
1.494
1.463
1.446
1.429
1.411
1.233
1.215
1.181
1.173
1.168
1.161
1.155
1.150
1.142
1.135
0.723
0.601
0.595
0.942
0.991
0.942 0.989
0.956 0.971
1.96
1.98
1.98
2
5.13
2.08 3.04
4
3.96
ppm
12
10
8
6
4
2
0

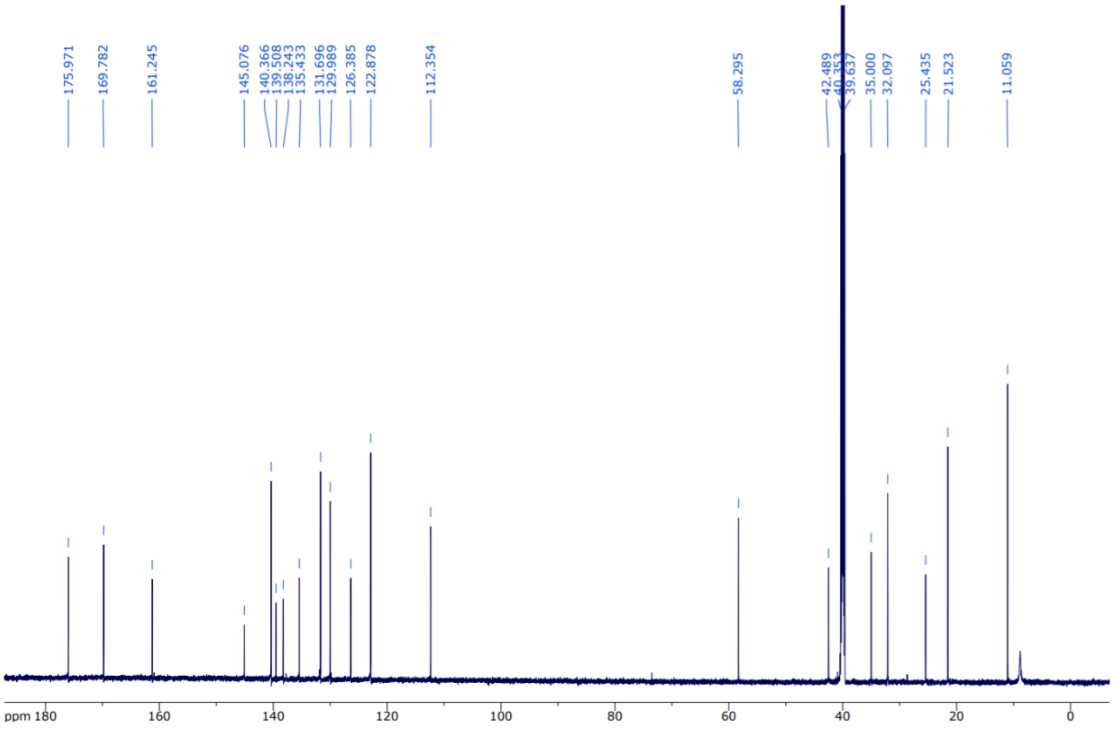
175.971
169.782
161.245
145.076
140.366
139.508
139.243
135.433
131.696
129.989
126.385
122.878
112.354
58.295
42.489
40.353
39.637
35.000
32.097
25.435
21.523
11.059
ppm 180
160
140
120
100
80
60
40
20
0

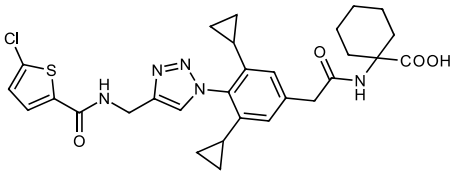
Cl
S
O
H
N
N=N
N
O
N
H
COOH

4i

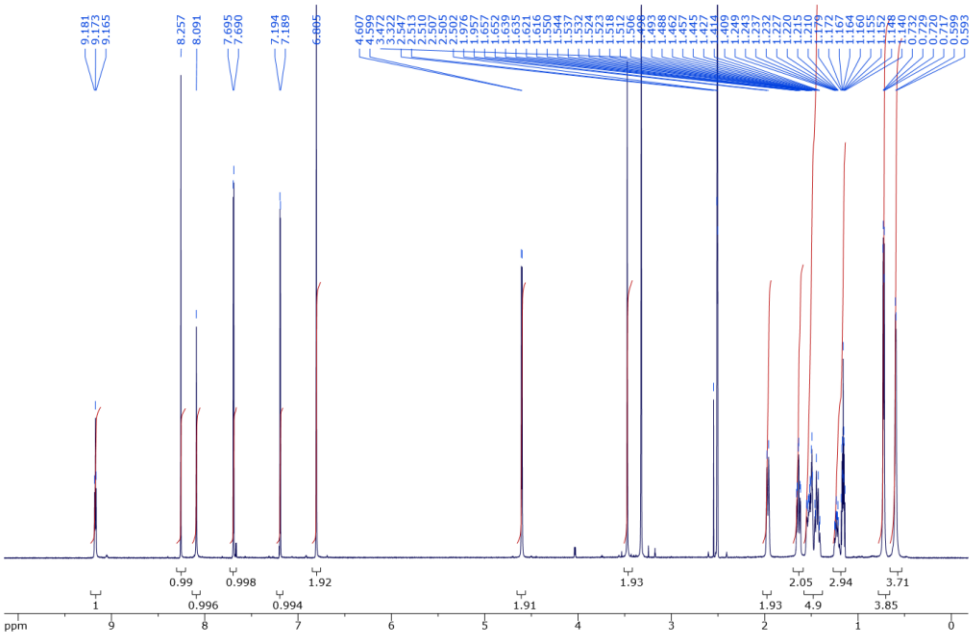
9.181
9.173
9.165
8.257
8.091
7.695
7.690
7.194
7.189
6.805
4.607
4.599
4.472
3.342
2.513
2.510
2.507
2.502
1.976
1.657
1.652
1.639
1.635
1.621
1.616
1.550
1.544
1.537
1.532
1.524
1.518
1.512
1.506
1.493
1.488
1.462
1.455
1.445
1.427
1.414
1.409
1.249
1.243
1.237
1.232
1.227
1.220
1.215
1.210
1.179
1.172
1.167
1.164
1.160
1.155
1.152
1.148
1.140
0.732
0.729
0.720
0.717
0.599
0.593
0.99
0.998
1.92
1.93
2.05
2.94
3.71
1
0.996
0.994
1.91
1.93
4.9
3.85
ppm
9
8
7
6
5
4
3
2
1
0

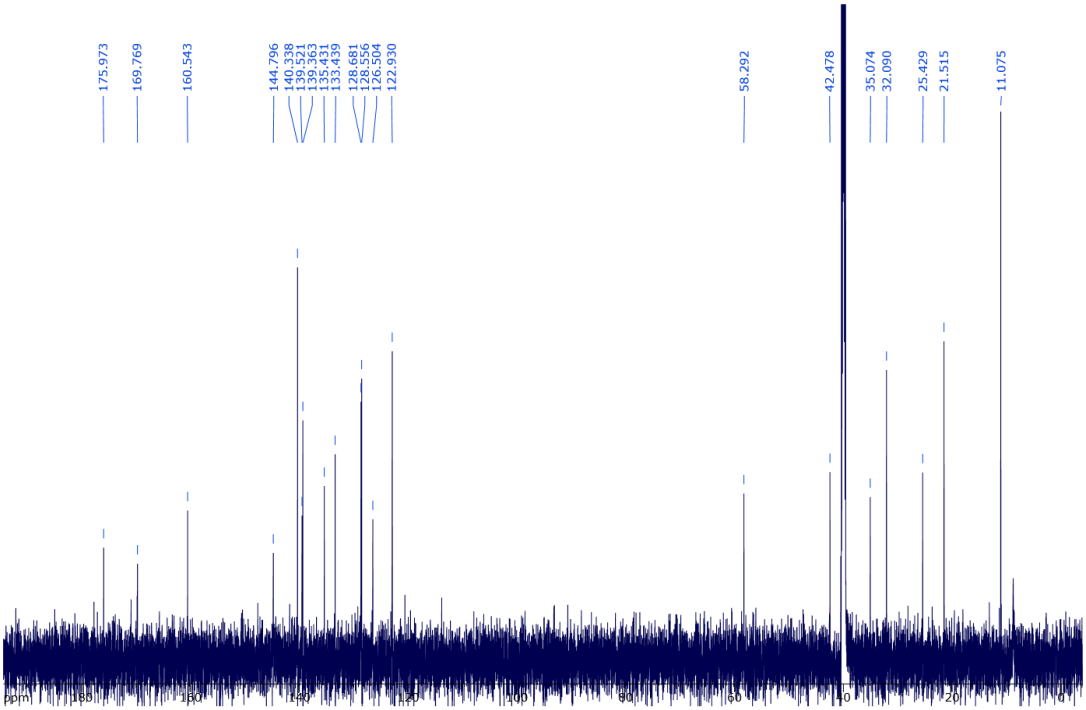
175.973
169.769
160.543
144.796
140.338
139.521
139.363
135.431
133.439
128.681
128.556
126.504
122.930
58.292
42.478
35.074
32.090
25.429
21.515
11.075
ppm
180
160
140
120
100
80
60
40
20
0

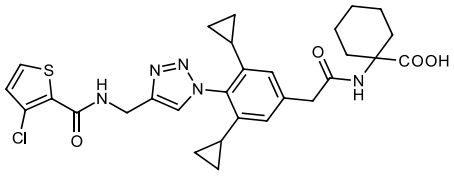
S
Cl
O
H
N
N=N
N
O
N
H
COOH

4j

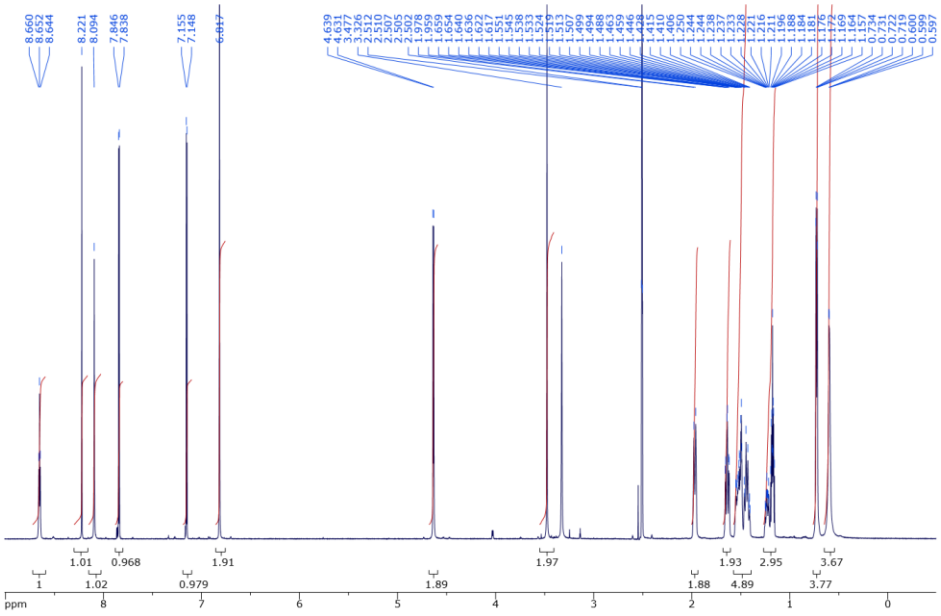
8.660
8.652
8.644
8.221
8.094
7.846
7.838
7.155
7.148
6.817
1.01
0.968
1.91
1.97
1.93
2.95
3.67
1.02
0.979
1.89
1.88
4.89
3.77
ppm

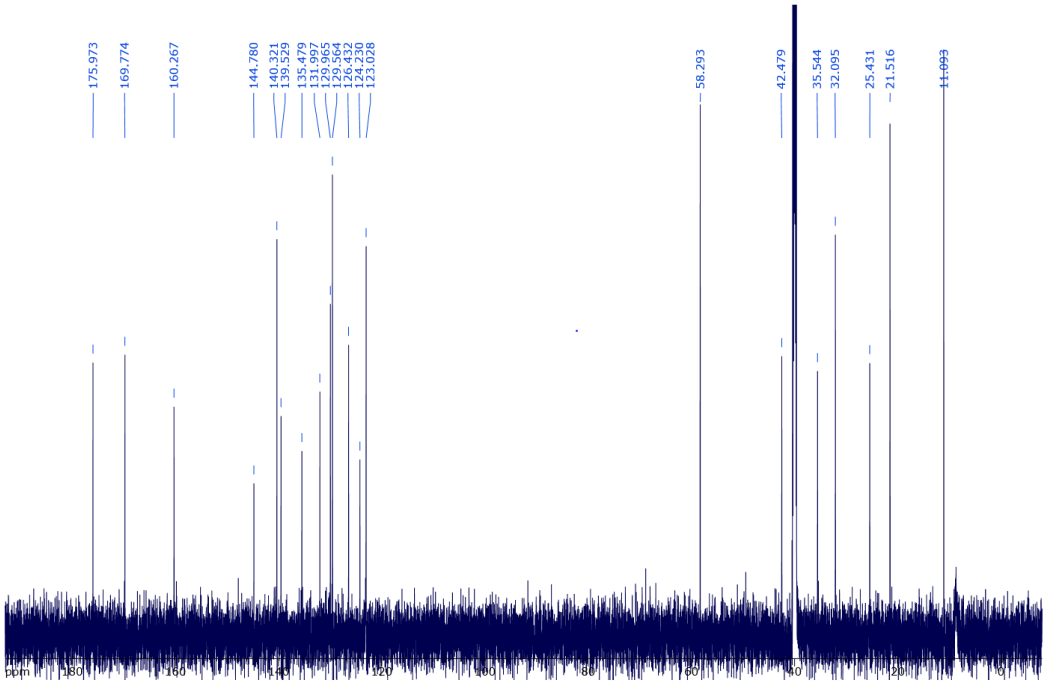
175.973
169.774
160.267
144.780
140.321
139.529
135.479
131.997
129.565
129.564
126.432
124.230
123.028
58.293
42.479
35.544
32.095
25.431
21.516
11.093
ppm

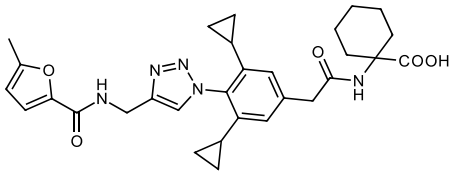
O
H
N
N=N
N
O
N
H
COOH

4k

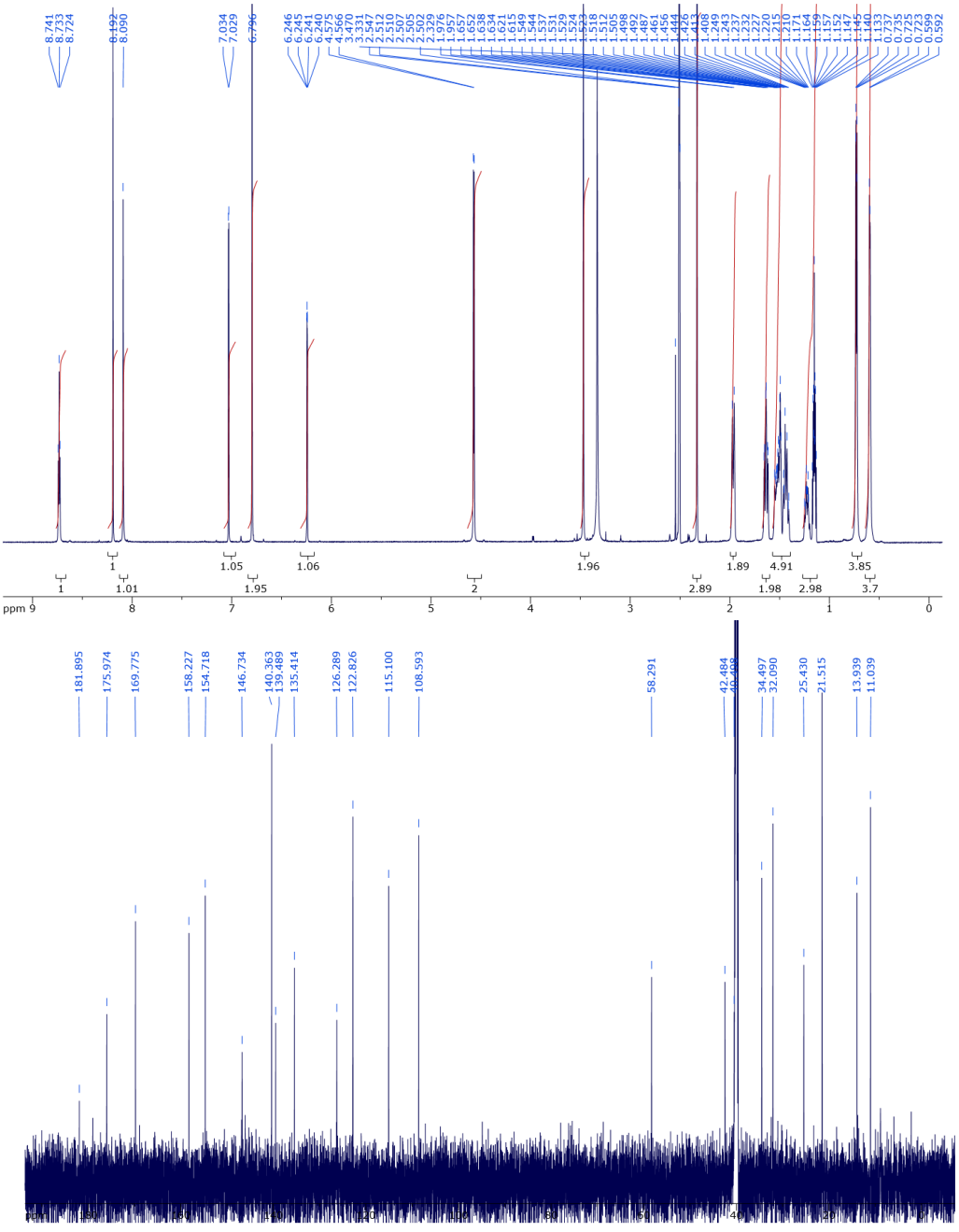
8.741
8.733
8.724
8.492
8.090
7.034
7.029
6.796
6.246
6.245
6.241
6.240
4.575
4.566
3.470
3.331
2.547
2.512
2.510
2.507
2.505
2.502
2.392
2.389
1.976
1.957
1.657
1.652
1.638
1.634
1.621
1.615
1.549
1.544
1.537
1.531
1.529
1.524
1.523
1.518
1.512
1.505
1.498
1.492
1.487
1.461
1.456
1.444
1.426
1.408
1.249
1.243
1.237
1.232
1.227
1.220
1.215
1.210
1.171
1.164
1.159
1.157
1.152
1.147
1.145
1.140
1.137
0.737
0.735
0.725
0.723
0.599
0.592
1
1.01
1.05
1.95
1.06
2
1.96
2.89
1.89
1.98
4.91
2.98
3.85
3.7
ppm 9
8
7
6
5
4
3
2
1
0
181.895
175.974
169.775
158.227
154.718
146.734
140.363
139.489
135.414
126.289
122.826
115.100
108.593
58.291
42.484
40.000
34.497
32.090
25.430
21.515
13.939
11.039

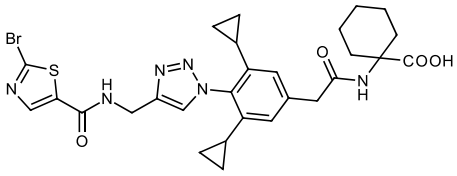
Br
S
N
H
N
O
N=N
N
O
N
H
COOH

4l

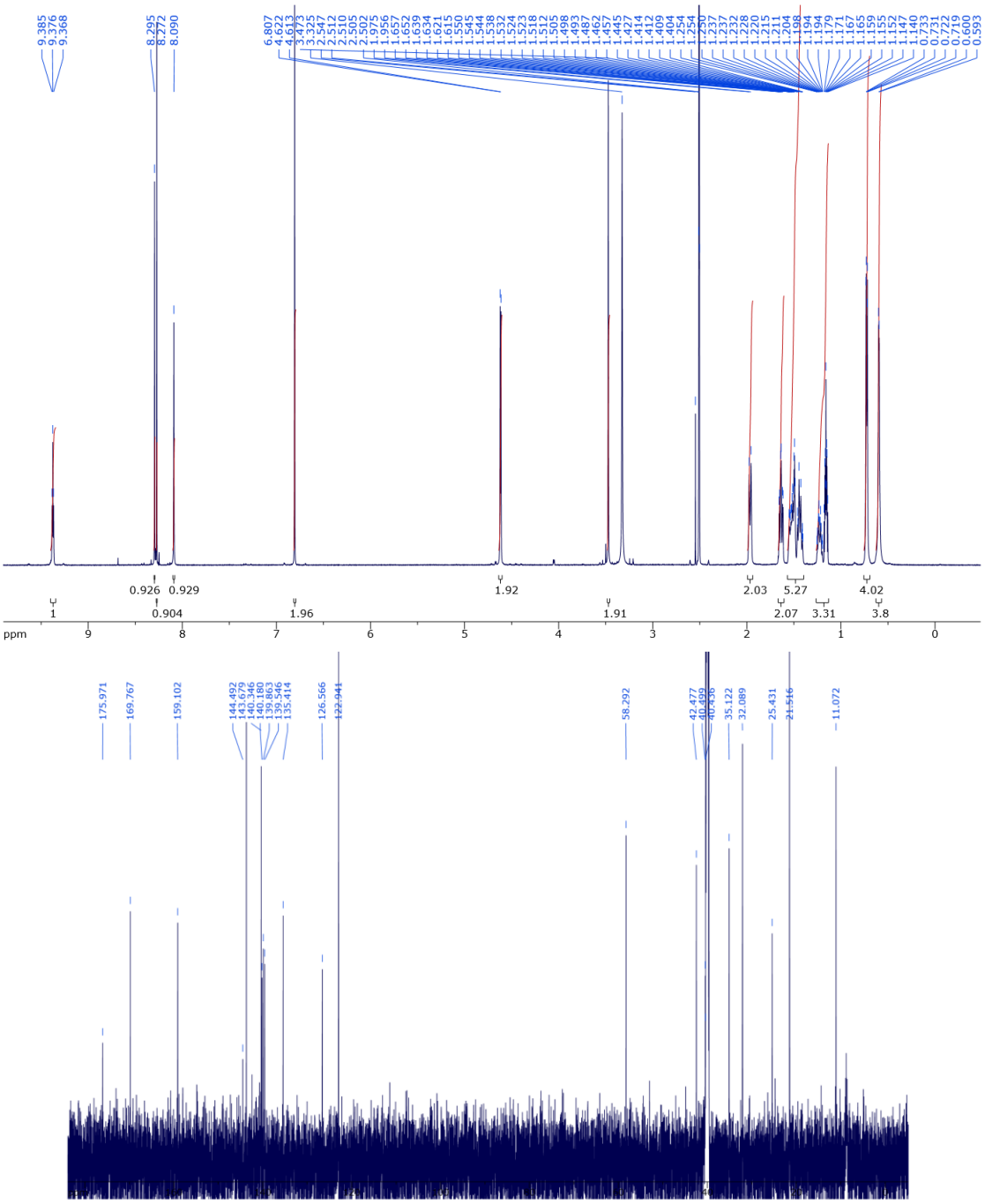
9.385
9.376
9.368
8.295
8.272
8.090
6.807
4.622
4.613
3.473
3.325
2.547
2.512
2.510
2.505
2.502
1.975
1.956
1.657
1.652
1.639
1.634
1.621
1.615
1.550
1.545
1.544
1.538
1.532
1.524
1.523
1.518
1.512
1.505
1.498
1.493
1.487
1.462
1.457
1.445
1.427
1.414
1.412
1.409
1.404
1.254
1.254
1.237
1.237
1.237
1.232
1.228
1.220
1.215
1.211
1.204
1.198
1.194
1.194
1.194
1.179
1.171
1.167
1.165
1.159
1.155
1.152
1.147
1.140
0.733
0.722
0.719
0.600
0.593
0.926
0.929
1.92
2.03
5.27
4.02
1
0.904
1.96
1.91
2.07
3.31
3.8
ppm
9
8
7
6
5
4
3
2
1
0
175.971
169.767
159.102
144.492
143.679
140.346
140.180
139.863
139.546
135.414
126.566
122.941
58.292
42.477
40.499
40.436
35.122
32.089
25.431
21.516
11.072

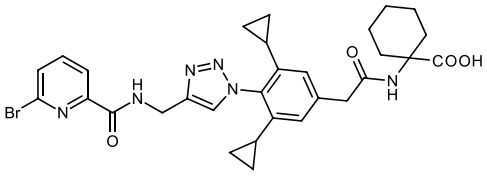
Br
N
O
H
N
N
N
O
N
H
COOH

4m

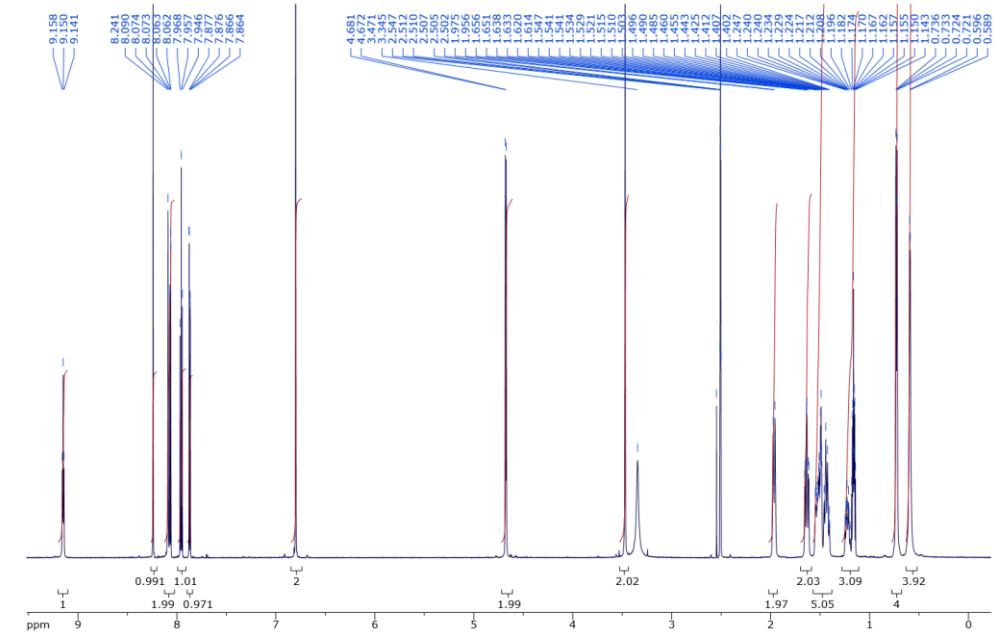
9.158
9.150
9.141
8.241
8.090
8.074
8.073
8.063
8.062
7.968
7.957
7.956
7.877
7.876
7.866
7.864
4.681
4.672
3.471
3.347
3.345
2.512
2.510
2.507
2.505
2.502
1.975
1.956
1.651
1.638
1.633
1.620
1.614
1.547
1.541
1.534
1.529
1.521
1.515
1.510
1.503
1.496
1.490
1.485
1.460
1.455
1.443
1.425
1.412
1.402
1.247
1.240
1.240
1.234
1.229
1.224
1.217
1.212
1.208
1.196
1.182
1.174
1.170
1.167
1.162
1.157
1.155
1.130
1.114
0.736
0.733
0.724
0.721
0.596
0.589
0.991
1.01
2
2.02
2.03
3.09
3.92
1
1.99
0.971
1.99
1.97
5.05
4
ppm

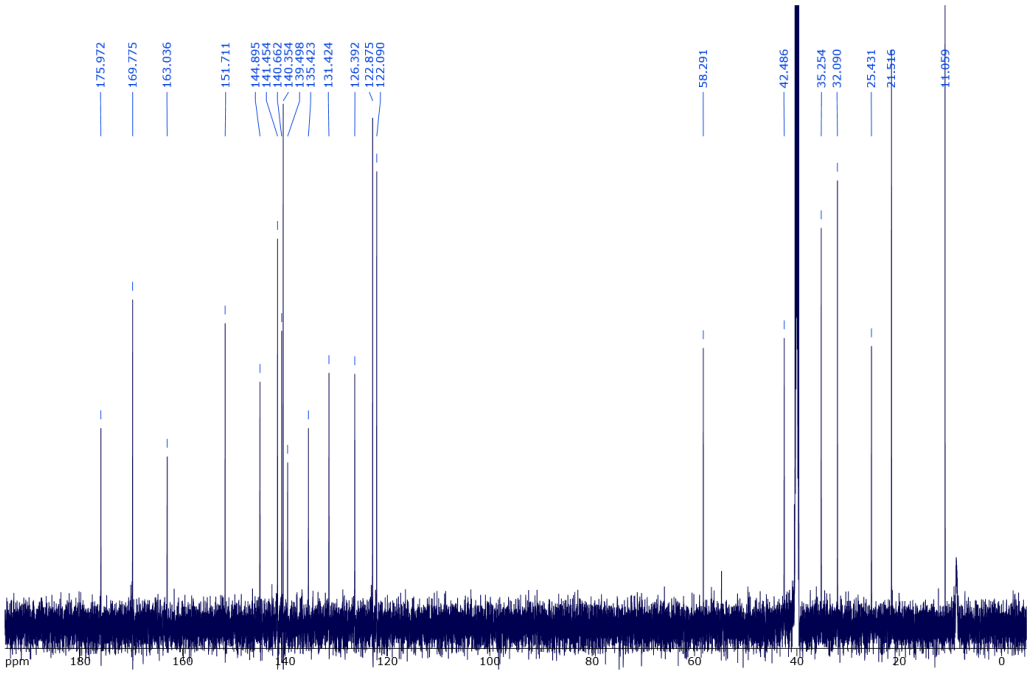
175.972
169.775
163.036
151.711
144.895
141.454
140.662
140.354
139.498
135.423
131.424
126.392
122.875
122.090
58.291
42.486
35.254
32.090
25.431
21.516
11.059
ppm

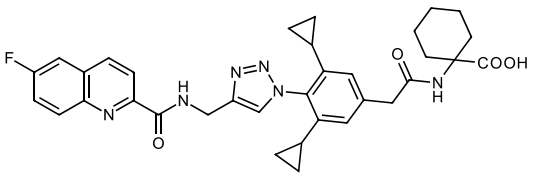
F
N
O
H
N
N=N
N
O
N
H
COOH

4o

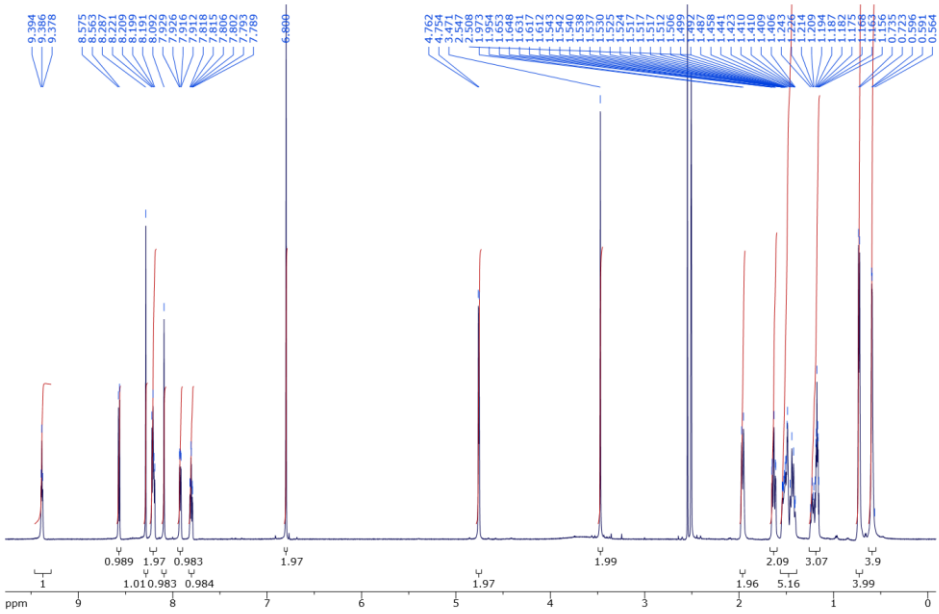
9.394
9.386
9.378
8.575
8.563
8.287
8.271
8.209
8.199
8.191
8.092
7.929
7.926
7.916
7.911
7.818
7.815
7.806
7.802
7.793
7.789
6.890
4.762
4.754
3.547
2.508
1.973
1.964
1.653
1.648
1.631
1.617
1.612
1.543
1.540
1.538
1.537
1.530
1.525
1.524
1.517
1.517
1.512
1.506
1.499
1.497
1.487
1.468
1.441
1.423
1.410
1.410
1.409
1.406
1.243
1.226
1.214
1.199
1.194
1.187
1.182
1.175
1.168
1.163
0.735
0.725
0.723
0.596
0.581
0.564
0.989
1.97
0.983
1.97
1.99
2.09
3.07
3.9
1
1.01
0.983
0.984
1.97
1.96
5.16
3.99
ppm
9
8
7
6
5
4
3
2
1
0

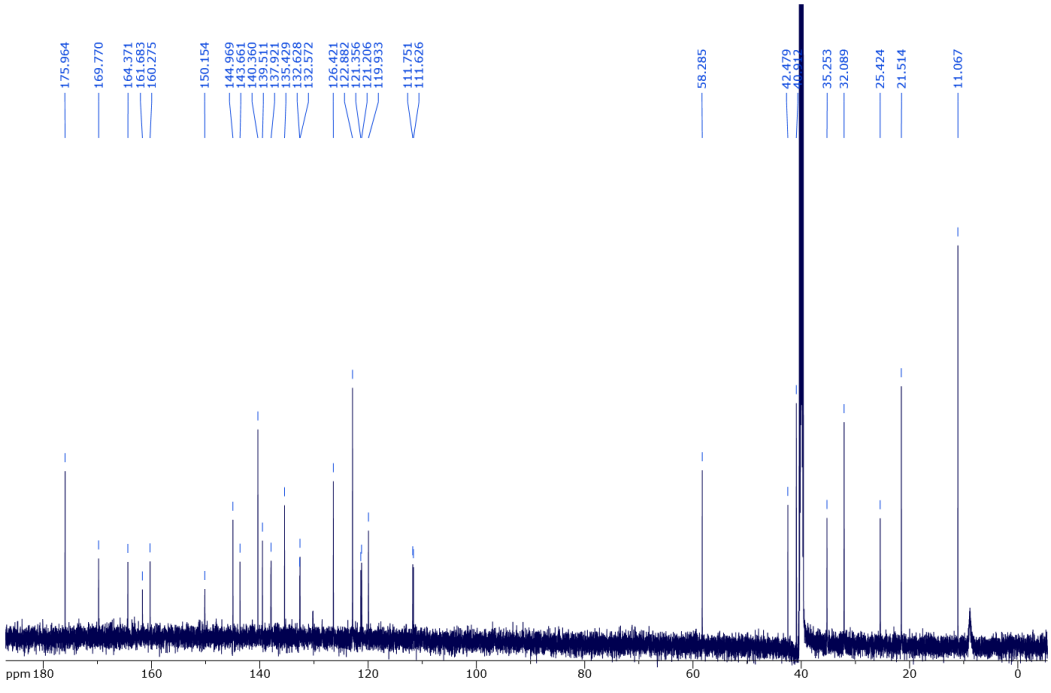
175.964
169.770
164.371
161.683
160.275
150.154
144.969
143.661
140.360
139.511
137.921
135.429
132.628
132.572
126.421
122.882
121.356
121.206
119.933
111.751
111.626
58.285
42.479
40.033
35.253
32.089
25.424
21.514
11.067
ppm
180
160
140
120
100
80
60
40
20
0

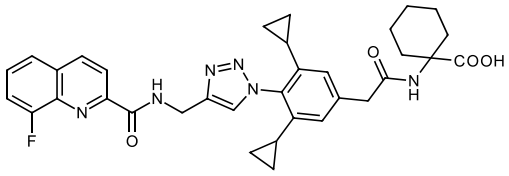
COOH
O
N
H
N
N
N
H
N
O
F

4n

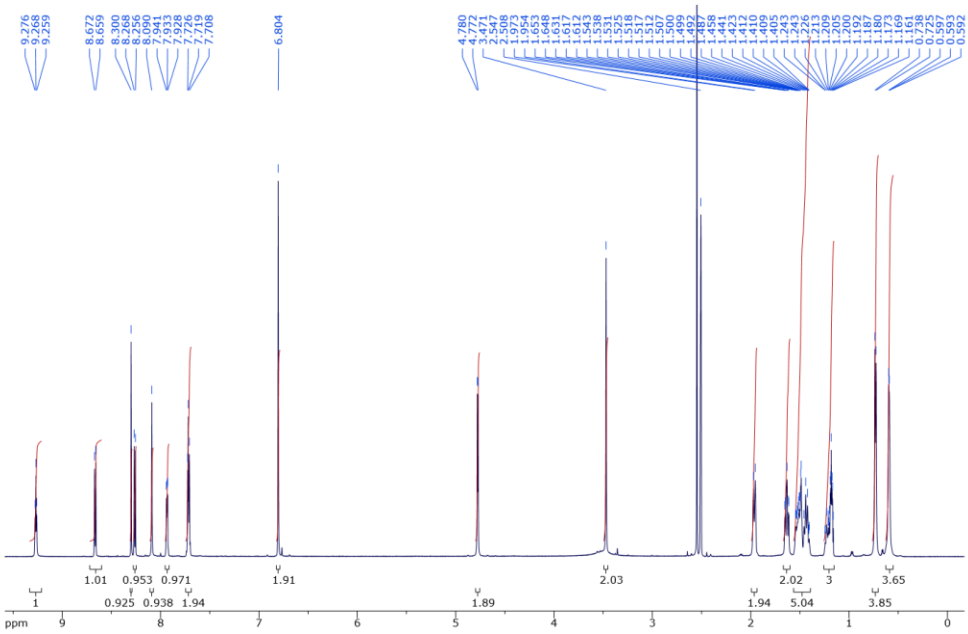
9.276
9.268
9.259
8.672
8.659
8.300
8.268
8.256
8.090
7.941
7.933
7.928
7.726
7.719
7.708
6.804
4.780
4.777
3.471
2.547
2.508
2.073
1.954
1.653
1.648
1.631
1.617
1.612
1.543
1.538
1.531
1.525
1.518
1.517
1.512
1.507
1.500
1.499
1.492
1.487
1.468
1.441
1.423
1.412
1.410
1.409
1.405
1.243
1.233
1.226
1.213
1.209
1.205
1.200
1.192
1.187
1.180
1.173
1.169
1.161
0.738
0.725
0.597
0.593
0.592
1.01
0.953
0.971
1.91
2.03
2.02
3
3.65
1
0.925
0.938
1.94
1.89
1.94
5.04
3.85
ppm
9
8
7
6
5
4
3
2
1
0

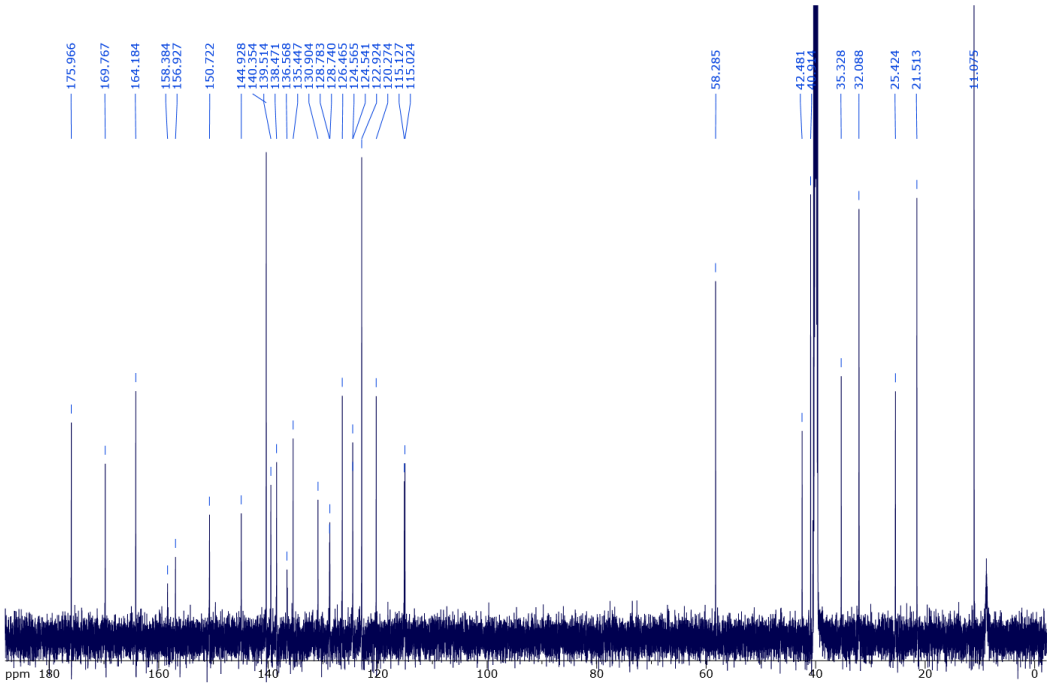
175.966
169.767
164.184
158.384
156.927
150.722
144.928
140.354
139.514
138.471
136.568
135.447
130.984
128.783
128.740
126.465
124.565
124.541
122.924
120.274
115.127
115.024
58.285
42.481
40.014
35.328
32.088
25.424
21.513
11.075
ppm
180
160
140
120
100
80
60
40
20
0

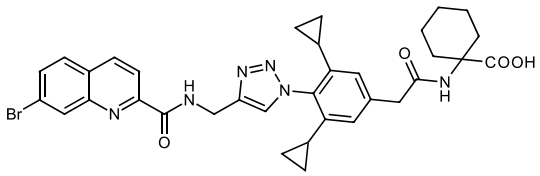

4p

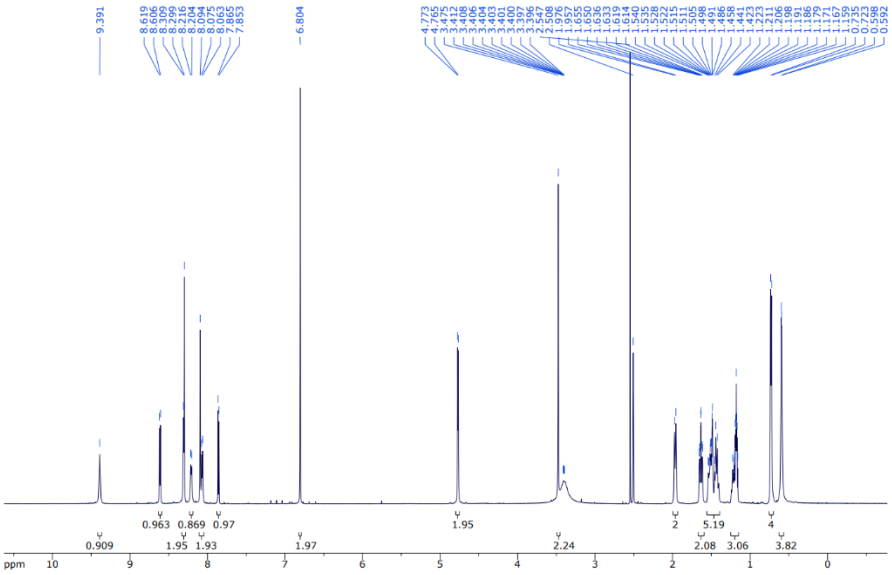

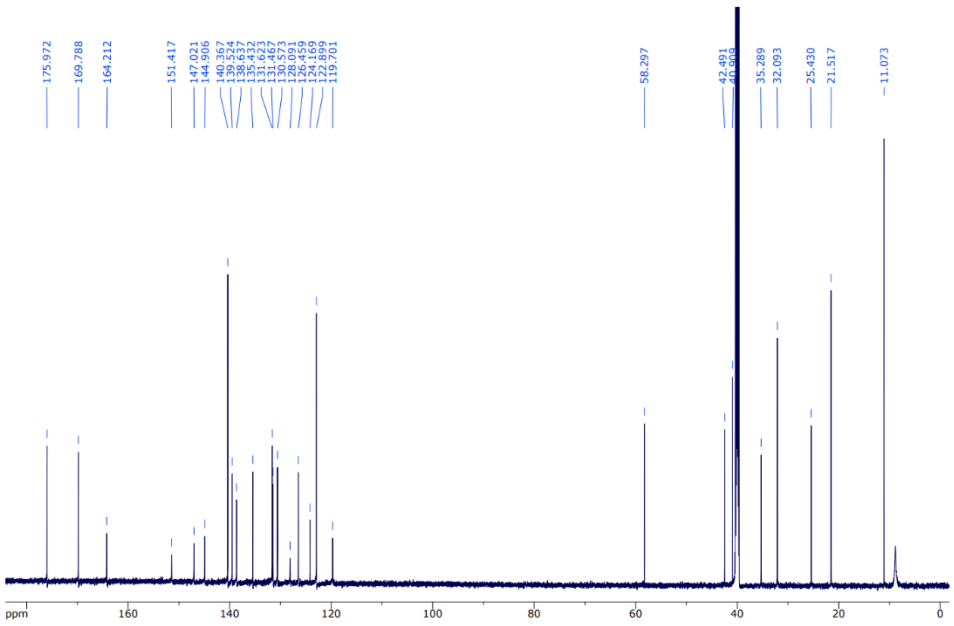

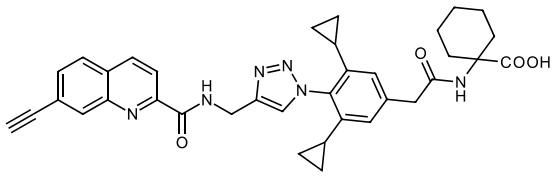

4q

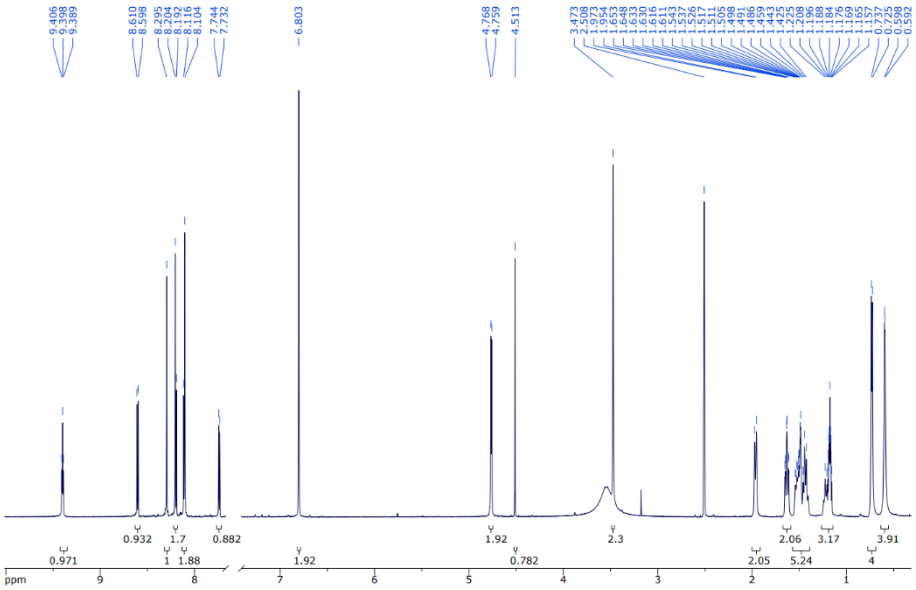

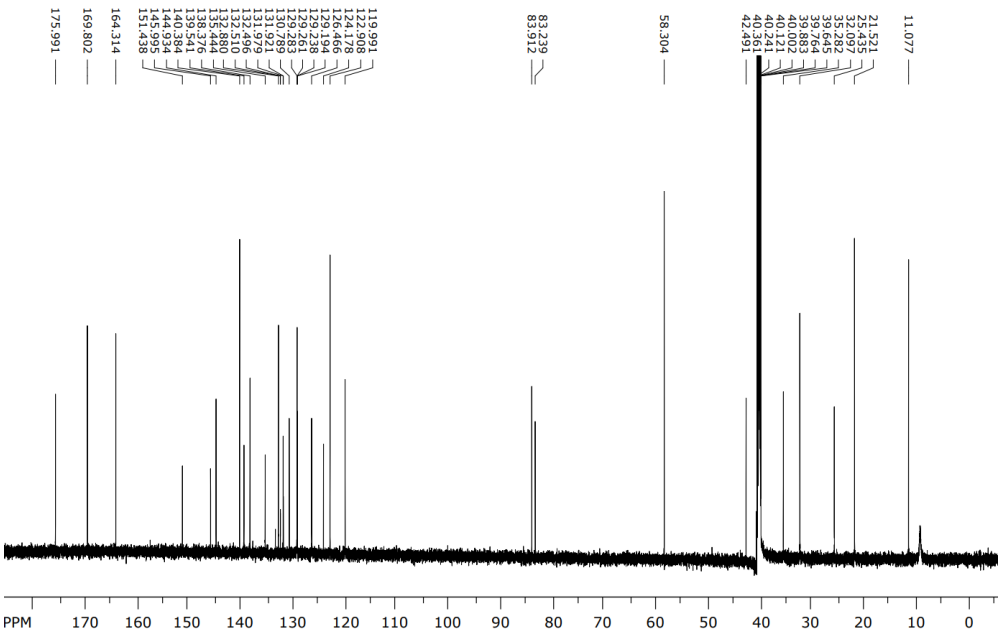

4r (TAMRA-ANT)

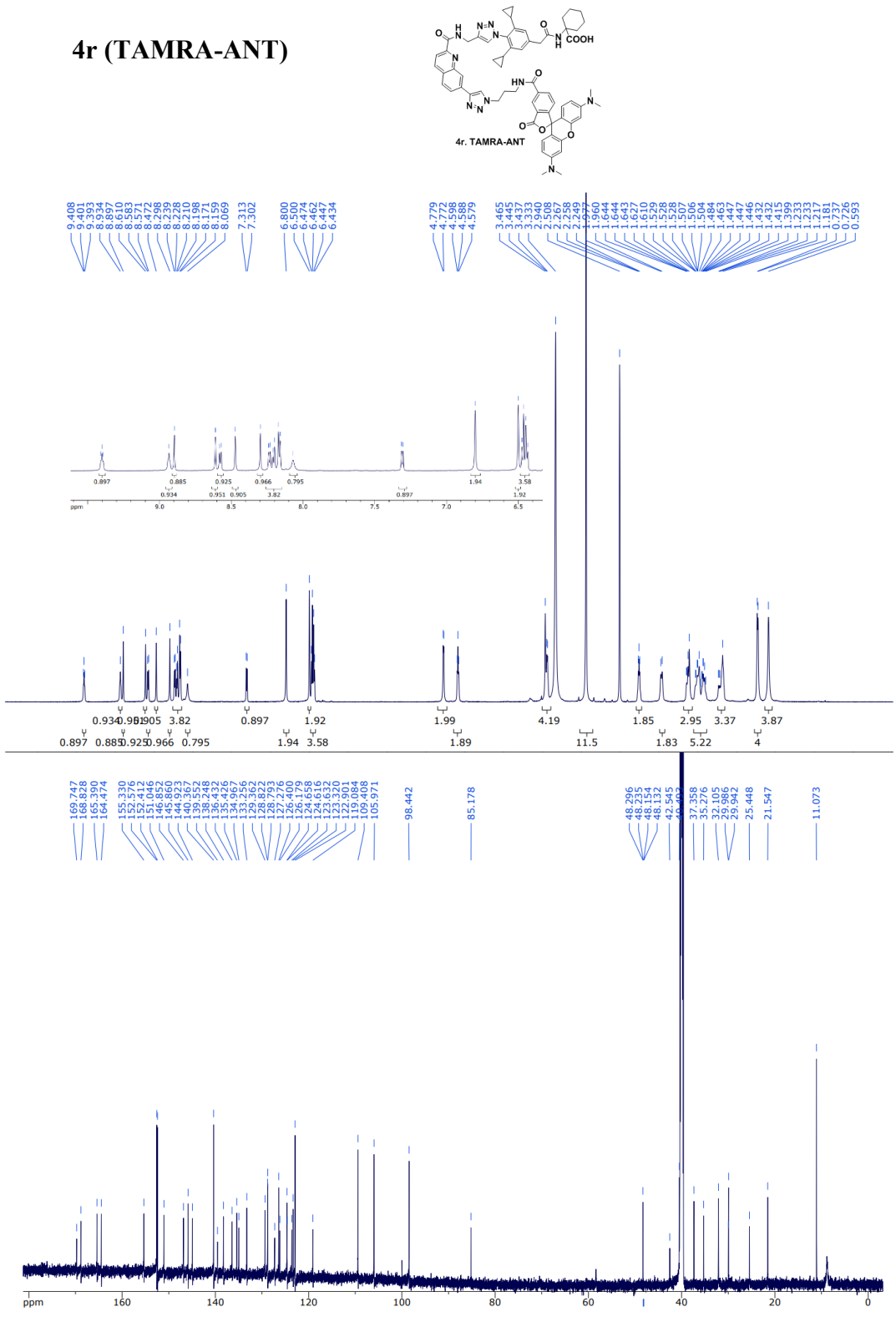

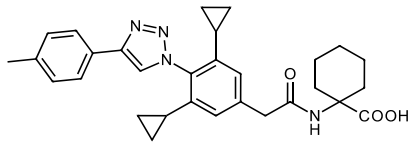
N
N
N
O
N
H
COOH

T1

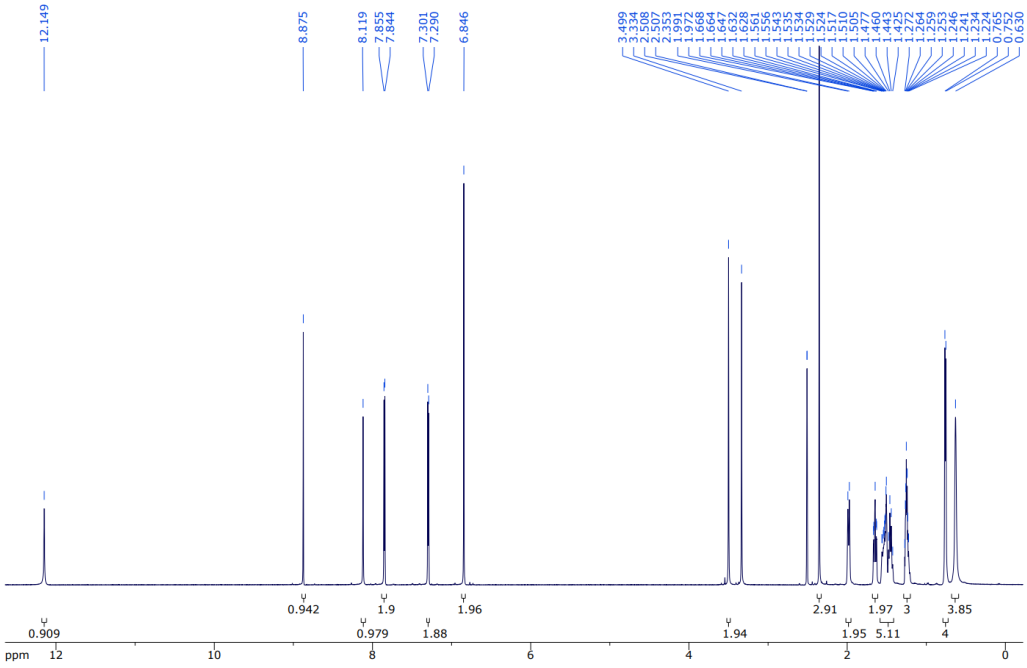
12.149
8.875
8.119
7.855
7.844
7.301
7.290
6.846
3.499
3.334
2.508
2.507
2.353
1.991
1.972
1.668
1.664
1.647
1.632
1.628
1.561
1.556
1.543
1.535
1.534
1.529
1.524
1.517
1.510
1.505
1.477
1.460
1.443
1.425
1.272
1.264
1.259
1.253
1.246
1.241
1.234
1.224
0.765
0.752
0.630
0.909
0.942
1.9
1.96
0.979
1.88
1.94
2.91
1.95
5.11
1.97
3
4
3.85
ppm
12
10
8
6
4
2
0

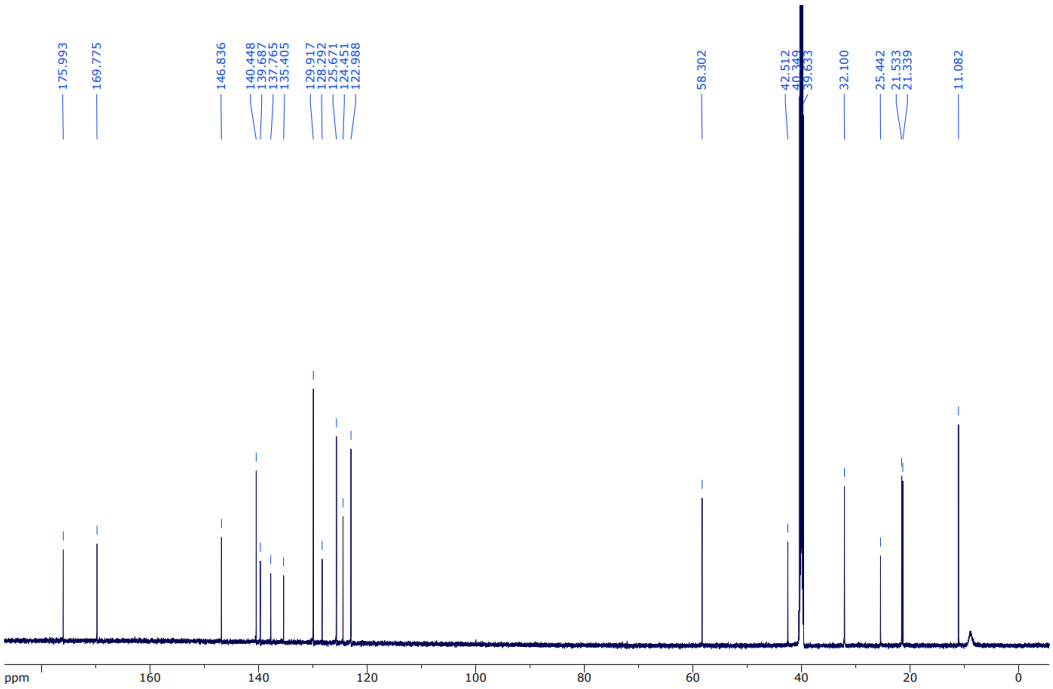
175.993
169.775
146.836
140.448
139.687
137.765
135.405
129.917
128.292
125.171
124.451
122.988
58.302
42.512
40.243
39.833
32.100
25.442
21.533
21.339
11.082
ppm
160
140
120
100
80
60
40
20
0

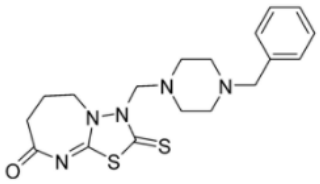

AA1

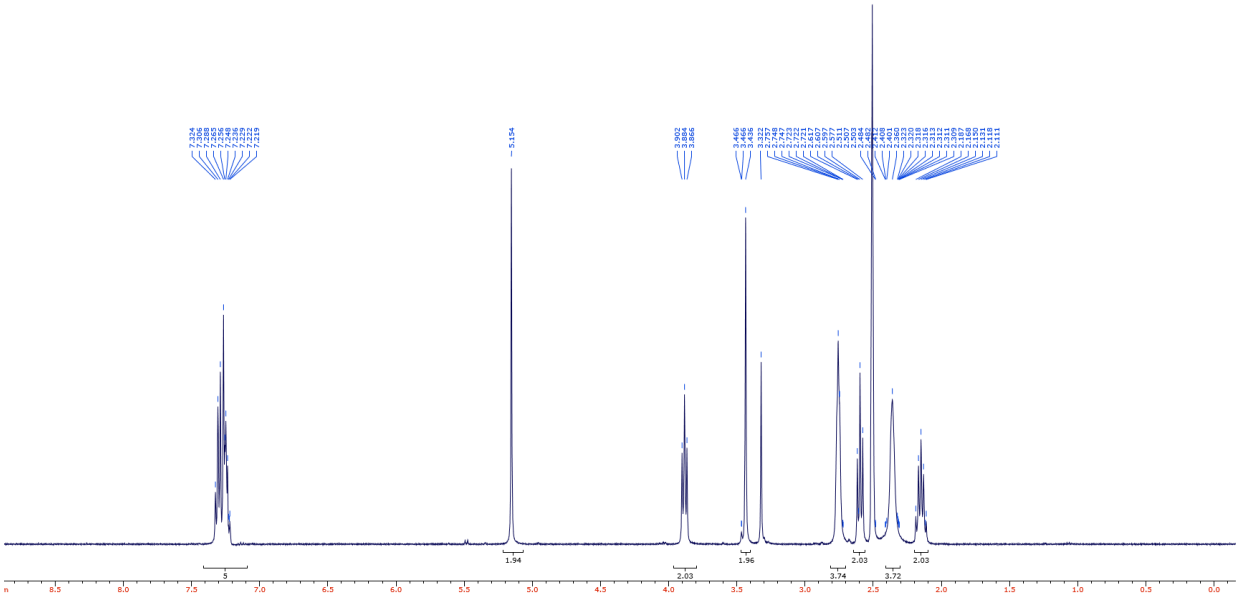

Dataset S1 (separate file): Table showing vendor IDs and structures (SMILEs notation) of the alkynes which produced click-reaction hits that gave >90% recovery in ΔN-HAB1 activity when tested in preliminary PYR1 mediated PP2C inhibition assay with ABA (5000 nM) and triazole hit (50000 nM). Hits were then retested at equimolar concentration with ABA (5000 nM) against representative receptors PYR1, PYL4, and PYL8 belonging to three subfamilies, column values indicating % activity of ΔN-HAB1 with individual receptors. Conversion of OPZ was measured by LC/MS analysis of click reactions by comparing the peak area of OPZ in the "click reaction" vs peak area of unreacted OPZ. The %-greening column indicates Arabidopsis seedling growth (measured by quantifying green cotyledon area normalized to seed number 4 days after stratification) treated with chemicals (1000 nM ABA and 10000 nM hit) relative to mock-treated control.

Dataset S2 (separate file): Table showing vendor IDs of aryl/heteroaryl carboxylic acids purchased from Combi-Blocks and structure (SMILEs notations) of propargyl amides obtained via polymer-supported chemistry. The resultant triazole library (106 members) was tested for antagonistic activity in presence of equimolar concentration with ABA (5000 nM) against representative receptors PYR1, PYL4, PYL8, column values indicating % activity of ΔN-HAB1. Table showing structure (SMILE notations) of precursor alkynes (**3a-n**) for triazole hits/ligands **4a-n**, resynthesized, purified (detailed synthesis and analytical data are shown in supplemental section), and retested for antagonistic activity. Hits were tested for antagonist-mediated recovery of PP2C activity in the presence of saturating ABA (5000 nM), PYL/RCAR, and ΔN-HAB1 proteins (both at 25 nM). EC_{50} values were obtained by non-linear fits of dose-response data to the 4 parameters log-logistic equation using the drc R package; assays were conducted in triplicate. Seedling growth was measured by quantifying green cotyledon area normalized to seed number 4 days after stratification; EC_{50} values indicate the concentration of the antagonist at 50% maximal green pixel area relative to mock control (1000 nM ABA); errors indicate standard deviation of experiments conducted in triplicate.

References cited

1. A. S. Vaidya, *et al.*, A Rationally Designed Agonist Defines Subfamily IIIA Abscisic Acid Receptors As Critical Targets for Manipulating Transpiration. *ACS Chem. Biol.* **12**, 2842–2848 (2017).
2. A. S. Vaidya, *et al.*, Dynamic control of plant water use using designed ABA receptor agonists. *Science* **366** (2019).
3. M. Okamoto, *et al.*, Activation of dimeric ABA receptors elicits guard cell closure, ABA-regulated gene expression, and drought tolerance. *Proc. Natl. Acad. Sci. U. S. A.* **110**, 12132–12137 (2013).
4. S.-Y. Park, *et al.*, Abscisic acid inhibits type 2C protein phosphatases via the PYR/PYL family of START proteins. *Science* **324**, 1068–1071 (2009).
5. Z. Otwinowski, W. Minor, Processing of X-ray diffraction data collected in oscillation mode. *Methods Enzymol.* **276**, 307–326 (1997).
6. P. D. Adams, *et al.*, PHENIX: a comprehensive Python-based system for macromolecular structure solution. *Acta Crystallogr. D Biol. Crystallogr.* **66**, 213–221 (2010).
7. P. Emsley, K. Cowtan, Coot: model-building tools for molecular graphics. *Acta Crystallogr. D Biol. Crystallogr.* **60**, 2126–2132 (2004).
8. V. B. Chen, *et al.*, MolProbity: all-atom structure validation for macromolecular crystallography. *Acta Crystallogr. D Biol. Crystallogr.* **66**, 12–21 (2010).
9. C. Ritz, F. Baty, J. C. Streibig, D. Gerhard, Dose-Response Analysis Using R. *PLoS One* **10**, e0146021 (2015).
10. S. Salentin, S. Schreiber, V. J. Haupt, M. F. Adasme, M. Schroeder, PLIP: fully automated protein-ligand interaction profiler. *Nucleic Acids Res.* **43**, W443–7 (2015).
11. R. A. Laskowski, M. B. Swindells, LigPlot+: Multiple Ligand–Protein Interaction Diagrams for Drug Discovery. *J. Chem. Inf. Model.* **51**, 2778–2786 (2011).
12. I. Jarmoskaite, I. AlSadhan, P. P. Vaidyanathan, D. Herschlag, How to measure and evaluate binding affinities. *Elife* **9** (2020).
13. J. Takeuchi, *et al.*, Designed abscisic acid analogs as antagonists of PYL-PP2C receptor interactions. *Nat. Chem. Biol.* **10**, 477–482 (2014).
14. R. Mega, *et al.*, Tuning water-use efficiency and drought tolerance in wheat using abscisic acid receptors. *Nat Plants* **5**, 153–159 (2019).
15. O. Pri-Tal, L. Shaar-Moshe, G. Wiseglass, Z. Peleg, A. Mosquna, Non-redundant functions of the dimeric ABA receptor Bd PYL 1 in the grass Brachypodium. *Plant J.* **92**, 774–786 (2017).
16. M.-J. Cao, *et al.*, ABA-mimicking ligand AMF4 in complex with ABA receptor PYL2 and PP2C HAB1 (2017) https:/doi.org/10.2210/pdb5vsr/pdb.
17. J. Takeuchi, *et al.*, Structure-Based Chemical Design of Abscisic Acid Antagonists That Block PYL–PP2C Receptor Interactions. *ACS Chem. Biol.* **13**, 1313–1321 (2018).